A MAGNETIC SURVEY OF THE SOUTHWEST PACIFIC OCEAN

Volume 1

by

DAVID IRWIN ROSS

Submitted for the Degree of

Doctor of Philosophy in Physics

at

Victoria University of Wellington

Wellington

New Zealand

April 1966

H.M.N.Z.S. Endeavour.

ABSTRACT

The design and construction of a free precession proton magnetometer which gives a reading of the field directly in gamma is described. This instrument has been used to obtain magnetic profiles across the Southwest Pacific Ocean during the 1963-65 summer Antarctic supply cruises of H.M.N.Z.S. Endeavour. The magnetic and bathymetric profiles obtained on these cruises have been analysed to determine the nature and structure of the oceanic crust in this region.

The region is divided into four divisions. (1) The New Zealand Plateau, with an almost continental crustal thickness. (2) The Southwest Pacific Basin, at a depth of 3,000 fathoms. (3) The Pacific-Antarctic Ridge, part of the world encircling mid-ocean ridge system. (4) The Ross Sea, an epicontinental sea across the Antarctic continental shelf.

Subtraction of the regional field from the magnetic results has enabled a regional field map of the area to be drawn. Comparison with earlier results indicates a westward drift of the earth's field of approximately 0.25°/yr. Some discussion of regional anomalies ($\sim$100 miles period) has been given.

Because of the excellent correlation of magnetic anomalies from track to track across the basin it has been possible to draw an anomaly contour map of this part. This map illustrates the predominantly east-west trend of features over the basin. To the north the features parallel the edge of the New Zealand Plateau. To the south the features swing more towards the Pacific-Antarctic Ridge. A major discontinuity is indicated along a direction 9°E of S meeting the Plateau just southwest of Antipodes Islands. If this discontinuity is extrapolated south to the ridge it meets it at approximately 180°E, where the ridge turns N-E towards Easter Island.

Across the ridge the magnetic pattern shows three distinct regions. Over the northern flanks large anomalies are evident but the correlation of anomalies from track to track is very poor. Further

south, across the upper flanks, the magnetic records are very much subdued. The extent of this region varies appreciably from track to track. Over the axis of the ridge large, steep-sided anomalies are obtained. These correlate well over part of the region studied. The southern flanks of the ridge are hidden by the Balleny Plateau which seems to form a link between Antarctica and the ridge in this region.

The bathymetry records obtained indicate a step-type formation over the ridge. A narrow median valley appears to exist along the axis of the ridge.

Some preliminary experimentation has been carried out with continual seismic profiling techniques over the region. The equipment that has been developed and the preliminary results obtained with it are discussed.

CONTENTS

Reprints of: 'Magnetic Anomalies South of the New Zealand Plateau'

'A 12V d.c. to 230V a.c. Silicon Controlled Rectifier Inverter'

are included in the envelope at the back of Volume 1.

LIST OF DIAGRAMS

INTRODUCTION

Over recent years interest in the nature and structure of the earth's crust beneath the oceans has increased enormously. The use of modern geophysical exploration techniques has enabled a vast amount of data to be collected over wide areas. There are however considerable regions of ocean about which little is known. The Southwest Pacific Ocean is one such region. With the commissioning of H.M.N.Z.S. Endeavour in 1962 as an Antarctic supply ship, and the equipping of her with facilities for carrying out scientific work at sea, it became possible for New Zealand scientists to carry out geophysical measurements in this little known region of the ocean.

This thesis describes the design and construction of a proton magnetometer and seismic profiler for use on Endeavour, and the results obtained to date with the equipment. These results are analysed, together with some earlier profiles, in an attempt to determine the nature of the earth's crust in this region and the processes occurring which form it.

The first three chapters contain mainly review material. A brief summary of results obtained elsewhere is given, together with a discussion of the types of measurements available and the problems involved. Earlier work over the region studied is also discussed. Chapters 4 and 5 discuss the design and construction of the magnetometer and seismic profiler respectively. The remaining chapters describe the results obtained, and discuss their significance.

It has been found necessary to refer the reader to a considerable number of diagrams. So these can be referred to easily while reading the script they have been included in a separate volume. The track chart, figure 23, showing the tracks over which results have been obtained, is mounted on an extension sheet so that it can be folded out clear of the other diagrams and can be readily seen for reference to track positions whenever required.

A brief summary of results obtained in December 1965 is included in Appendix 2. These tracks are not shown on the track chart and are not included in the discussion in the main script. On the whole they confirm earlier results.

Acknowledgements

I would like to gratefully acknowledge the assistance of the following people during the course of the work described in this thesis.

Dr. D. A. Christoffel for first interesting me in geophysical measurements at sea and for his continued interest and help in many ways since the commencement of this work. Professor D. Walker and other members of the academic staff of the Physics Department for help and discussions on matters arising from the thesis. The technical staff of the Physics Department for their help with equipment, particularly Mr. W. Brown of the Physics Workshop who did the major part of the work involved in the construction of the magnetometer fish and hydrophone arrays, and Mr. B. E. G. Goodger, Physics Department Electronic Technician, for considerable help in the design and construction of the electronic equipment. The D.S.I.R., Royal New Zealand Navy, and officers and men of H.M.N.Z.S. Endeavour for their cooperation and help with the project. I would also like to thank the following people, who as research assistants, helped with the operation of the equipment onboard H.M.N.Z.S. Endeavour; Messrs. S. T. Reid, G. Harvey, M. Bartle, G. Linford, and R. K. Falconer.

For help in the correction of the script I would like to thank Mrs. D. McL. Ross and for typing the final copy Mrs. Helen Gray. Mrs. Barbara Winchester for drawing the anomaly contour and magnetic trend maps across the basin region, figures 40 and 41, and Mrs. Adams for copying all diagrams. Mr. M. King took the photographs of the equipment, figures 5, 14, and 19. Finally I would like to thank my

wife for her considerable help and encouragement during the course of this work.

Some financial assistance was obtained for the project from a Grant-in-Aid from the University Grants Committee.

CHAPTER 1

THE EARTH'S CRUST UNDER THE OCEANS

1.1 General

Two divisions of the earth's crust are immediately obvious - the continents and the oceans. That the crustal structure beneath the continents and oceans is markedly different has only become apparent in recent years through the use of seismic exploration techniques. Ewing and Press (1955) and Gutenberg (1955) have shown that the depth to the Mohorovicic discontinuity in oceanic regions is only about 11 km, whereas in continental regions it is about 35 km. Gravity measurements have confirmed the deductions from seismic results. Figure 1 shows the standard crustal sections deduced by Worzel and Shurbet (1955) from gravity and seismic measurements.

Investigations of the structure of the continents have long been going on. With the advent of modern geophysical methods of exploration it has become possible to obtain information on the oceanic crust. The improvement of the echo-so under during the war enabled topographical maps of the deep ocean regions to be made. Heezen et al.(1959) have divided the ocean floor into three major morphological divisions; continental margin, ocean-basin floor, and mid-oceanic ridge. In the Atlantic, Indian, and South Pacific oceans each of these divisions accounts for about one third of the total area. Moreover it has been shown (e.g. Heezen and Ewing, 1956) that the mid-oceanic ridge forms an essentially continuous world encircling belt, 40,000 miles long. Its structure and origin are therefore fundamental to the origin of the oceans, and indeed must play a large part in the evolution of the whole crust.

Some 'master force' which is capable of acting on a world wide scale is required to explain world wide features of the earth's

crust. Three such 'master forces' are; contraction or expansion of the earth, subcrustal convection currents, and crustal displacement with or without convection. Chadwick (1962) has reviewed a number of theories of mountain building processes incorporating these 'master forces'.

In the explanation of oceanic features the 'master force' that has received most favour is that of subcrustal convection currents with consequent crustal displacement (Dietz, 1961; Wilson, 1961, 1965; Menard, 1958; 1960; Vening Meinesz, 1962). That such convection currents do exist, and have their upwelling along the crest of the mid-ocean ridge as is generally assumed, is supported by heat flow measurements across the ridge system.

With the increased use of geophysical measurements at sea over the last decade considerable knowledge has been accumulated about the major features of the oceans. Any theory on the formation of the oceans must be consistent with the large number of facts available.

1.2 Continental Margins

This region consists of the continental shelf, slope and rise, and any marginal plateau which may occur at a depth of less than 1200 fathoms. Wide variations in the form of the continental margins occur throughout the world. Thompson (1957) has classified continental shelves into three broad classes; polar shelves, middle latitude shelves, and tropical shelves. He considers the shelf to be a wave cut platform formed at a time when the sea level was considerably lower than at present.

Heezen et al.(1959) have described in some detail the variations in form of continental margins that have been studied. Guilcher (1963) has classified margins according to assumed origin. He considers five possible types of margin; the erosional and constructional classic type, the constructional subsiding type, the flexured type, the downfaulted or

block faulted type, the fissured type. He concludes that, "the continental margins appear to have a mainly diastrophic or constructional origin. Marine erosion in shallow and coastal waters, of which wave abrasion is probably less important, is responsible for some of the features, but its action has been of limited extent."

In connection with continental shelves Bullard states, "All that can be deduced from the observations is that the shelf was formed in at least two stages. In the first, more or less flat lying sediments were laid on a subsiding basement, then a scarp formed at the outer edge and the existing regime set in. The scarp could be formed by normal faulting, as Heezen et al.(1959) suggest, or by erosion or, conceivably, by continental drift splitting a relatively narrow sediment-filled basin and converting it into the shelves of two opposing continents."

One of the features of continental margins is the large number of canyons which cut the region. These appear to be channels by which sediment from the continent is transported across the continental shelf to the adjoining deep sea regions. It was earlier thought that all these canyons had been cut by rivers at some time when the present shelf was above sea level. However many of these canyons continue across the continental slope to considerable depths, and some have even been traced across deep ocean basins (Ewing et al.1953). To account for the erosion of these deep channels requires deep ocean currents which travel for considerable distances.

Daly (1936) suggested that turbidity currents could be the cause of these canyons. Since then this idea has gained considerable support. From calculations on the sequence of breaks in submarine cables after the 1929 Grand Banks earthquake, Heezen and Ewing (1952) were able to show that turbidity currents could travel at the required speed for considerable distances. Kuenen (1953) considers two distinct types of canyon exist. One, drowned rivers, and two, turbidity current cut canyons, the latter occurring across continental slopes. This is now generally accepted.

1.3 Ocean Basins

Heezen and Laughton (1963) have discussed the types and occurrence of deep ocean basins, and also their possible origins. The main feature of these deep basins is the remarkable smoothness of the topography across them. The most plausible way of explaining this remarkable flatness is that proposed by Heezen, Ewing, and Ericson (1951). They suggested that the abyssal plains are regions where the original topography has been buried by deposits of turbidity currents. Support for this hypothesis was obtained from the occurrence of graded sand layers and shallow water foraminifera in cores from the abyssal plains, and also from observations on the sequence of breaks in the submarine cables after the 1929 Grand Banks earthquake.

Seismic measurements over deep ocean basins suggest that the average crustal section consists of $\frac{1}{2}$-1 km of low velocity sediments, a 1-2 km layer of velocity 4.5 - 5.5 km/sec, and 4-6 km of oceanic crustal rock in which the seismic velocity is about 6.5 km/sec (Ewing and Ewing, 1959; Hill, 1957). This second intermediate velocity layer may consist of consolidated sediments (Hamilton, 1961), although Vine and Wilson (1965) consider this layer to be the main source of magnetic anomalies.

The mean heat flow over the ocean basins (approximately $1.08 \mu cal/cm^2$ sec) appears to be very close to the mean continental value (Bullard 1963). Because of the small thickness of the oceanic crust the majority of this heat must come from the mantle. The constancy of the measured heat flow across deep ocean basins suggests that these regions have been stable for some time (Reitzel, 1963).

1.4 Mid-ocean Ridge

The mid-ocean ridge system has been described by Heezen and Ewing (1963). Considerable work has been done over various parts of the ridge system. The greatest portion of this has been concentrated along the Mid-Atlantic Ridge. Although it appears that the mid-oceanic

ridge is essentially a continuous world encircling feature, as suggested by Ewing and Heezen (1956), the various sections making up the complete system exhibit quite marked differences. For example the East-Pacific Rise is a broad rise with gentler slopes than the Mid-Atlantic Ridge (Menard, 1960). Nor is there evidence of a median rift valley associated with the rise. Such a rift valley is a characteristic feature of the Mid-Atlantic Ridge. Similarly strongly positive magnetic anomalies have been found characteristic of crossings of the rift valley in the North and South Atlantic, but this is not so across the rift valley of the Indian Ocean (Heezen, 1962). On the other hand Rothé (1954), Heezen and Ewing, (1963), Sykes (1963) and Menard (1960), have shown that the crest of the ridge is associated with shallow earthquakes along its whole length.

Where heat flow measurements have been made across the crest of the ridge system, it is found that high values occur along the crest, with low values being associated with the flanks. Measurements across the Mid-Atlantic Ridge have been made by Gerard (1962), and Nason and Lee (1962, 1964). Measurements across the East Pacific Rise have been made by Bullard et al. (1956), Von Herzen (1959), Von Herzen and Uyeda (1963), and Langseth et al. (1965).

As already mentioned magnetic measurements across the Mid-Atlantic Ridge seem to show characteristic large anomalies associated with the rift valley. Similar large anomalies are associated with the Red Sea (Drake and Girdler, 1964). Measurements across the East Pacific Rise show a lineated anomaly pattern which closely parallels the Rise.

The structure of the crust and upper mantle under the Mid-Atlantic Ridge and East Pacific Rise has been deduced from seismic refraction and gravity measurements by workers in the Lamont Geological Observatory, (Le Pichon et al., 1965; Talwani et al., 1965). They find that the crust does not thicken under the ridge but that the crest is underlaid by an anomalous low-velocity mantle. This work

followed on from earlier work by Ewing and Ewing (1959) and Raitt (1956). Ewing and Landisman (1961) have summarized the known facts about the mid-ocean ridge system as follows.

"1. The mid-ocean ridge system is continuous and can be traced with certainty through a 40,000 mile world encircling belt, which passes through the Atlantic, Indian, Pacific, and Arctic oceans.

2. A deep narrow median valley or trench from 20-80 miles wide and $\frac{1}{2}$ - $1\frac{1}{2}$ miles deep is a characteristic feature of the ridge through the Atlantic and Indian oceans. Apparently the valley is not conspicuous in the Pacific.

3. A seismic belt in which all shocks are shallow focus, is continuous along the ridge and coincident with the median valley (in so far as the valley position is known).

4. The earthquake belt and an associated rift system extend into continental areas in several places.

5. In contrast to land mountain systems, this range of submarine mountains consists of a thin upper layer with seismic velocities of about 4.5 - 5 km/sec and a mass 30 - 40 km thick in which the velocity is about 7.3 km/sec.

6. The ridge shows a striking tendency to bisect the oceans through which it passes, if we grant that the southeast Pacific is an exception."

Menard (1958) has suggested that the various gradational forms of median elevations found in ocean basins may be stages in development. The sequence of forms suggested is as follows.

"1. A very broad seismically active rise with many volcanic islands and sea-mounts but, few, if any guyots, e.g. East Pacific Rise.

2. A narrower, steeper, seismically active rise with volcanic

islands and guyots side by side, e.g. Mid-Atlantic Ridge in the North Atlantic.

3. A narrow, steepsided, seismically inactive ridge lacking volcanic islands but with many guyots and atolls, e.g. Tuamotu Ridge and Mid-Pacific Mountains."

Menard, together with many other investigators, considers that the observed facts about the ridge system can be explained by the convection current hypothesis. This suggests that the ridge is formed over an upwelling convection current in the mantle. A difficulty with this idea is to work out a suitable convection current pattern which fits all the available data.

In connection with the convection current hypothesis mention should be made of the suggestion of Dietz (1961). He considers the upward convection current along the ridge as being the source of new crustal material, which spreads away from the ridge across the adjacent sea floor until it is finally added to the base of the continental regions. Thus he considers the mid-ocean ridge as being the primary source of the crustal material. Some discussion on Dietz' paper is published in Nature (1961).

Hess (1954, 1955) has suggested an alternative theory for the origin of the ridge system. His theory relies on the expansion which occurs with the serpentization of olivine according to the reversible equation;

$$\text{Olivine} + H_2O = \text{Serpentine} + \text{heat}$$

If water is gradually supplied from the interior of the earth, that part of the mantle above the $500^{\circ}C$ isotherm will be subject to the reaction going to the right. This involves a density change of from 3.25 - 2.60 and hence results in an increase in the height of the column. Conversely, if the isotherm rises in a serpentized area, the reaction goes to the left. The subsequent collapse of a ridge can therefore be easily explained.

Evison (1960) has suggested that the growth of continents by plastic flow and their subsequent encroachment into the ocean basins, would cause a redistribution of material in the upper mantle and a consequent upwelling of the central part of the oceans.

CHAPTER 2

GEOPHYSICAL MEASUREMENTS AT SEA

2.1 Problems Associated with Measurements at Sea

Three major problems arise with measurements at sea. The first of these arises from the fact that the ocean floor is at an average depth of $2\frac{1}{2}$ miles below the sea's surface. All probing of the ocean crust must therefore be carried out from a distance. This obviously increases the difficulties encountered.

The second problem is that of obtaining a stable platform from which to carry out measurements. Until recently this made magnetic and gravity measurements at sea impossible, and still presents a major problem in the design of surface ship gravimeters. The problem of carrying out magnetic measurements has been overcome by the development of total field magnetometers which can be towed behind the ship.

The third problem is that of accurate navigation. This is a real problem in regions, such as the area studied, where electronic navigational aids do not exist. Where good astronomical observations are obtained, positional accuracy of a few miles can be realised. But when, because of weather conditions, dead reckoning must be relied on, large errors may occur. Such large errors make the correlation of records from track to track very difficult.

In carrying out seismic measurements a further factor arises. This is the requirement of a quiet hydrophone to enable the weak reflected or refracted signals to be picked up. This may mean shutting down the ship's engines and other auxillary equipment during the listening period.

2.2 Measurements Possible at Sea

Despite the problems involved, techniques have been

developed to carry out a wide range of measurements and so obtain an accurate picture of the oceanic crustal structure. With modern techniques the available measurements include; bathymetric, seismic, heat flow, magnetic, and gravity measurements, as well as deep sea sampling and photography. A summary of the techniques used follows.

2.2.1 Bathymetric measurements

The development of the modern echo-sounder has enabled the topography of the ocean floor to be mapped. With echo-sounders as standard equipment on ocean-going vessels, detailed charts have been drawn for large regions of the oceans. However the conventional sounder does not give accurate depths, nor does it resolve fine detail in deep water. To overcome these shortcomings Luskin et al. (1954) constructed a precision depth recorder which enabled them to obtain an accuracy of 1 fathom in 3000 fathoms. The P.D.R. has become standard equipment on oceanographic ships, and has enabled the features of the deep ocean to be studied in detail and physiographic diagrams to be drawn (e.g. Heezen et al., 1959; Heezen and Tharp, 1961; Menard, 1964).

2.2.2 Seismic measurements

Seismic measurements have been among the most useful in furthering a knowledge of the structure of the ocean crust. Both reflection and refraction techniques have been used extensively at sea. (Ewing, 1963; Shor , 1963). Single ship refraction measurements have been made using sono-radio buoys as the receiving station (Hill, 1963). Basically seismic measurements supply information on the number and thickness of the sub-surface strata, together with the velocity of sound in each. Thus the structure of the crust below the ocean regions can be determined, and the way in which it varies from one region to another. In this way anomalous regions can be selected for more detailed study.

Recently a continuous seismic reflection technique has been developed for the study of sediment layering and basement topography (Ewing and Tirey, 1961). With this technique the thickness and structure of the sediments can be determined over large areas while the ship is cruising at its normal speed. Hersey (1963) has reviewed the method and given some results. Improvements in the hydrophone arrays and sound sources used, have enabled good results to be obtained in deep ocean regions while cruising at speeds of up to 10 knots.

Surface wave studies have been used to determine average crustal structure, particularly in continental margin regions (Ewing and Press, 1950, 1952; Oliver and Dorman, 1963). These studies have also shown that the upper mantle is different under the oceans to that under the continents (Dorman et al., 1960). Both contain a region of low shear velocity. Under the continents this region is at a depth of approximately 100-200 km, while under the oceans it is from 50-200 km. It is also a much more pronounced feature under the oceans.

2.2.3 Heat flow measurements

Heat flow measurements at sea have been described by Bullard (1963). The rate of flow of heat through unit area of the ocean floor is given by the product of the temperature gradient through the sediments and the conductivity of these sediments. The temperature gradient is measured by a probe forced into the ocean floor. The conductivity is determined by measurements on samples brought up by a coring tube.

Measurements show that the average oceanic value agrees well with that of the continents. Measurements of the radioactivity of rocks indicate that the continental heat flow arises from radioactive sources in the crust. Because of the thinness of the oceanic crust however, the heat flow over oceanic regions must arise from sources below the Mohorovicic discontinuity. Heat flow measurements over the ocean ridge regions generally show high values over the crest and low values

over the flanks, suggesting an upwelling convection current along the crest of the ridge.

2.2.4 Magnetic measurements

With the development of the fluxgate magnetometer for the detection of submarinesduring the second world war, it became possible to make accurate measurements of the earth's magnetic field over oceanic regions. The subsequent development of the proton precession magnetometer made shipborne measurements more reliable, since the proton magnetometer is an absolute instrument while the fluxgate requires frequent calibration. A review of magnetic methods at sea has been given by Bullard and Mason (1963), together with some of the detailed results obtained off the coast of California (Mason and Raff, 1961; Vacquier et al., 1961). These latter results illustrate how structural trends can be deduced from magnetic records. They indicate an essentially north-south lineated pattern across which several large fracture zones cut. Correlation of magnetic records across these zones indicates the displacement that has occurred. Measurements indicate a left lateral slip of 265 km along the Pioneer and 1185 km along the Mendocino faults.

2.2.5 Gravity measurements

Until recently continuous gravity measurements at sea were impossible. Considerable work had been done previously with pendulum instruments in submarines (Vening Meinesz, 1929, 1941). Accuracies of a few milligals were obtainable provided the wave accelerations were less than about 6000 milligals.

The development of the La Coste (La Coste, 1959; Harrison, 1959), and the Graf Sea (Worzel, 1959) gravimeters, made continuous gravity measurements possible on surface ships. These instruments have been used with some success in the last few years under normal sea conditions. Worzel and Harrison (1963) have reviewed the problems

of gravity measurements at sea and have presented results obtained over the main ocean structures. Gravity measurements enable detailed crustal sections to be determined, particularly if seismic results are also available.

2.2.6 Deep sea floor sampling

The problems involved in obtaining samples from the deep sea floor are quite considerable. Dredgings from rock outcrops suggest that basalt is the main oceanic rock type. Considerable information on the surface of the sea floor is now being obtained with deep sea photographic techniques (Edgerton, 1963). These techniques have been found particularly useful for studying small features not resolved by echo-sounding surveys (Laughton, 1963).

Cores of deep sea sediments can give a lot of information on rates of sedimentation and methods of sediment transportation, as well as considerable information on past climatic conditions. Much of the history of the earth's surface is hidden in the sedimentary record of the ocean floor. Unfortunately it is still impossible to sample all but the top few layers of this record.

Early corers relied on gravity to drive them into the sediments. Their velocity of fall was limited by the rate at which the cable could be let off the winch. This limited their penetration to a few feet. Various methods of obtaining greater penetration have since been devised and improved on. Piggot (1936) designed a corer which used explosives to drive the coring tube into the sediment. Petterson and Kullenberg (1940) devised a vacuum core sampler for deep sea sediments. Hvorslev and Stetson (1946) described a free-fall coring tube in which the coring tube with attached weight was allowed to fall freely from some specified height above the ocean bottom. The higher velocities obtained in this way enabled considerably longer cores to be collected than was previously possible with a gravity corer.

Considerable distortion of cores normally occurs in their collection, particularly with long cores. Piggot (1941) discussed the factors influencing the distortion, and deduced relations for these factors based on experiments with glacial varve deposits.

2.3 Possible Measurements in the Present Study

For the present study facilities were made available aboard H.M.N.Z.S. Endeavour during her summer Antarctic supply cruises. Because of the tight schedule for these trips, all measurements had to be made while the ship was underway at an average speed of 10-12 knots. Although some control over the tracks followed, within the bounds of 165°E - 180°E, was possible, other factors often necessitated a change in course over part, or all, of the proposed track.

The ship carried an 'Edo' echo-sounder which generally operated well in all depths encountered, providing reasonable bathymetric profiles along the tracks followed. However, because of the small scale on the deep range (6000 fathoms), and the inherent inaccuracies of the instrument, it was not possible to obtain detailed information on topographical features in deep ocean regions.

With the facilities available, a total field magnetometer could be installed for the measurement of total magnetic field. Rumbaugh and Alldredge (1949) described the fluxgate magnetometer. To measure the total field the fluxgate head must be aligned with the earth's field. This is accomplished by mounting three fluxgate units perpendicular to one another, and using two of these to align the third by means of a servo system. The measuring head is used as a null detector, the actual field value being determined from the current required in a set of field cancelling coils. Obviously the accuracy of the instrument depends on the stability and accuracy of the field cancelling system. The instrument therefore requires frequent calibration for absolute measurements. Miller and Ewing (1956) first used a towed fluxgate magnetometer at sea.

The proton magnetometer has the advantage of being an absolute instrument. Also the detecting coil requires no elaborate aligning system since the frequency of the precession signal is directly proportional to the magnitude of the total field. However the amplitude of the signal does depend on the orientation of the coil relative to the field direction, becoming zero when the coil and fields are aligned. This rarely presents any problem however. Hill (1959) first used the proton magnetometer at sea and since then it has largely replaced the fluxgate.

For these reasons a proton magnetometer was constructed for the present study. The theory and operation of the magnetometer, together with details of construction are given in chapter 4.

One other type of measurement was possible with the facilities available on H.M.N.Z.S. Endeavour. This was the measurement of sediment structure and thickness by means of the seismic profiling technique. However two major obstacles had to be overcome. These were the attainment of a quiet hydrophone at speeds of 10-12 knots, and the problem of a suitable sound source. Since the Endeavour's main cargo on these trips was aviation fuel for the American Base at McMurdo Sound, restrictions were placed on the type of sound source used. However it was felt that useful experience would be gained by incorporating this equipment in the programme. The equipment used and the problems encountered are discussed in chapter 5.

2.4 Information Obtained from Total Magnetic Field Measurements

The interpretation of the data obtained from a survey of the earth's magnetic field is based on the fact that the field is uniform over areas of magnetically homogeneous composition, but is measurably distorted in regions of inhomogeneous composition. The actual field measured at any point is the sum of the regional value of the earth's field, and the anomalous field due to any disturbances. Since the earth

behaves approximately as a uniformly magnetized sphere, the regional field will increase reasonably uniformly from the equator to the poles.

Subtracting the regional field from the records obtained then leaves the local anomalous field caused by variations in local structure, plus any time fluctuations of the field of periods less than several hours. Fluctuations with periods greater than this will tend to be included in the regional field.

Three types of variations in local structure can give rise to a magnetic anomaly. (1) A change in topography of a magnetic rock structure. Except for highly magnetic shallow sources this is usually of minor importance. (2) A change in lithology of the rock structure. This is usually regarded as the major factor in interpretation, as large scale changes in lithology do occur, involving considerable susceptibility contrasts. (3) A change in remanent magnetization of a rock structure, either in direction or magnitude. The importance of considering this has only become apparent recently (Girdler and Peter, 1960; Green, 1960). In the case of basalts the ratio of the remanent to the induced magnetization is often high (Ngata, 1956), so that variations in remanence may lead to quite large anomalies. An important point to note in this case is that if the direction of the remanent magnetization changes over a region of otherwise uniform composition, an anomaly will result.

The shape of the observed anomaly will depend on a number of factors. The most important of these are the shape of the source and its depth. However the direction of magnetization and the direction of traverse over the source, will also influence the shape of the anomaly. The actual amplitude of the anomaly depends primarily on the magnetization of the source and hence its susceptibility.

Obviously there are too many variables to obtain a unique solution from the magnetic data alone. However if sufficient results are available to map an area, an idea of the shape of the source can be obtained. By comparison with theoretical anomalies over standard bodies approximating to the source, an estimation of the depth and

susceptibility of the source can be obtained. For simple bodies, e.g. dykes, it is possible to obtain theoretical formulae for the computation of model bodies, the associated anomalies of which can be closely fitted to the actual anomalies observed. Since the most common sources encountered at sea appear to be bodies which are very long compared to their width and depth, the dyke model is generally a good approximation to the actual source, and two dimensional models are all that are required to obtain a good fit between the observed and calculated anomalies.

Hence although a unique solution for the source of an anomaly is unobtainable, a reasonable picture of the structure of the magnetic basement may be built up. Furthermore a magnetic map of a region will show changes in structure across the region. Since we can only obtain profiles from H.M.N.Z.S. Endeavour, the problem is to obtain sufficient profiles with reasonable positional accuracy to build up a picture of the basement structure across the region.

2.5 Information Obtained from Seismic Profiles

To help in the analysis of the magnetic data as much other information as possible is required. A profile of the ocean floor is obtained by the ship's echo-sounder. Information on sediment layering and thickness would give indications of the history of the ocean floor. Basement topography may be completely masked by sediment deposition. Unless the basement topography is known magnetic effects which are in fact due to topography may be interpreted as due to some other cause. The seismic profiler can supply this missing information. By the use of a high energy, low frequency sound source, penetration of the sediment layers can be accomplished, and reflections obtained from the intermediate boundaries down to the basement rock. By noting the time between successive reflections, the thickness of the various sedimentary layers may be determined, assuming reasonable values for the velocity of sound in the layers.

CHAPTER 3

THE REGION STUDIED

3.1 Nomenclature

The area covered by the present study is that region of ocean lying between New Zealand and McMurdo Sound crossed by the Antarctic supply ship H.M.N.Z.S. Endeavour. Figure 2 shows the region divided into the three major morphological divisions; continental margins, ocean basin, and mid-ocean ridge. The fact that it contains these three major oceanic provinces makes it an important area to study.

In discussing the region the following nomenclature has been used.

New Zealand Plateau. The marginal plateau surrounding New Zealand and extending to the mid-depth of the marginal slope, (Brodie 1965). It includes the Campbell Plateau, the region of the New Zealand Plateau lying to the south east of New Zealand.

Subantarctic Slope. The steep slope marking the southern edge of the New Zealand Plateau (Brodie, 1965).

Indian-Antarctic Ridge. The broad ridge extending from about 50°S, 120°E to the Balleny Islands. Approved by the British National Committee on the Nomenclature of Ocean Bottom Features. (Herdman et al, 1956).

Macquarie-Balleny Ridge. The ridge extending from Macquarie Island to the Balleny Islands and joining the Indian-Antarctic Ridge at about 60°S. Proposed by the British Committee (Herdman et al., 1956).

Pacific-Antarctic Ridge. As proposed by the British Committee (Herdman et al., 1956) this is a broad ridge extending from 40°S 112°W to 65°S 180°W. In the present discussion the connection between the Indian-Antarctic Ridge and the Pacific-Antarctic Ridge, i.e. the region of the ridge system lying between 180°W and 160°E, will be

referred to as part of the Pacific-Antarctic Ridge.

Southwest Pacific Basin. The basin bounded by the Pacific-Antarctic Ridge, the Macquarie-Balleny Ridge, the New Zealand Plateau, the Tonga and Kermadec Trenches, and latitude 15°S (Wiseman and Ovey, 1954).

Balleny Plateau. The plateau-like region at a depth of approximately 2000 fathoms lying between the Balleny Islands and Scott Island, and bounded on the north by the Pacific-Antarctic Ridge, and on the south by the Antarctic continental shelf. To the east it abutts onto the western edge of the deeper Pacific-Antarctic Basin which extends to the east between Antarctica and the Pacific-Antarctic Ridge.

Ross Sea. In the present discussion this is defined as the shallow marginal sea across the Antarctic continental shelf between 165°E and 150°W.

3.2 General Description of the Region

Brodie (1965) has described the morphology of the New Zealand Plateau in some detail. For the most part it lies at depths of less than 500 fathoms. Evidence from rock samples collected from the islands of the southern plateau, Auckland, Campbell, Antipodes, Bounty, and Chathams, suggests that it is continental in nature. Measurements of crustal thickness by earthquake surface wave dispersion methods give values of 17-25 km over most of the plateau (Adams, 1962; Officer, 1955). Thus the crustal thickness appears to be intermediate between that of continental and deep oceanic regions.

At the southern boundary of the New Zealand Plateau the sea floor falls steeply across the Subantarctic Slope to the abyssal floor of the Southwestern Pacific Basin. Over the part of the basin in which most of the present measurements have been made it extends to about latitude 60°S. The depth of the basin is 2700-3000 fathoms.

To the south the basin is bounded by the Pacific-Antarctic Ridge, part of the mid-ocean ridge system. The ridge extends from

about 60°S - 66°S, the crest lying around 63° - 65°S. This portion of the ridge is complicated to some extent by the juncture with the Macquarie-Balleny Ridge in the vicinity of 62°S, 165°E.

South of the ridge the tracks cross the comparatively shallow Balleny Plateau. At about 70°S the floor again begins to slope up as the Antarctic continental shelf is approached.

The Ross Sea is an epi-continental sea over an abnormally deep continental shelf. Wherever it occurs, the Antarctic continental shelf appears to be considerably deeper than that normally found (Lisitzin and Zhivago, 1960). Results of measurements of earthquake surface wave dispersion across the Antarctic suggest that the Ross Sea has a crust of almost continental thickness (Evison et al, 1960).

3.3 Prior Measurements South of the New Zealand Plateau

Very few geophysical measurements have been made over the deep ocean region south of the New Zealand Plateau.

Bathymetry measurements have been made for some time by ships supplying the Antarctic bases on Ross Island. Spot soundings were made by the early explorers crossing these waters but the first reasonably detailed profiles seem to be those obtained by Roos (1937) on the second Byrd Antarctic Expedition. On this expedition depths were measured every seven miles along the complete track between New Zealand and Antarctica, with additional readings being taken where the depth was changing rapidly. Continuously recording deep sea echo-sounders have been standard equipment on U.S. Deepfreeze vessels for some years now but have only been operated on the N.Z. Antarctic supply ship since the summer of 1962-63. Portions of profiles obtained by the Deepfreeze ships have been published in the U.S. Navy Hydrographic Office reports (1962, 1965). A profile obtained aboard H.M.N.Z.S. Endeavour has also been recently published (Brodie, 1965)

Total magnetic field profiles over the region have been

published by Christoffel (1961), Adams and Christoffel (1962), and the U.S. Navy Hydrographic Office (1962, 1965). These measurements suggest magnetic lineations which tend to parallel the Pacific-Antarctic Ridge. Christoffel obtained correlations across his two tracks which he extended across the basin region. The proposed magnetic lineations had a direction closely paralleling that of the bathymetry. A number of additional profiles have been obtained by the staff of Geophysics Division of the D.S.I.R. These have not yet been published. Two of these profiles have been lent for use in the present analysis.

Some sediment cores have been obtained in the region, particularly south of the ridge and in the Ross Sea (Hough, 1950; Thomas, 1959; Lisitzin, 1962). These give evidence of different climatic conditions occurring in the Antarctic in the past. They also indicate that the predominant sediments are the 'iceberg sediments', i.e. sediments transported away from the continent by icebergs.

No seismic reflection or refraction, gravity or heat flow measurements have been made in the deep ocean regions to date. However some indication of crustal thickness has been obtained from earthquake surface wave dispersion measurements. As already mentioned Evison et al., (1960), have suggested that the Ross Sea area has a crust of almost continental thickness. Adams (1964) has used this method to obtain an average crustal thickness for the Pacific-Antarctic Ridge. He obtains an average thickness of 6 - 7 km. Sykes (1963) has presented a map of earthquake epicentres for the South Pacific Ocean for the period 1957-1963. Most of the epicentres lie near the plotted crests of the mid-ocean ridges. Several possible fracture zones are suggested from the epicentre data.

Some work has been done over the Ross Sea. Lepley (1964) has discussed the geomorphology of the Eastern Ross Sea. Bentley et al. (1960) have carried out gravity measurements across West Antarctica and deduced the crustal structure, including that of the Ross Sea. Their

results suggest a crustal thickness of 28 km for the Ross Sea region. Bennett (1964) has described a gravity and magnetic survey of the Ross Ice Shelf area. Other magnetic results obtained include those of Christoffel (1961) and Robinson (1964), the latter being confined to the McMurdo Sound area. The lack of strong magnetic anomalies over the area has been interpreted as indicating that the magnetic basement is at a considerable depth as would be expected for a continental region. Bennett finds poor correlation between gravity and magnetic anomalies, also indicating that the source of the magnetic anomalies is deep.

CHAPTER 4

THE PROTON MAGNETOMETER

4.1 General Principles

The method of measuring the earth's magnetic field by determining the frequency of free precession of protons in this field, was first reported by Packard and Varian (1954), although the principles of nuclear induction on which the method is based were discussed some eight years earlier by Bloch (1946). Waters and Phillips (1956) and Waters and Francis (1958) described practical instruments using this principle.

The principle of the free precession proton magnetometer is as follows. In the earth s magnetic field the protons in a sample of water align themselves in directions approximately parallel and antiparallel to the field, a slightly greater number pointing along the parallel direction. If N_1 is the number of protons in the parallel direction, and N_2 the number in the antiparallel direction, then

$$N_1 - N_2 = N(1 - \exp-(\frac{\mu F}{kT}))$$

where μ = magnetic dipole moment of the protons,

F = earth's total magnetic field,

T = absolute temperature,

k = Boltzman's constant,

N = total number of protons in the sample.

Thus a small magnetic moment is produced along the direction of the earth's field equal to $(N_1 - N_2)\mu$. If a magnetic field $H > F$ is applied at an angle to the direction of the earth's field, a magnetic moment will be produced in the direction of the resultant of this applied field and the earth's field. For $H >> F$ the resultant field will have a direction and strength approximately equal to H. The magnetic moment produced in

the direction of H will approach its maximum value (equal to $\mu N(1 - \exp-(\frac{\mu H}{kT}))$) exponentially with a time constant T_1, the spin-lattice relaxation time which for protons in water is a few seconds. If after a suitable time the applied field is removed in a time short compared to the Larmor precession period (equal to $\frac{2\pi}{\gamma_p F}$, where γ_p is the gyromagnetic ratio for protons), the magnetic vector will not follow the decreasing resultant field. Instead it will return to its original value and direction in the earth's field by precessing around that field direction at a frequency equal to the Larmor precession frequency, $\frac{\gamma_p F}{2\pi}$. The precessing magnetic vector will induce an e.m.f. in a coil around the water sample. The frequency of this e.m.f. provides a measure of the earth's field. At the moment of removal of the magnetic field H, the individual protons whose component sum produces the vector, begin to precess in phase. However as the magnetic field varies slightly at each individual proton because of the assymetrical field contribution from neighbours, a loss of phase will occur with time, in turn causing a diminution of the signal. Thus the observed signal decays exponentially with a time constant T_2, the spin-spin relaxation time. For protons in water $T_1 \doteq T_2$. T_2 is however reduced if a magnetic gradient exists across the sample due to nonuniformity of the external field. Both T_1 and T_2 are reduced by the presence of paramagnetic ions in the water sample.

4.2 Design of the Magnetometer

Before a detailed description is given of the various sections of the magnetometer, a general discussion of the requirements of the apparatus may be profitable in order to obtain a picture of the complete apparatus.

As already shown, the frequency of the proton precession signal is directly proportional to the ambient magnetic field at the sample. Thus a measurement of the magnetic field requires a measurement of the frequency of the precession signal before it has

time to decay into the "noise". The equipment therefore consists basically of a switching unit, to polarize the proton sample at regular time intervals; an amplifier, to amplify the small induced e.m.f. to a usable level; a counter system, to measure the signal frequency; and a recorder, to read the counter output and record the value obtained.

4.2.1 Switching of the Polarizing Current

To obtain a proton precession signal from a sample of water, the protons must first be polarized by a large magnetic field in a direction approximately at right angles to the ambient field. The angle between the polarizing and ambient fields affects only the amplitude of the signal. Elementary theory shows that the amplitude of the signal should be proportional to $\sin^2 0$, where 0 is the angle between the two field directions. Measurements made by Bullard et al. (1964) indicate that this relation is not strictly correct, but depends on the rate at which the polarizing field is reduced. The polarizing field is produced by passing a current of several amperes through a coil around the sample. To obtain a precession signal of reasonable amplitude induced in a signal coil around the sample the polarizing field must (1), be present for a time long compared with the spin-lattice relaxation time of the protons, so that sufficient protons are aligned with the field, and (2), be reduced in the sample to a very small value compared with the ambient field in a time short compared with the Larmor precession period. It is convenient to combine into a single coil both the polarizing field coil and the signal pick-up coil. The switching unit is therefore required to switch the coil onto the preamplifier input a short time after the polarizing current has been cut off; sufficient time being allowed for the switching transients in the coil to decay so that the amplifier is not damaged, or its amplifying conditions altered.

4.2.2 Amplification of the Precession Signal

The voltage induced in a coil of N turns enclosing a sample of volume V, is given by Fairi and Svelto (1962) as;

$$E = \frac{\chi \mu_0 w \eta N^2 iV}{\sqrt{2}\, b^2}$$

where χ = nuclear paramagnetic susceptibility of protons in water,

μ_0 = permeability of free space,

w = angular frequency of the precession signal,

i = polarizing current (polarizing field assumed at right angles to the earth's field),

b = coil length,

η = factor which depends on the ratio of radius to length of the coil.

For a coil of 1000 turns enclosing a sample volume of a litre and polarized by a current of 2 amperes, the theoretical signal voltage is a few microvolts.

In practice the maximum obtainable signal may be less than this for the following reasons.

(1) The polarizing field is not reduced to zero instantaneously as assumed in the derivation.

(2) The polarizing field is not normally at right angles to the ambient field.

(3) The magnetization produced in the sample approaches its maximum value exponentially, so that in practice it may be considerably less than the theoretical value.

(4) The signal decays exponentially with a time constant T_2. Although this is approximately 3 seconds for protons in pure water in a uniform field, it may be considerably reduced by impurities in the water, particularly small quantities of paramagnetic ions, and by local field gradients.

The apparatus must therefore be able to detect signal levels of approximately 1 microvolt. This voltage level must then be amplified to several volts so that the frequency can be measured. A total gain of at least 10^6 is therefore required. For reliable frequency measurements the signal-to-noise ratio at the amplifier output must be reasonably high.

Because of the large number of turns of the signal coil, any stray fields in the vicinity will induce an e.m.f. in the coil which will be amplified and recorded by the counter along with the precession signal. Although at sea this is not a major problem, on land it is, since effective shielding, particularly from power frequencies, is very difficult. The signal-to-noise ratio can be improved by tuning the coil and amplifiers to the precession frequency. The reduction of the bandwidth however, necessitates continual tuning when the magnetometer is used in areas where considerable variations occur in the magnetic field. In practice a compromise must be made to ensure a sufficiently good signal-to-noise ratio to obtain consistent frequency measurements, while reducing the necessary tuning adjustments to a minimum.

4.2.3 Frequency Measurement of the Precession Signal

(a) The conventional magnetometer

Having obtained the required amplification of the precession signal, its frequency must then be measured to the required accuracy. An accuracy of 10 gamma is sufficient for normal use at sea, since the anomalies of interest usually have amplitudes of several hundred gamma. To obtain this accuracy in a field of 50,000 gamma requires a frequency measurement of 1 part in 5,000. Because of the decay of the signal, the measurement must be made in less than a second. Since the precession frequency is around 2.5 kc/s direct counting of the signal will not give the required accuracy. The normal method of determining the frequency is to use the precession signal to gate a counter connected to a high frequency oscillator (100 kc/s or more). In this way the time for a set number of cycles of the precession signal can be measured to the required degree of accuracy. The precession frequency, and hence the magnetic field, can then be calculated.

(b) The direct reading magnetometer

Although it is normal to measure the period of the precession

signal as described above, it would be more convenient to obtain a reading of the field directly. This could be done if the frequency of the signal could be measured directly to the required accuracy, since to obtain the field from the frequency only requires multiplication by a constant factor. Such a multiplication factor can easily be built into the counter so that the readout given by the counter is in gamma rather than in cycles per second.

The problem is to measure a frequency of approximately 2.5 kc/s to an accuracy of 1 in 5000, in a time less than 1 second. Since the field is given by $F = \frac{2\pi f}{\gamma_p}$, the period of the precessional signal is $\frac{2\pi}{F\gamma_p}$, and the required counting time for a direct reading to the nearest 10 gamma is $\frac{2\pi 10^4}{\gamma_p} \doteq 2.35$ seconds, as the counter can only count whole cycles. This counting time could be reduced if the frequency of the signal could be increased in some way. For example, if the frequency could be multiplied by a factor of ten, then the required counting time would be reduced by the same factor of ten. Such a method of obtaining a direct frequency count without requiring a long counting time, is used in the present magnetometer. In this particular case the frequency of the precession signal is multiplied eight times in the main amplifier. This means the required counting time is reduced to 0.29362 seconds for an accuracy of 10 gamma. This has proved to be a reasonable counting time for use at sea, but is somewhat long for use in the vicinity of buildings where the gradient is such that a relaxation time of less than 1 second is often obtained.

4.2.4 Recording of the Field Value

For continual use at sea some form of recording the field values obtained by the counter is required. An analogue presentation of the field versus time is the most convenient form of presentation. Since the counter gives a binary digital output, this must first be converted to the decimal system and then recorded in analogue form on a chart recorder. The simplest method of obtaining a decimal analogue readout

from the counter is to put a relay circuit in each of the binary outputs of the counter which are to be recorded, and arrange for these to switch in standard resistors in a potentiometric circuit across which the recorder is connected.

4.3 The Magnetometer Circuitry

A block diagram of the complete magnetometer may now be drawn. Such a diagram is shown in figure 3. A description of the circuitry of the individual parts of the magnetometer will now be given.

4.3.1 The Preamplifier

It has already been shown that a total gain of 10^6 is required in the amplifiers. To ensure a stable system it is preferable to make the amplifier in two parts; a preamplifier, which may be incorporated in the fish towed behind the ship, and a main amplifier which contains the main filter and multiplication circuits.

The main problem associated with the amplification of the precession signal is to obtain a satisfactory signal-to-noise ratio. To reduce noise generated in the amplifiers and that picked up from stray fields, a narrow bandwidth is used.. However this has little effect on noise pulses of the type generated in the cable connecting the coil in the fish to the amplifiers on the ship. A cable of at least 100 yds. is required to ensure the ship's magnetic field is negligible at the sample. Since the cable is continually moving through the water considerable microphonic noise is generated by it, and this appears at the amplifier input along with the wanted precession signal. The amplitude and quantity of this cable noise depends on the cable used. With careful design and construction of the cable the noise generated may be reduced to a very low level. However commercial cable normally available is very microphonic. To improve the signal-to-noise ratio at the ship end of such a cable, the precession signal must be amplified before leaving the fish. Incorporating the preamplifier in the fish has a number

of practical disadvantages.

(1) Power must be supplied to the preamplifier either by a battery in the fish or via the cable.

(2) Tuning of the preamplifier and coil is difficult.

(3) The preamplifier must be situated sufficiently far from the bottle containing the water sample that the effect of any magnetic material, e.g. the switching relay, is negligible.

(4) The fish must be exceptionally well sealed.

Hill (1959) has used a system in which the preamplifier is in a second fish connected to the main fish containing the bottle by a 3 metre length of screened cable. In his arrangement the coil is tuned by a stepping relay in the preamplifier fish. Christoffel (1961) used a similar arrangement but with the bottle and preamplifier mounted in a single long fish.

Because of the greater simplicity of the shipboard preamplifier this was the system first used. However it was found that without special non-microphonic cable the noise level was too high to obtain reliable counts. A preamplifier was therefore constructed for incorporating in the fish.

The circuit of the preamplifier used, together with the input and switching circuitry, is shown in figure 4. The relay, Re, used to switch the coil from polarizing line to preamplifier, is the only magnetic material used in the preamplifier. It was found that a distance of 30 inches between coil and relay was sufficient for the latter to have a negligible effect on the precession signal. The preamplifier and coil could therefore be included in a single 3 ft. fish. To overcome the problem of tuning the input the coil is damped by resistor R_2, so that a single value of the tuning capacitor C is sufficient to cover the range of frequencies between New Zealand and Antarctica. The input stage of the preamplifier uses one of the 12 volt series of valves. The reason for this is that, should the preamplifier be connected to the coil before the

polarizing transients have decayed, it will be subjected to large voltage transients*. These would destroy a transistor. Hence if a transistor is used, it must be safe-guarded by a device which will protect the transistor and at the same time will not increase the input noise level if subjected to transients as high as several hundred volts. A valve will recover from such transients in a very short time without any appreciable after effects. On the other hand a valve requires a relatively large current for its filament. The filament supply should therefore be on the ship where it can be easily changed. The gain of the preamplifier was approximately 500 over a frequency range of 1-4 kc/s. Outside this frequency range the gain decreased rapidly. Even so the equivalent input noise level was almost 10 microvolts. Figure 5 is a photograph of preamplifier and relay mounted ready for assembly in the fish.

To supply the preamplifier and coil with power, and get the signal back to the ship, requires a total of five leads to the fish. The conductors are used as follows: (1) polarizing supply for the coil, (2) supply for the switching relay, (3) supply for the preamplifier, (4) preamplifier output, (5) earth return for all leads. It is necessary to have separate supply lines for the relay and coil since, if the relay is across the coil during the collapse of the polarizing field, it will considerably increase the time taken for the field to decay and hence reduce the precession signal. A 4-conductor screened cable which was obtained locally has been found satisfactory, the screen being used as the earth return. The use of the screen for carrying power and signal introduces some noise into the system, particularly after the cable has been used for some time. This presumably arises from movement of the woven wires making up the screen. Experience has shown that the use

* These switching transients can be practically eliminated by a modification of the normal switching circuit. This problem is therefore largely overcome and a satisfactory all transistor preamplifier has been constructed and used successfully (see Appendix 1).

of the screen for carrying power or signal should be avoided if possible. Unfortunately no other more suitable cable, which was also strong enough to take the towing strain, was available.

4.3.2 The Main Amplifier and Frequency Multiplier

This consists of a tuned amplifier followed by a frequency multiplier to multiply the frequency of the precession signal eight times.

Tuning of the amplifier is accomplished by a twin-T network in a negative feedback loop around the second amplifier stage. The twin-T network has the characteristic of passing all frequencies except that given by the null condition. Since it is in a negative feedback loop, all frequencies except the null frequency will be highly attenuated in the amplifier. With high gain in the loop a high 'Q' is obtainable for the tuned circuit. Advantages over the normal L-C tuning are that a continuously variable centre frequency may be obtained, even at low frequencies, and also a variable bandwidth, the latter simply by varying the feed-back applied across the stage. To vary the frequency of the twin-T network a 3-ganged element is normally required. The circuit shown here uses a single differential capacitor as tuning element. This variation was pointed out by Dunn (1951).

Frequency multiplication is accomplished by a series of doubler stages. The normal methods of frequency multiplication require highly tuned circuits and so are unsuitable when the input signal is varying over a wide frequency range as in the present application. The present circuit uses the fact that a full-wave rectifier doubles the fundamental frequency of an input sinewave. Hence the frequency range of this doubler circuit is unlimited.

The circuit of the first two stages is shown in figure 6a. A low pass filter is included between the two stages to reduce the harmonics generated by the rectification process. This is necessary to ensure a uniform output waveform from the second doubler. For this particular application no adjustment of the filter is required since the frequency

range we are interested in is only 2-3 kc/s. The cut-off frequency of the filter can therefore be set above the highest frequency required, and still attenuate the harmonics of the lowest frequency sufficiently. In the present case the cut-off frequency was set at 6 kc/s, and the frequency of 'infinite' attenuation, given by the resonant frequency of the parallel L-C combination, at 10 kc/s.

For the third doubler stage use was made of the Schmidt trigger included after the two full-wave rectifier stages. The inclusion of the Schmidt trigger in the amplifier is advantageous, since it provides a constant output for all input signals above a specified level and rejects all others. Hence it can be set to discard all noise below a specified level and will convert the decaying precession signal into a constant amplitude output signal, thus providing a specified voltage level for the frequency counter to accept. In the present circuit, figure 6b, the doubling action is obtained as follows. The output from the Schmidt trigger is a square wave of constant amplitude. This is differentiated, providing a positive and negative pulse for each cycle of the input wave. The positive pulses are fed to an inverter amplifier, appearing as negative pulses at the output. The negative pulses from the differentiator bypass the inverter and are added to the pulses from the inverter at the final amplifier stage. Hence at the final amplifier input, two negative pulses are obtained for every cycle of the waveform at the input of the Schmidt trigger. Thus a frequency doubling action is obtained. The amplitude of the pulses is of such a magnitude as to completely saturate the final amplifier stage, so that a 12 volt peak to peak square wave output signal is obtained.

The complete amplifier circuit is shown in figure 7. Included in the circuit is a sound channel feeding a small speaker. This is invaluable for monitoring the precession signal and tuning the amplifier. The total gain of the circuit is 10^4, a 1 mv signal at the input being sufficient to trigger the Schmidt trigger with the gain control turned

right up. The bandwidth is variable over the range 100-1000 c/s and the centre frequency over the range 1.8 - 3.0 kc/s. The total current drain for the circuit is 20 ma and this is reduced to 10 ma with the OC72 speaker output stage switched off.

4.3.3 The Frequency Counter

It has already been pointed out that the frequency counter will give a reading of the magnetic field directly in gamma if it counts the multiplied precession signal for a time of 0.29362 seconds. The frequency counter therefore consists of an ordinary decade counter whose counting time is controlled by an accurate time device which allows it to count the input signal for a period of 0.29362 seconds each time a signal is received from the fish. Provision must be made for discarding the first few counts from the fish, since these may contain switching transients and other 'noise' associated with the switching of the coil from polarizing line to preamplifier input.

A block diagram of the complete counter unit is given in figure 8. The operation of the counter is as follows. During the polarizing period of the magnetometer cycle, counter A is reset to 9,000, counter B to 100,000 - 29,362 i.e. 70,638, and gate A to open. Gate B is initially closed. On completion of the polarizing period the reset line is opened and counter A begins to count the signal from the amplifier. On reception of the 1,000th count, counter A sends a pulse to open gate B, allowing the 100 kc/s crystal oscillator signal to be passed to counter B. When counter B has received 29,362 counts from the oscillator it in turn sends out a pulse which closes both gates and so stops any further counts from entering counter A. The reading given by counter A is then the field value in units of 10 gamma. Provision is made for changing the initial reset count of counter A from 9,000 to 8,7,6, or 5,000, thus discarding 1,2,3,4, or 5,000 counts respectively. Provision is also made for setting the reset value of counter B to any value between 0 and 99,999, thus providing a counting time of from

1 second to 10^{-5} second. This adjustment of the reset value of the counters is made possible by bringing out the reset lines of the binary units in each decade concerned to a 4-pole 10 position switch. Thus each of the decade units can be reset to any number between 0 and 9.

All binary, decade, and pulse shaper units used were from the range of Philips circuit blocks. The oscillator circuit is of standard design and is shown in figure 9.

4.3.4 The Recorder Readout Unit

The basic potentiometric readout circuit to obtain an analogue presentation of the last two counter decades is shown in figure 10a. The chart recorder is connected across R. The current through R, and hence the voltage drop across it, is determined by which of the switches S_1-S_8 are closed. S_1-S_4 are operated by binary units 1-4 making up the first decade of the counter, and S_5-S_8 by the four binary units in the second decade. The switches are controlled by the state of the binary unit to which they are connected. By having the resistors R_1-R_8 in the correct ratio the current through R can be made proportional to the counter reading. The resistor R is made variable to allow adjustment of the full-scale reading.

Initially Philips relay units (consisting of a relay plus a switching amplifier) were used for the switches S_1-S_8. These however proved unreliable as well as being bulky and requiring their own power supply. They have now been replaced by the silicon transistor switch shown in figure 10b. This switch is designed to run off the counter supply. The complete two-decade readout fits on a printed board 4 inches square. The potentiometer in the emitter circuit is used to adjust the current through each switch when in the on condition, and hence to adjust for the correct current through the readout resistor R. The leakage current through these transistors is so low that they behave as practically perfect switches. During the polarizing and counting period the recorder is returned to zero by opening the supply line to resistor R with a relay in the switching unit. When the counter has

completed a count the relay contacts are closed and the recorder reads the value obtained.

4.3.5 The Switching Unit

A convenient cycling time for the magnetometer at sea is about $\frac{1}{2}$ minute. This means the switching unit must send a polarizing current of several amperes to the coil once every $\frac{1}{2}$ minute. To obtain a strong precession signal the polarizing time must be long compared to the spin-lattice relaxation time of the protons. A polarizing time of 10 seconds is convenient. At the end of the polarizing period the field must be reduced rapidly to zero and the preamplifier input switched on to the coil. As well as this, provision must be made for resetting the counter during the polarizing period, and the recorder during the polarizing and counting periods. The circuit of the switching unit is given in figure 11. This is the conventional circuit except for the addition of the relay in the fish (see for example Waters and Francis 1958). The microswitch S_2 controlling the polarizing relay is operated by a cam on a 1 rev/min synchronous motor. Relays Re_2 and Re_3 are slugged to delay their opening. Re_2 has a short delay (20 ms), Re_3 a much longer delay ($\frac{1}{2}$ min.) so that it does not open until the counter has completed a count.

As already mentioned a serious cause of trouble with the proton magnetometer is the large transients which occur when the polarizing current is broken. This causes arcing at the relay contacts, as well as possible damage to the input stage of the preamplifier. Also, because of the transients circulating in the coil, the polarizing field is not reduced to zero instantaneously, and the precession signal is reduced. On the other hand, if the polarizing current is decreased to reduce these transients, the precession signal is also reduced since the magnetization produced in the sample is proportional to the polarizing field.. A simple variation of the circuit shown in figure 11 has been found to overcome this problem and greatly improve the

precession signal. Instead of using the microswitch to switch the current to the relay as in the figure, it is used to switch the primary current to the supply transformer, i.e. a microswitch is used for S_1. On opening S_1 the current to the coil decays relatively slowly at first, the rate of decay being controlled by the amount of filter capacitance in the circuit. During this part of the decay the protons are able to follow the resultant field direction because the rate of change is sufficiently slow. However when the supply voltage has fallen below the holding voltage for the main relay the current to the coil is suddenly broken, the polarizing field is removed, and precession about the ambient field direction occurs. Measurements on the coils used show that the current falls to about 0.2 amperes before the relay drops out. The polarizing field at this instant is still about 20 oersteds, so that the resultant field direction has changed very little. Under these conditions no arcing occurs at the relay contacts and what transients do still remain can be easily damped out. The precession signal obtained is due to the magnetization produced by the maximum polarizing field applied so that no reduction in signal occurs.

Included on the switching unit chassis is the power supply for the amplifier and counter. The circuit of this is given in figure 12.

4.3.6 Design of the Fish

Three main problems occur in the design of the fish. These are (1) it must be effectively sealed to keep out sea-water, (2) it must be fairly simple to strip down, (3) it must tow smoothly through the water at speeds of up to 12 knots, without any spinning or jerking that will cause wear on the towing cable.

An exploded view of the fish is given in figure 13. With the P.V.C. casing used some difficulty was experienced with sealing the fish, particularly when using them in the cold Antarctic waters. Most of this trouble would probably be overcome by using a high pressure P.V.C. casing. Wear on the towing cable has been reduced by

reinforcing it where it enters the fish with a length of rubber sleeving, and also by stabilizing the fish with a 10' x 1' length of canvas tail. The canvas tail has proved very effective. Without it failure of one or more of the conductors occurred within 2-3 days. Since the tail has been used one fish has had six weeks in the water at towing speeds of up to 13 knots without any appreciable cable wear occurring.

Figure 14 is a photograph showing the layout of the coil and preamplifier in the fish.

4.3.7 Coil Design

Fairi and Svelto (1962) have given equations for determining the dimensions of a coil for optimum signal-to-noise ratio. For use at sea the coil dimensions are largely determined by the size of the fish. A reasonably large water sample is preferable to obtain as large a precession signal as possible. Since field gradients at sea are very small a long bottle may be used. The number of turns in the coil determines both the induced signal and the required current to produce a specified polarizing field. The coils used consisted of approximately 2,000 turns around a sample volume of approximately 600 cm^3. The length of the coils was 25 cm.

4.3.8 Absolute Accuracy of the Magnetometer

The absolute accuracy of field measurements obtained with the magnetometer depends on the accuracy of the frequency measuring system. This is primarily determined by the time for which the counter gate is open. Because of the fast rise-time of the pulse from the counter which operates the gate ($\sim 0.5 \mu$sec) there is little likelihood of any appreciable error arising from variations in the gating level of the gate. The stability of the 100 kc/s crystal is given by the manufacturers as 2 parts/10^6/$^\circ$C. Thus a temperature variation of 20°C would only cause an error of 2 gamma in the field value. Errors in the timing counter represent only 1 or 2 gamma. This includes the possible error in the value for the gyromagnetic ratio. Thus the

absolute accuracy should be well within the reading accuracy of ± 10 gamma (i.e. ± 1 count).

A further factor which will affect the field values obtained is the magnetic field of the ship. Bullard and Mason (1961) conclude that if the sample is more than two ships' lengths astern of most ships the magnetic disturbance is less than 3 gamma. In the case of H.M.N.Z.S. Endeavour experiments carried out on the ice beside the ship have shown that the effect of the ship is certainly less than 10 gamma for a towing distance of 250 ft. or more.

4.3.9 Performance

During each of the trips with the magnetometer some improvements have been made. Although some improvements are still required to make the equipment completely reliable and able to be run continuously by technicians or research assistants with little prior experience, it is now developed to such a stage where it is possible to obtain extremely good precession signals, and hence accurate magnetic profiles, over long periods of time. Figure 15 is an oscilloscope photograph of the precession signal obtained on the return trip in February 1965. This signal was initially recorded on magnetic tape with a microphone held close to the amplifier speaker. Although some deterioration of the signal has occurred due to the recording of background noise and subsequent replaying through the oscilloscope, the decay envelope is clear. As can be seen the signal lasted for a good eight seconds before being lost in the noise. Figure 16 is a photograph of part of the record obtained on this trip. Over the whole 2,000 miles of return trip the only miscounts that occurred were due to a flat preamplifier battery. A total of $1\frac{1}{4}$ hours of record was affected in this way and most of this was still quite readable. These results indicate the advantages of using a preamplifier in the fish.

CHAPTER 5

THE SEISMIC PROFILER

5.1 Principle

The seismic profiler is essentially a high power echo-sounder which, by virtue of its low frequency sound source, can penetrate the sediment layers of the ocean floor and thus provide information on sediment layering and basement topography. A hydrophone, towed behind the ship, is used to receive the weak echoes from the bottom and sub-bottom layers. Since the profiler receiver is required to have a fairly wide bandwidth, it is necessary to obtain a quiet hydrophone while still proceeding at normal cruising speed. The echoes received by the hydrophone are normally recorded as a function of depth and position on an electro-sensitive paper recorder, similar to that of a normal echo-sounder. Recording the echoes in this way facilitates correlation from shot to shot. Ewing and Tirey (1961) have described a profiler which they have used for refraction and reflection work, while Hersey and Knott (1963) have described profiler equipment used by personnel of the Woods Hole Institute.

5.2 The Sound Source

To obtain sediment penetration of several kilometres it is necessary to use a high energy, low frequency sound source. Four types of sound source have been used with some success. They are; (1) explosives, (2) sparker, (3) boomer, (4) gas-gun.

Explosives were used in the original work of this kind but they have three main disadvantages. (1) They are somewhat dangerous to use. (2) Unless floated near the surface the sound pulse is prolonged due to bubble pulses and surface echoes, hence reducing the possible resolution. (3) Large numbers are required in order to cover a

reasonable area with closely spaced shots, and so obtain good data density. On the other hand they have the advantage of requiring no elaborate installations.

The sparker (Knott and Hersey, 1956), a high tension spark discharged under water, has been used successfully in shallow water regions (Beckmann et al., 1959). High energy sparkers have also been used with some success over deep ocean regions (Hersey, 1963). They are however a very inefficient sound source (~ 0.07% of the electrical energy converted to sound energy, Anderson, 1953), and thus require a very high electrical energy (up to 25,000 joules) to obtain appreciable sediment penetration in deep sea regions. Because of the high electrical energies required the spark contacts require renewing after several hours use.

The boomer was developed by Edgerton and Hayward (1964). A large current is passed through a flat coil between two aluminium plates. Eddy currents induced in the plates cause them to fly rapidly apart, producing a cavitation volume between the plates which acts as the sound source. This device has been used with considerable success in deep water but like the sparker requires large electrical energies (13,000 joules) to obtain appreciable penetration.

Various types of gas-guns have been developed for use with continuous seismic profilers. The earliest of these relied on the explosion of a mixture of propane and oxygen (Beckmann et al., 1959), or some other explosive gas mixture. Zaunere and Ewing (1963) described a gun using a diesel and air mixture. More recently the possibility of utilizing a burst of high pressure air released from a fast acting valve has been investigated by Ewing and Zaunere (1964). This idea has the advantage of being comparatively simple and since it only requires a supply of high pressure air, it is both reliable and safe.

During the trips in December 1963 and February 1965 hand grenades were used as a sound source. The use of an explosive source

in the early stages of this work was preferred since no elaborate installations were required. Hand grenades are a convenient explosive to use on a ship, and in fact the only type that was permissable when H.M.N.Z.S. Endeavour was carrying fuel. However they have the disadvantage that with a seven second fuse they sink to a depth of about 150 ft before exploding. This means that the sound pulse is complicated by both a bubble pulse, which is dependent on the depth at which the grenade explodes (Arons and Yennie, 1948) and also a reflection from the surface of the water. Figure 17 is an oscilloscope photograph of a grenade shot received by the hydrophone array. The sound pulse consists of three major groups of waves, each lasting approximately 0.05 seconds. Each major group of waves is made up of 8 or 9 waves with periods of approximately 0.006 seconds. Such a sound pulse causes considerable confusion in the reflected signals received from the different layers. For this reason an air-gun along the lines described by Ewing and Zaunere (1964) has been constructed for use on future trips. The gun, figure 18, acts essentially as a fast acting valve which allows a burst of air at a pressure of 3000 p.s.i. to escape into the water, thus generating the sound pulse. Immediately after the air is released the low pressure air in the larger cylinder returns the piston to its firing position ready for another shot. With careful adjustment of the pressures in the two supply lines, and the rate of supply of air, the time interval between shots can be controlled over a reasonable range; from 10-60 seconds for example. Provision for the installation of a 3000 p.s.i. compressor unit is being made aboard H.M.N.Z.S. Endeavour. The use of the gun has however been restricted to times when the ship is not carrying JP-4 jet aircraft fuel.

5.3 The Hydrophone Array

One of the difficulties in receiving the weak echoes from the sub-bottom layers is to ensure a quiet hydrophone so that a reasonable

signal-to-noise ratio is obtained. One method, used with limited success on the first trip, is to slacken off the hydrophone cable for each shot (Ewing and Tirey, 1961). This allows the hydrophone to sink slowly during the listening period, thus eliminating the majority of the flow noise. The method requires a winch, capable of hauling in 600 ft of cable between shots, which will allow the cable to pay out freely during the listening period. Unfortunately the winch that was available on H.M.N.Z.S. Endeavour was not suitable and proved to be a constant source of trouble.

A second method of reducing towing noise in the hydrophone, and one which has become standard practice in the last two years, is to use an array of hydrophones enclosed in an oil-filled plastic hose. The streamlining effect of the plastic hose itself reduces the flow noise. A further reduction in noise is obtained by arranging the outputs of individual hydrophones to add for the near vertical travelling echo, while tending to cancel for the nearly horizontally travelling noise signals. An array of hydrophones connected in parallel will produce the desired signal-to-noise improvement. The spacing of the elements and overall length of the array will depend on the desired signal frequency range (Edgerton and Hayward, 1964).

Two different arrays have been used in the present work. The first of these used five Hall-Sears type MP4 hydrophones enclosed in a 60 ft length of 2 inch diameter hose while the second used the much smaller MP7 hydrophones enclosed in a 1 inch diameter hose (Figure 19). The smaller diameter array proved the most successful and enabled sub-bottom reflections to be obtained in water depths of 1000 fathoms with the ship travelling at a speed of 10 knots.

5.4 Profiler Electronics

Some experimentation has been carried out with the profiler electronics. The basic requirements are:

(1) a high gain low noise amplifier capable of amplifying frequencies down to 20 c/s,

(2) a variable bandpass filter for improving the signal-to-noise ratio in the desired frequency range,

(3) a variable density recorder and print amplifier for plotting the results continuously as received,

(4) a tape recorder for recording the signals on magnetic tape to facilitate analysis of the data back in the laboratory.

Some form of signal compression is required in the print amplifier to extend the dynamic range of the electro-sensitive paper.

In the equipment used so far the tape-recorder amplifier has been used as the main amplifier. It has been found however that the incorporation of a preamplifier in the hydrophone array would greatly improve the signal-to-noise ratio. A number of Philips integrated circuit amplifiers type OM200 have been obtained for this purpose. These units are capable of a power gain of 80 db and require 1 ma at 1.3 v to run them. The preamplifier and battery can easily be installed in the plastic hose enclosing the hydrophone array.

A block diagram of the profiler which will be used on future trips is shown in figure 20. A variable delay is incorporated in the trigger circuit to enable the stylus to be delayed for a specified time after the shot-instant before starting its sweep, thus providing an expanded scale in deep water regions. The microphone input on the tape-recorder mixer amplifier is used for coding the magnetic tape. A 1 kc/s signal is fed on to the second track of the tape-recorder to provide automatic speed control of the recorder on playback. The standard 50 c/s 230 volt supply has been described by Ross and Goodger (1965).

An obsolete asdic recorder, obtained from the New Zealand Navy has been adapted for recording the signals received from the

hydrophone array. The main modification has been the replacement of the D.C. motor which drove the paper and stylus in the asdic recorder by a synchronous motor. This can be driven off the ship's 60 c/s supply, or if greater accuracy is required, off the standard 50 c/s supply. A number of different types of electro-sensitive paper have been tried. Muirhead mufax recording paper has proved to have a reasonable dynamic range. The amplifiers designed for use with this paper are shown in figure 21. The maximum gain of the amplifiers is 10^5. 30 db of compression is available in the compression amplifiers. Also included in this figure is the circuit of the trigger used to engage the magnetic clutch that operates the stylus. This circuit uses the Philips series 10 circuit blocks and has a variable delay of from 0-8 seconds in four steps. Two sweep speeds are available on the recorder, 3 in/sec and 1 in/sec. The flyback switch automatically resets the trigger relay at the end of the sweep so that the stylus is returned to its starting point ready for the next shot.

5.5 Results Obtained with the Seismic Profiler

The use of hand grenades as a sound source has enabled experience to be obtained with different types of hydrophone and enabled suitable methods of obtaining a system quiet enough for the reception of the weak signals to be designed. However, useful profiles of any appreciable length have not so far been obtained.

A 5-10 minute shot schedule was used on the trips. This interval is too long to ensure reliable correlation from shot to shot, particularly when the records are poor. Because of the factors already mentioned it is almost impossible to obtain good clear reflection records using hand grenades as a sound source.

Figure 22 shows two successive reflections obtained over the Campbell Plateau. The time interval between these two shots was 5 minutes. It is difficult to trace sediment layers from such records although there are definite indications of a deepening of the reflectors

from (a) to (b). The strong sub-bottom reflector on (a) is absent from (b) indicating a considerable increase in depth of this reflector between the two shots. This is in agreement with the magnetic records which suggest considerable basement relief across the Plateau.

CHAPTER 6

BATHYMETRIC AND MAGNETIC RESULTS

6.1 Introduction

Tracks on which results presented in this chapter were obtained are shown on the map of figure 23. Bathymetry profiles were obtained over tracks b, d, e, h, and j. Total field profiles were obtained over the greater part of all tracks. Those on tracks b, d, h, and j, were obtained with the magnetometer described in chapter 4. Those on other tracks were obtained as follows.

Tracks c and f: Dr. D. A. Christoffel (1961, Adams and Christoffel, (1962).

Tracks a and e: Unpublished results obtained by personnel in the Geophysics Division of the Department of Scientific and Industrial Research and kindly lent for the present work by Dr. T. Hatherton.

Tracks g and i: Results obtained by American scientists aboard the icebreaker U.S.N.S. Staten Island during 1961 and published by the U.S. Navy Hydrographic Office (1962).

6.1.1 Navigational Errors

In comparing results obtained on different tracks and plotting structural trends from the records, the most important errors that occur are due to difficulties involved with accurate navigation. This is particularly so south of 55^{o}S, as weather conditions in these regions often make astronomical observations impossible for periods of 2-3 days or more.

In drawing the tracks and computing the ship's hourly position for the reduction of the results, a straight course between two reliable astronomical fixes was assumed unless a change of course was indicated in the ship's log book. The actual distance travelled in each hour was then calculated by correcting the hourly log readings by a

factor which was the ratio of the actual distance between the two fixes and that shown by the log. In this way the majority of errors occurring are smoothed out over a reasonable distance.

From an analysis of tracks which cross, or are close to each other, it would appear that while errors of 5-10 miles do still occur, appreciably larger errors rarely, if ever, occur.

6.1.2 Time Fluctuations of the Magnetic Field

The magnetic field measured at any point is not constant but continually changing. Two distinct types of change occur; transient fluctuations, and long term secular changes. The transient fluctuations arise from causes outside the earth. Since the periods of these fluctuations range from very short periods to periods of a few days, they may produce anomalies on the magnetometer records which are indistinguishable from anomalies produced by variations in crustal structure. The secular variation on the other hand is due to causes within the earth and has a period of 500-1000 years. Hence the secular variation can only be observed by comparing results over a period of years.

The short period fluctuations may be removed from the observed records if magnetograms from a nearby magnetic observatory are available. In the present investigation these were available from Amberley and Scott Base. It is however unlikely that either of these records represent the fluctuations occurring over the 2000 miles of intervening sea. Direct subtraction of large variations from the records is therefore impossible. The records from Scott Base probably represent the maximum fluctuations over the region because of the high latitude of the station (78°S), and can therefore be used as a control. It is safe to assume that time variations over the greater portion of the tracks will be considerably less than these. For example, the diurnal variations at Amberley are some twenty times less than those at Scott Base. Also in oceanic surveys such as the present, only

Table 1.

K_p, C_i, C_p, A_p, K_{Fr}, R_z, and Selected Days, December 1963

Day[1]	3-hr Range Indices K_p[2]								Sum	Prel.[3] C_i	C_p[4]	A_p[5]	3-hr Range Indices K_{Fr}[6] Values	Sum	Prov.[7] R_z
	1	2	3	4	5	6	7	8							
1 q	1+	1−	1o	1−	1−	2+	1o	2+	10o	0.2	0.2	5	1011	1212	9	22
2	2o	3−	2+	1+	3+	3+	3−	3o	21−	0.9	0.7	12	1221	3323	17	21
3 D	4−	4+	6−	4+	5−	4o	4+	5−	36−	1.4	1.4	36	3454	4334	30	20
4 D	3+	4+	4o	3−	4−	4−	4−	5o	30+	1.2	1.2	25	3442	3325	26	20
5 D	5−	4o	3o	3+	4+	4o	5−	4o	32o	1.3	1.2	28	4422	3343	25	20
6 D	4−	4o	4−	3−	4+	4o	4−	4−	30−	1.2	1.1	23	4432	3333	25	16
7	3+	3o	3o	3o	4−	3o	3−	2o	24−	0.8	0.8	15	3322	3321	19	14
8	3−	4−	3+	3−	3+	3o	3−	2o	23+	0.8	0.8	14	2442	3222	21	13
9	1o	2o	3−	3o	3−	2o	0+	0o	14−	0.3	0.4	7	0123	2111	11	33
10 Q	0o	0o	0+	0o	0o	0o	0o	0o	0+	0.0	0.0	0	0000	0000	00	24
11 Q	0o	1−	0o	0+	1−	0+	0+	0+	3−	0.0	0.0	2	0100	1101	4	23
12 q	1o	0+	0+	1−	0+	0o	1−	3−	6o	0.1	0.1	4	1011	0003	6	13
13	3o	3+	1o	1+	1o	1−	2−	1+	13+	0.3	0.4	8	2311	1111	11	8
14	1o	1+	2−	1+	3+	4−	3o	3o	18+	0.7	0.6	11	1212	3333	18	7
15	2o	2−	2+	2+	2−	2+	2o	1o	15+	0.3	0.4	7	1122	2221	13	0
16	3−	2−	1−	1o	1+	3−	1+	2−	13o	0.3	0.3	7	2111	1212	11	0
17 q	2+	0o	1o	0o	0+	1o	1+	1o	7o	0.1	0.1	4	2000	1121	7	7
18 Q	1−	0o	1−	1o	0+	0o	0o	1−	3+	0.0	0.0	2	1011	1000	4	17
19	0o	0o	0o	0o	1−	2−	1+	4−	7+	0.3	0.2	4	0000	1224	9	8
20 D	3+	3+	5−	3o	3+	3−	4o	3o	27+	1.2	1.0	20	2333	3232	21	17
21	1o	1+	3−	2−	2+	3+	2−	4o	18o	0.8	0.6	11	1122	2213	14	11
22	2−	3−	3o	2+	4−	2o	3+	3−	21+	0.8	0.7	13	1332	3122	17	11
23	1+	1+	4−	3+	0+	3+	3+	3+	20o	0.9	0.8	13	1244	0323	19	9
24	3+	2−	1−	0+	2o	3o	3o	3−	17−	0.6	0.5	10	2100	2222	11	16
25 Q	0o	0o	1o	3−	1−	0+	0+	0o	5o	0.0	0.1	3	0012	0000	3	8
26 q	0+	2o	1−	1o	1−	1−	1−	2−	8−	0.1	0.1	4	1201	0111	7	7
27 q	1+	1+	2+	0+	2−	1−	1−	0+	9−	0.1	0.2	4	1220	2111	10	0
28	2−	2−	3+	2−	1+	2o	4−	3+	19−	0.7	0.6	11	1231	1133	15	0
29	4−	2o	2o	4o	4−	4−	3+	2+	24o	1.0	0.9	17	3224	4322	22	0
30	2+	1+	0+	1−	2o	2o	1−	2−	11o	0.3	0.2		2100	1101	6	0
31 q	1o	0+	1−	1−	1−	0+	0o	1+	5o	0.1	0.0	3	0001	0001	2	0
									Means	0.53	0.50	11				11.8
									No. of days	31	31	31				31

[1] Five quiet days (Q), ten quiet days (Q or q), five disturbed days (D) selected by Committee on Characterization of Magnetic Disturbances, J. Veldkamp, Kon. Nederlandsch Meteorologisch Institut, DeBilt, Holland.

[2] Geomagnetic planetary 3-hr range indices K_p prepared by Committee on Characterization of Magnetic Disturbances, J. Bartels, Chairman, University, Göttingen, Germany.

[3] Preliminary magnetic character figures C_i prepared by J. Veldkamp.

[4] Magnetic character figures C_p prepared by J. Bartels.

[5] Average amplitudes A_p (unit 2 γ) prepared by J. Bartels.

[6] Fredericksburg 3-hr range indices K ($K9$ = 500 γ); scale values of variometers in γ/mm: D = 2.75, H = 2.45, Z = 3.00, prepared by J. V. Hastings, Observer-in-Charge, Fredericksburg Magnetic Observatory, Corbin, Virginia.

[7] Provisional sunspot numbers (dependent on observations at Zurich Observatory and its stations at Locarno and Arosa) prepared by M. Waldmeier, Swiss Federal Observatory, Zurich, Switzerland.

Table 2.

K_p, C_i, C_p, A_p, K_{Fr}, R_z, and Selected Days, February 1965

Day[1]	3-hr Range Indices K_p[2]								Sum	Prel.[3] C_i	C_p[4]	A_p[5]	3-hr Range Indices K_{Fr}[6]		Prov.[7] R_z
	1	2	3	4	5	6	7	8					Values	Sum	
1 q	3−	2o	1o	1o	0o	0o	0o	0+	7o	0.1	0.1	4	3211 0001	8	14
2 Q	0+	2−	1−	0o	0o	0+	1−	1o	5−	0.0	0.0	2	0200 0011	4	13
3 q	1o	1+	1o	1−	1o	0+	1−	3o	9o	0.3	0.2	5	2110 1013	9	13
4	3o	2+	2+	3−	2o	2+	3−	2−	19o	0.6	0.6	10	3223 2221	17	13
5 q	2−	1+	1−	1o	1+	2−	2−	1+	11−	0.4	0.2	5	0201 1111	7	10
6	3o	1+	2−	0+	3o	5−	3+	2+	20−	1.1	0.8	14	3120 3433	19	23
7 D	4−	5+	6−	3+	4o	4+	3o	3−	32o	1.4	1.3	31	3454 4422	28	23
8 D	1+	1−	1+	2−	1−	2o	5o	5+	18o	1.0	0.9	17	1112 1244	16	17
9	3−	2o	1o	2+	3o	3+	2+	2o	19−	0.8	0.6	10	2112 3322	16	23
10	2+	3+	3−	3+	3−	2+	2o	2+	21o	0.7	0.7	12	2333 2112	17	17
11	2o	3−	4o	1o	1+	2o	3−	2o	18−	0.6	0.6	10	2241 1122	15	17
12 Q	2o	1+	1o	2−	1o	0+	0+	0o	8−	0.1	0.1	4	1122 1000	7	23
13 Q	1−	0o	1+	1o	1−	1+	2−	2−	8+	0.4	0.1	4	0011 1111	6	25
14	2−	3−	3+	1−	2+	1+	3−	2o	20−	0.8	0.7	11	1233 2122	16	16
15	3o	2o	1o	2−	3o	4o	2−	3o	19+	0.9	0.7	12	3211 2323	17	23
16	2+	3o	1o	3−	1+	1+	1−	1+	13−	0.2	0.3	6	2311 1111	11	15
17 Q	2−	0o	0o	1o	2−	0o	0o	1−	5o	0.0	0.0	2	2001 2001	6	8
18 q	0o	0o	0o	0+	1+	1o	1o	3o	7−	0.4	0.1	4	0000 1012	4	8
19 Q	0+	2−	1−	1−	1o	1−	1−	2o	7+	0.2	0.1	4	0201 0011	5	0
20	2−	1o	2−	1o	1+	2o	1o	2−	11o	0.3	0.2	5	1121 1112	10	0
21 D	2+	5−	2+	3+	3+	3+	3o	3−	25o	0.9	0.9	17	2523 2222	20	7
22 q	2o	1−	1o	1−	1−	2−	2+	2+	10−	0.1	0.2	5	2010 0122	8	0
23 D	3o	3−	2−	3−	3+	4+	5−	4−	24o	1.1	1.0	18	2222 3343	21	0
24	1−	3o	2−	3−	2o	1+	2−	3+	19o	0.7	0.6	11	3322 2123	18	13
25 D	1+	1−	1−	1−	2−	1+	1o	3o	19+	0.8	0.8	14	4122 1112	14	15
26	2o	3+	3−	2−	2−	2+	2−	1+	15+	0.5	0.4	7	2132 2211	14	22
27	3−	2−	2−	3−	3o	3−	1o	3−	17−	0.6	0.5	9	2113 3222	16	24
28	1+	1−	1−	1+	1+	2o	2o	1+	13+	0.3	0.3	6	3200 1121	10	18
									Means	0.55	0.46	9			14.3
									No. of days	28	28	28			28

[1] Five quiet days (Q), ten quiet days (Q or q), five disturbed days (D) selected by Committee on Characterization of Magnetic Disturbances, J. Veldkamp, Kon. Nederlands Meteorologisch Instituut, DeBilt, Holland.

[2] Geomagnetic planetary 3-hr-range indices K_p prepared by Committee on Characterization of Magnetic Disturbances, University, Göttingen, Germany.

[3] Preliminary magnetic character figures C_i prepared by J. Veldkamp.

[4] Magnetic character figures C_p prepared by University, Göttingen, Germany.

[5] Average amplitude [illegible] prepared by University, Göttingen, Germany.

[6] Fredericksburg 3-hr-range indices K_{Fr} (K_9 = 500 γ); scale values of variometers in γ/mm: D = 2.78; H = 2.43; Z = 3.30 prepared by R. W. Koberry, Observer-in-Charge, Fredericksburg Magnetic Observatory, Corbin, Virginia.

[7] Provisional sunspot numbers [illegible] observations at Zurich Observatory and its stations at Locarno and Arosa prepared by M. [illegible], Swiss Federal Observatory, Zurich, Switzerland.

K_p, C_i, C_p, A_p, K_{Fr}, R_z, and Selected Days, March 1965

Day[1]	3-hr Range Indices K_p[2]								Sum	Prel.[3] C_i	C_p[4]	A_p[5]	3-hr Range Indices K_{Fr}[6]		Prov.[7] R_z
	1	2	3	4	5	6	7	8					Values	Sum	
1	1o	1+	0+	1+	2+	3+	2−	1+	13−	0.6	0.3	7	1101 1111	7	13
2	0o	1+	1+	1+	2o	3+	3+	2o	15−	0.6	0.4	8	0112 2232	13	0
3 D	3+	4−	4o	3o	3+	5−	5−	4o	31−	1.4	1.2	26	3333 3342	24	0
4 D	4o	6o	4o	3+	2o	1+	1o	1−	22+	0.8	1.1	21	3542 1010	16	8
5	0o	1−	2o	3+	2o	2−	2o	2−	13+	0.5	0.3	7	0123 1111	10	7

periods of a limited range need to be considered. Very short period fluctuations can be averaged out of the magnetometer records over deep sea regions during analysis since here the depth of the crustal sources requires a broad anomaly. On the other hand long period fluctuations of periods greater than several hours, are removed from the profiles as a regional trend and hence have no effect on local structural interpretations. They may however appear as regional anomalies on the regional field map.

Copies of the world geomagnetic data available (Lincoln, 1964, 1965) for December 1963, and February, March 1965, are given in tables 1 and 2. The measurements at sea were made during the periods 6th-14th, 24th-31st, December 1963, and 14th-19th February, 24th February - 2nd March 1965. It will be noted that the days of recording in December 1963 included seven of the ten selected quiet days and only one of the five selected disturbed days. This last was only the second day out from Christchurch. In February, March 1965 the days of recording included three quiet days and one disturbed day.

Variations of up to 100 gamma do occur in the Scott Base records. Only four cases of fluctuations which might be attributed to crustal sources appear in the magnetograms. Two of these occurred when the ship was north of latitude 50°S and are therefore unlikely to affect the records appreciably. The other two occurred when the ship was in the vicinity of latitude 60°S. It is believed that any effects of the transient fluctuations remaining in the plotted anomaly profiles obtained during December 1963 and February 1965 are insignificant compared to structural effects.

6.2 Bathymetry of the Region

Figure 24 shows four echo-sounding profiles obtained between New Zealand and Antarctica, and one obtained between New Zealand and Balleny Islands. These profiles illustrate the division of the region into the three major provinces.

6.2.1 New Zealand Continental Margin

(a) New Zealand Plateau. The bathymetry of the New Zealand Plateau has been described fully by Brodie (1965). Over the southern region shown in the profiles of figure 24, i.e. the Campbell Plateau, the surface is essentially smooth and in general slightly concave, before the gradient increases towards the marginal slope.

(b) Subantarctic Slope. This steep slope marks the edge of the New Zealand Plateau. Profile h is a normal crossing of the slope and illustrates the steepness at this crossing. The steepest slope on this crossing is 1:4 from 1300-1800 fathoms. Profiles b and e are also close to normal crossings and show that the steep gradient of profile h is not an isolated example. There is evidence of canyons cutting through the slope. The reversals of slope occurring on profile d, which crosses the slope almost tangentially, are most likely explained in this way. Such canyons presumably provide channels for the transport of sediment off the plateau to the ocean basin.

At the foot of the slope the gradient decreases to 1:100 - 1:500 across the continental rise before reaching the essentially flat ocean basin to the south. The extent of the rise is not great, generally 50-60 miles, suggesting comparatively little sediment accumulation at the foot of the slope. Thus the sediment carried off the plateau is probably spread across the basin for some considerable distance.

6.2.2 Southwestern Pacific Basin

This is a true ocean basin with a depth of 2,700-3,000 fathoms. Menard (1964) calls this region one of five "most normal regions" of the Pacific Basin. The maximum observed relief on the profiles of figure 24 is less than 300 fathoms. An exception is profile j which is across the western edge of the basin and crosses a large seamount at 57°S. It is a sharp peak rising 6000 ft above the surrounding basin floor.

The present echo-sounder installed on H.M.N.Z.S. Endeavour

makes accurate measurements of small topographical features in this region impossible. However the basin does appear to exhibit the features of an abyssal basin, the surface of which has been considerably smoothed by sediment, presumably carried off the plateau in the form of turbidity currents.

Average gradients across the basin are in the order of 1:2000 to 1:3000 away from the plateau, tracks e and h. However on track d the gradient is of the order of 1:3000 towards the plateau south of the slight rise at 55°30'S, and on track b the gradient changes from about 1:3000 away from the plateau to 1:1800 towards the plateau at about the centre of the basin.

6.2.3 Pacific-Antarctic Ridge

The boundary between the basin and the ridge flanks seems to be fairly sharp, being marked by an increase in the relief and a general decrease in the average depth of the floor. The northern flanks are characterised by relief as great as 4000 ft, and can be divided into step provinces similar to those described by Heezen et al. (1959) for the Mid-Atlantic Ridge, figure 25.

Over the Mid-Atlantic and Indian-Antarctic ridges there appears to be a deep median rift valley running through the crest of the ridge (Heezen et al., 1959). A narrow median valley probably also exists along the crest of this portion of the Pacific-Antarctic ridge, figure 25. The topography across the crest is very broken being marked by a number of steep-sided peaks and valleys. Peaks with a height of 7000 ft are not uncommon. In this respect too it resembles the Indian and Atlantic ridge systems. Note the deep narrow valley on the southern edge of the crest which may be a continuous feature along much of the ridge studied.

The marked asymmetry of the ridge in this region is interesting and is in contract to most other parts of the mid-ocean ridge system studied. This asymmetry is presumably due to the proximity of the Antarctic continent to the ridge in this region. There appears to be a

plateau region linking the ridge to Antarctica, similar to the Azores Plateau in the North Atlantic and Crozet Plateau in the Indian Ocean. This region is called the Balleny Plateau in this discussion and covers an area of approximately 100,000 sq. miles.

6.2.4 Balleny Plateau

The topography across the plateau is surprisingly smooth, particularly considering its proximity to the ridge crest. The depth is approximately 2000 fathoms, so the southern flanks of the ridge will be beneath it. Little detail on the fine structure of the sea floor is available from the echograms. However the smoothness of the floor indicates considerable smoothing by sediment, presumably carried north from the continent by icebergs.

Several large seamounts, including Scott Island and the Balleny Islands, protrude through the floor of the plateau, indicating volcanic activity in the region.

6.2.5 Antarctic Continental Margin

(a) Antarctic Slope. At the southern edge of the Balleny Plateau the floor slopes up towards the Antarctic shelf. The average gradient over the continental rise is of the order of 1:150, although the rise is made up of a number of steps across which the gradient is considerably less than this. This region of the continental rise is quite extensive, reaching out across the Balleny Plateau a distance of up to 200 miles. This is to be compared to the marginal rise south of New Zealand where it occupies only 50-60 miles. In depth the rise extends from about 1000-2000 fathoms. This large area covered by the rise is suggestive of considerable sediment deposition in this region.

At about the 1000 fathoms level the gradient abruptly increases to about 1:15, corresponding to the continental slope region. On the profiles shown the slope continues unbroken to a depth of 300 fathoms where the gradient again levels off across the Ross Sea.

(b) Ross Sea. As mentioned in chapter 3.1 the Ross Sea is

an epicontinental sea across a continental shelf of unusually great depth. Profiles over this region of the Ross Sea show an initial bank at a depth of about 200 fathoms near the northern edge of the shelf, after which the depth increases again towards the continent. Taylor (1930) suggested that the Pennell Bank was a vast terminal moraine. This was strengthened by results of dredging over the bank by Roos (1937). Lisitzin and Zhivago (1960) report similar terminal moraines along the offshore edge of the continental shelf west of the Balleny Islands. It seems that these shallow banks are a feature of the Antarctic shelf.

6.2.6 Sediment Transport South of the Ridge

The bathymetry south of the ridge illustrates the different method of sediment transport occurring in this region. The predominant sediments occurring here are the "iceberg sediments" (Lisitzin, 1962). Considerable material has been removed from the land by glacial action. This material is carried far out to sea by the icebergs formed when the glaciers descend to the sea and calve. Hence instead of the sediment being deposited on the continental shelf and subsequently carried off in the form of turbidity currents, as occurs in the case of normal continental regions, the majority of sediment in this region is deposited towards the northern extremity of the shelf, or over the deep sea regions north of the continental slope. According to Lisitzin the iceberg sediments predominate to approximately $65^{\circ}S$, i.e. just south of the crest of the ridge. With such a method of deposition the sediments tend to build up across the continental rise producing an extended rise as observed. The smoothness of the Balleny Plateau is probably also a result of these ice-rafted sediments. Records from a seismic profiler operated across this region should indicate the thickness of these sediments and whether or not they are underlaid by more irregular relief.

6.3 Comparison of Magnetic and Bathymetric Profiles

Figures 26-30 show the total magnetic field and bathymetric profiles obtained during the two Antarctic cruises. It should be noted that navigational errors do not enter into comparisons between the magnetic and bathymetric records as both were obtained at the same time.

Between Christchurch and 47°S the tracks cross the southern portion of the Chatham Rise, and the Bounty Trough. Except on track h where a large anomaly occurs on the northern side of the Bounty Trough, there is little magnetic activity over this region.

Over the smooth Campbell Plateau the magnetic records are extremely irregular, figure 26. Large steep-sided anomalies occur, characteristic of a shallow source. The anomalies indicate a very magnetic basement which rises close to the surface of the sea floor in a number of places across the Plateau and probably exhibits considerable relief which has been buried by sediments deposited on the Plateau. Three major anomalies appear on the tracks over this region. The southern-most of these appears to be associated with the southern edge of the Plateau.

The Subantarctic slope marks the southern boundary of the steep-sided anomalies observed over the Campbell Plateau and the beginning of the gentler anomalies characteristic of deep ocean regions. Across the Southwestern Pacific Basin there is no obvious relief which could cause the large anomalies observed, figure 27. Although there is a lack of detail in the echograms, it does appear that here also the source of the anomalies has been buried by sediment.

South of 60°S the tracks cross the foothills and crest of the Pacific-Antarctic Ridge. Over much of this region there is unlikely to be much sediment covering. Yet here also there is little obvious correlation between the bathymetric and magnetic records, figure 28. This lack of correlation suggests that variations in topography are not

a major cause of anomalies over the deep ocean regions, although they will have a modifying effect on the shape of the anomalies. Such conclusions agree with results obtained elsewhere (Drake et al., 1963; Vine and Matthews, 1963; Vine and Wilson, 1965).

In general the crest of the mid-ocean ridge system is characterised by both large relief and large magnetic anomalies. Heezen et al. (1959) found a systematic positive anomaly over the central rift valley of the Mid-Atlantic Ridge. On the other hand Hill (1960), found no obvious magnetic anomaly associated with the valley. He also states that in the vicinity of the valley the size of the magnetic anomalies are not significantly different from those found elsewhere.

In the present results there is no evidence of a large positive anomaly being consistently associated with the rift valley. On profile b there is a large positive anomaly across the central valley. This anomaly is the largest over the crest and is flanked by two sharp negative anomalies. The deep valleys on either side of the central valley have no obvious anomaly associated with them. On profile e there is no obvious anomaly associated with the crest at all, although a negative anomaly of 350 gamma is a notable feature of the crest. This is particularly so as it is the only negative anomaly within 180 miles of the crest, figure 42. The deep valley at $64^{\circ}45'S$ however produces no noticeable effect on the magnetic record. Profile h is also notable for the negative anomaly occurring over the crest of the ridge, this time nearly 600 gamma. It should be noted that this anomaly is associated with the topographical high just north of the rift valley.

These results suggest a change in the ridge in the vicinity of profile e, i.e. $175^{\circ}E$. To the west it exhibits features similar to those described by Heezen et al. (1959) for the Mid-Atlantic Ridge. To the east the main anomaly is negative and does not appear to be associated with any major rift, although there still appears to be a rift valley south of the main anomaly.

Two complete profiles have been obtained across the Balleny Plateau, figure 29. One of these, profile h, is a north-south profile and the other, profile j, a predominantly east-west one. The latter is plotted in terms of distance travelled from a reliable midday fix ($66^{\circ}38'S$, $162^{\circ}33'E$) rather than degrees of latitude as for all other profiles. Profile j is interesting because it crosses a seamount in the Balleny group which appears to be reversely magnetized. The mount, at 40 miles ($67^{\circ}08'S$, $163^{\circ}21'E$ approximately) rises from a depth of 1200 fathoms to within 330 fathoms of the sea surface. The magnetic record across the mount shows an isolated negative of -1100 gamma magnitude. The size of the anomaly indicates a high magnetization. Hence it can only be explained by reverse magnetization. Such a classic example of a reversely magnetized seamount is rare and provides evidence that large volumes of reversely magnetized rocks do occur.

A second mount at 65 miles (approximately $67^{\circ}25'S$, $167^{\circ}47'E$) appears to be partly composed of reversely magnetized rock also. This mount comes within 50 fathoms of the surface. The observed anomaly across it is largely positive but with a large narrow negative dip in its centre, suggesting that the mount is composed of a reversely magnetized block of rock enclosed by normally magnetized rock. Hence it appears to have been formed in two stages, the central core while the earth's magnetic field was in the opposite direction to the present field, and the outer flanks while the field was normal.

Profile j approximately parallels the Pacific-Antarctic Ridge over the greater part of its length, yet it will be noticed that the wavelength of the anomaly pattern is not appreciably different to that of profile h, at right angles to the ridge. (The scale of the two profiles is not exactly the same, 50 miles compared to one degree of latitude). Thus there is no evidence of lineations paralleling the ridge at the latitude of this profile. Results obtained by the U.S. Navy Hydrographic Office (1962) for a track approximately paralleling the ridge between latitudes $90^{\circ}W$ and $120^{\circ}W$ suggest that considerably longer anomaly

wavelengths should be obtained if the ridge flanks extend this far south.

Over the greater part of the Balleny Plateau there is little evidence of a source on the sea floor for the observed anomalies. It appears that here too the source is generally buried.

Only one magnetic profile of any appreciable length has been obtained over the Ross Sea. This is presented with the corresponding bathymetry profile in figure 30. The lack of anomalies on this profile is in agreement with the findings of Christoffel (1961) and is what would be expected across a continental shelf.

6.4 The Regional Magnetic Field

As can be seen from the total magnetic profiles, the anomaly baseline increases as one proceeds from New Zealand to Antarctica. This is a result of the latitude variation of the earth's normal field. Before analysing the records in terms of crustal structure it is convenient to remove this regional field trend.

6.4.1 Removal of the Regional Trend

Various methods of removing the regional trend are available. One may assume that the earth's field is primarily a dipole field and calculate the theoretical regional variation along the tracks. This of course takes no account of higher order effects which form an appreciable part of the earth's field. In some regions a polynomial in latitude and longitude has been fitted to the results and this polynomial used to describe the regional variation (Grant, 1957; Bullard and Mason, 1963).

Over the region of the present survey the inclination of the earth's field is of the order of 80° or more. One would therefore expect the anomalous field due to crustal variations to increase the total field obtained, i.e. one would expect to obtain only positive anomalies in the total field measured. If this were so, and the anomalies were reasonably well separated, it would be possible to obtain the

regional field variation along a profile simply by drawing a smooth curve through the base of the observed anomalies. In fact, while the majority of the observed anomalies do appear to be normal positive anomalies, there are a number which are definitely not and must be assumed to be negative. These probably arise from reversely magnetized regions. However it is still possible to obtain a reasonable curve for the regional field variation by the method described, and this appears to be preferable to a simple averaging process.

This was therefore the method used in the present analysis. Figure 31 shows a portion of the total field results obtained with the assumed regional variation drawn on it.

6.4.2 The Regional Field Map

Figure 32 shows a chart of the region with the total field variation for epoch 1964.5 drawn on it. The regularly spaced contours, and the agreement across widely spaced tracks, indicates the validity of the method of subtracting the regional field from the profiles. The map indicates a position of maximum intensity in the region of 67°S 140°E. Burrows (1963) gives the position of the dip pole for 1962 as 67½°S 140°E. Watford et al. (1965) give the position for 1965.0 as 66.5°S 139.9°E.

6.4.3 Comparison with earlier charts

Three earlier total magnetic field maps which include all or part of this region have been published. The first of these, published by the U.S. Hydrographic Office (1955), differs widely from the present map. It shows a maximum intensity of 72,000 gamma in the region of 60°S 170°E. The present map gives a value of just under 66,000 gamma at this point. Further the map suggests that in the region of maximum intensity (67°S 140°E) the maximum value is not likely to exceed 69,000 gamma.

Nagata (1962) has published a total field map for Antarctica for epoch 1957.5 which includes part of the region considered here. He gives a maximum field of 70,000 gamma in the region of 69°S 141°E

Comparison of his map with that presented here suggests a marked north-westerly drift of the field in the period 1957-64.

Christoffel (1961) gives a total field map over this region for 1959. Appreciable differences exist between this map and the present one also. North of 60°S Christoffel's field contours tend to be situated approximately 30' to the north of those presented here. South of latitude 60°S the discrepancy is somewhat larger. The difference here is consistent with a predominantly westward drift in the field pattern.

These comparisons indicate a definite westward drift in the field pattern. This is in agreement with world-wide observations (Fleming, 1948; Elsasser, 1950; Bullard et al., 1950). An average value for the velocity of drift for this century appears to be about 0.2-0.3°/yr. However Vestine (1953) has shown that there is evidence that the velocity of the westward drift fluctuates by about 20% in 50 yrs.

Adam et al (1964) have estimated the rate of drift of the centres of world anomalies and of the isodynams outlining them. For the North American, African, and East Siberian anomalies they find that the rate of movement is almost constant for the period 1880-1955, and differs considerably for all three anomalies. They obtain values of 0.12°/yr, 0.21°/yr, and 0.15°/yr for the North American, African and East Siberian anomalies respectively. They suggest the different drift velocities may be associated with the different depths in the core of the current vortices which produce them.

In the construction of a world magnetic chart for epoch 1965, Watford et al. (1965) have adopted a value for the movement of the south magnetic pole of 14 km/yr in a northwesterly direction.

The velocity of westward drift obtained from a comparison of Christoffel's map and the present one is approximately 0.25°/yr for the region between 50°S and 60°S. South of 60°S there is an increase in the drift. To bring the two 67,000 gamma isolines into coincidence requires a drift of nearly 1°/yr. Nagata (1962) noted that the secular

variation near the south magnetic pole was large.

Thus it appears that differences occurring between the two maps can be explained by the westward drift of the non-dipole component of the earth's magnetic field. Hence it seems possible to obtain a value for the drift of the field from the comparison of total field maps drawn from the data obtained from widely spaced profiles. Since little is known about the secular variation in this region (Cullington, 1963), such comparisons can prove very useful.

6.4.4 Regional Anomalies over the Region

In subtracting the regional field from the magnetic records long period anomalies, (i.e. periods of 100 miles or more) are also removed from the records. Anomalies of periods around 100 miles can arise from large scale variations in the thickness of the magnetic basement rocks. Two effects can cause the required change in thickness. (1) A gradual change in the depth of the basement rock over a large area such as could occur over the mid-ocean ridge. Rapid changes in depth such as occur across the edge of the New Zealand Plateau will not produce a regional anomaly but rather a small local anomaly over the edge of the Plateau. (2) A gradual change in the depth of the Curie point isotherm and hence in the base of the magnetic basement. The first effect will be very small for the changes in depth that occur and is not likely to be observed unless the magnetic rock is very thin, e.g. layer 2 only, as suggested by Vine and Wilson (1965). The second effect may be considerably larger since heat flow measurements across such regions as the mid-ocean ridge suggest large changes in the level of the Curie point isotherm. Thus appreciable regional magnetic anomalies may occur across some parts of the ocean, and it would be interesting to see if any can be detected in the present survey. It is difficult to obtain accurate values for these anomalies because of the problem of removing the earth's normal field. However by assuming

a linear variation for the earth's field over distances of approximately 100 miles, the anomalies may be detected, and approximate values of their amplitude obtained. This has been done for tracks a-e, h, j. The results obtained are plotted in figures 33 and 34. The first of these shows the anomalies obtained over the plateau and basin regions, while the second shows those across the ridge. These figures illustrate that appreciable anomalies do occur and that they can be correlated to some extent across the tracks, and hence with the region the tracks cross.

On all except tracks c and d there is no apparent anomaly over the Plateau. Tracks c and d, which in fact cross in the central portion of the Campbell Plateau, both contain large negative anomalies. The fact that no such anomaly occurs on the tracks on either side of c and d, indicates that the source of the anomaly is long and thin. It is difficult to explain this anomaly in terms of a decrease in the depth of the Curie point isotherm.

Immediately south of the edge of the Plateau there is a positive anomaly of 100-150 gammas on all tracks. This indicates an appreciable thickening of the basement at this point. Such a thickening at the continental edge would be in agreement with the ideas of Dietz (1961) that the oceanic crust tends to be thrust under the continent, and also of a descending convection current with consequent lowering of the Curie point isotherm. On all tracks except h there is a further positive anomaly over the basin. The correlation here however is not so good.

On all tracks across the ridge the flanks are characterized by a positive anomaly indicating an increase in the depth of the Curie point isotherm and hence a low in the heat flow value. The axial zone is characterized by a zero or small anomaly, while records south of the crest indicate a further positive anomaly on the southern flank. Thus there appears to be a definite increase in the depth of the Curie point isotherm away from the crest of the ridge. Heirtzler and Le Pichon

(1965) have observed a similar effect on several profiles across the Mid-Atlantic Ridge.

Figure 35 is a map of the region with the observed anomalies plotted on it. Although there is some doubt about the amplitude of anomalies, so that too much reliance cannot be placed on the contouring shown in the figure, it is believed that the general trends shown by the shading are real and worthy of further attention.

6.5 Total Field Anomaly Profiles

With the regional magnetic field subtracted from the total field profiles, comparison of the anomalies across the tracks is very much simpler.

6.5.1 Campbell Plateau

Figure 36 shows the anomaly profiles obtained across the southwestern part of the New Zealand Plateau. Three of these profiles (c, e, f) were obtained with a digital readout magnetometer. Over regions where the magnetic field fluctuates rapidly (e.g. south of 48°S) these profiles may have suffered some smoothing due to the averaging process used in plotting them.

North of 48°S, across the Bounty trough, the profiles are relatively smooth. This correlates with an increase in the basement depth under the trough. A large anomaly occurs at 45°35'S on profile h. The anomaly is too far south to be associated with the Bank's Peninsular volcanics, and as yet its cause is unknown. It does appear to be a local feature since it has not been observed on any other profiles presented here. It does however appear similar to an anomaly on Adam's profile (Adams and Christoffel, 1961) which he puts at about 47°30'S.

The three profiles obtained using the magnetometer constructed (profiles b, d, h), illustrate the complexity of the record south of 48°S. The large sharp anomalies indicate a shallow magnetic source and because of this the profiles probably reflect, at least to some extent,

the basement topography across the region. Correlation of anomalies between the profiles is on the whole good. On the other hand because of the complexity of the records it is difficult to determine whether the large anomalies A-F (figure 36) on the northern side of the edge of the plateau are associated with the plateau edge, and a more or less continuous feature, or not. Nevertheless an interesting picture is obtained if these large anomalies are assumed to be due to a single feature. Figure 37 shows a line drawn through these anomalies joining up with a line through the large anomalies along $49^{\circ}20' - 48^{\circ}20'$S (anomalies G-K) together with the bathymetry contours of the region. The correlation between the edge of the plateau and the line of magnetic anomalies is remarkable and indicates that these anomalies might well be due to a continuous basement ridge running around the edge of the Plateau, very like an enclosing wall. Between the two lines of anomalies the basement seems never very far from the surface as is indicated by the sharpness and detail of the profiles, and the whole region is obviously a complex one. A third set of large anomalies, L-O, probably represents a further ridge running across the Plateau. This ridge is dotted in Figure 37. The validity of these correlations can only be proved by a more detailed survey of the entire region.

6.5.2 Basin Region

Figure 38 shows the anomaly profiles across the basin obtained on the nine tracks shown on the track chart, figure 23. There is a marked similarity about all the profiles. Christoffel (1961) first pointed out the similarity of the profiles across this region. With the addition of the two tracks for December 1963 the validity of the correlation was further demonstrated (Christoffel and Ross 1965). Figure 39 shows the four tracks and assumed correlation suggested in this paper. The tracks obtained during February 1965, and those made available by D.S.I.R. have enabled an accurate picture of the trend of magnetic features across this region of the basin to be obtained. The features are clearly shown in the anomaly contour map which has been drawn for the region, figure 40. In drawing this contour map some adjustment of position of the southern portions of some of

the profileswas required to fit the patterns where tracks crossed or approached very close to each other. There is therefore some doubt as to the positional accuracy of the southern-most features. A maximum error of ± 5 miles would seem reasonable. Apart from the interesting fact that the continuous features are observed over such long distances, the most striking feature of the map is the displacement of anomalies along a line striking 9°E of S, and running between 51°S 177°E, 58°S 178°E. Contours associated with similar features have been made continuous across this line although they may not be, particularly if the displacement is across a fault zone. Correlation of anomalies across the line is very good suggesting a real discontinuity in the basement features giving rise to the anomalies. The displacement of similar features to the north of the basin is approximately 180 miles but this decreases appreciably towards the south. Evidence of differential movement on the two sides of the line of discontinuity is obtained from a closer study of the profiles. It will be seen that profiles a to e are of approximately the same length with a slight decrease from a to e. Profile g is on the other hand very much compressed, suggesting that it is under considerable pressure. On the eastern side of the line profiles h and i are considerably longer than the other profiles, suggesting that on this side the pressure has been released. In figure 41 the magnetic features shown in the contour map, together with the tracks over which they were obtained, are drawn over a bathymetric map of the basin. The relation between the magnetic features and the edge of the New Zealand Plateau is striking. This immediately suggests that the reason for the compression of the crust to the west of the discontinuity is that there the crust is being forced against the continental mass, while to the east the obstruction is further to the north, either because this part of the Plateau has moved along a continuation of the 'fault' or because this was its original shape.

If the 'fault' line is produced south to the ridge it intersects the ridge at approximately 65°S 180°E. This is the region where the ridge turns northeast towards Easter Island. There does not however appear to be a discontinuity of the ridge in this region. The low seismicity of this part of the ridge (Sykes, 1963) would also suggest that there is no major fracture zone meeting the ridge here.

6.5.3 Ridge Region

The anomaly profiles over the Pacific-Antarctic Ridge are shown in figure 42. The similarity of the profiles so noticeable on the records across the basin is not obvious over this region (Christoffel and Ross, 1965). Over shorter distances there certainly is some correlation and it seems probable that a similar magnetic grain to that obtained across the basin region would show up in a detailed survey. However with the results available at present it is impossible to follow the magnetic pattern which was so clear across the basin south across the ridge foothills. The exact reason for this loss of correlation is uncertain, but is certainly due to the presence of the ridge and indicates a change in the source of the anomalies south of the basin. The fact that there is little correlation between bathymetric records over the ridge suggests that topographical effects may be partly the cause.

The ridge anomalies fall into three general categories.* The axial anomaly, upper flank anomalies, and lower flank anomalies. The axial zone is characterised by a large steep-sided anomaly and is from 30-80 miles wide. On the three tracks obtained between 165°E and 175°E the axial anomaly is a large positive anomaly flanked by two narrow negative ones. These anomalies correlate well across the three tracks.

*Heirtzler and Le Pichon (1965) have recognised similar zones across the Mid-Atlantic Ridge. Their axial zone corresponds to the upper flank zone of the present discussion.

To the east of 175°E the correlation between axial anomalies is not so good, although track h is similar to those west of 175°E except for the deep negative portion. On track g, and also on other tracks crossed by U.S.N.S. Staten Island east of 180°E (U.S. Navy Hydrographic Office 1962), the axial zone seems to be appreciably wider and contains larger anomalies than over this region.

Profile a is interesting as this track has crossed the crest of the ridge at a very low angle (figure 23), and so has followed the axial zone for some distance. If the magnetic lineations tend to parallel the ridge, one would expect considerably longer anomaly wavelengths on this track than on a normal crossing. This however is not so. The whole of the axial zone exhibits extremely sharp magnetic peaks, individual peaks ranging from 500-1000 gamma. These peaks are as sharp as any on the more normal crossings. This profile emphasises the need for a detailed survey over the region in future work rather than continuing to obtain isolated profiles.

Immediately north of the axial zone the magnetic record on most tracks is comparatively subdued. The width of this zone varies considerably but covers at least the region of the high fractured plateau of figure 25, and in some cases extends across the upper step. On the southern side of the axial zone the ridge pattern is confused by the close proximity of Antarctica and the presence of the Balleny Plateau. Any anomalies over this plateau characteristic of the ridge are likely to be masked by the effects of the plateau. The few anomalies that do occur over the exposed ridge south of the axial anomaly are of large amplitude similar to those over the lower flanks on the northern side.

To the north of the upper flank region of subdued anomalies there is a sudden and marked increase in the anomaly amplitude. This increased amplitude continues across the lower flanks, although there is a tendency for a slight decrease as the basin is approached.

6.5.4 Anomalies South of the Ridge

Results across the region south of the ridge are limited. This is because fog and ice conditions often prevent the towing of the magnetometer. Insufficient results are available to make comparisons across the tracks worthwhile. Those results obtained in this region have already been discussed, together with the bathymetry profiles, in section 6.3.

CHAPTER 7

THE SOURCE OF THE OBSERVED ANOMALIES

7.1 Introduction

In interpreting the magnetic records one would like to be able to determine the form of the source causing the anomalies. As pointed out in chapter 2.4 a unique solution for the source is impossible without considerably more information, but a reasonable model which fits both the observed anomalies and known facts and ideas about the crustal structure, can often be determined. Such simple models can be very useful in elucidating effects occurring in the crust. In attempting to obtain reasonable models for the sources the first step is to obtain estimates of the susceptibility, and particularly the shape and depth, of the source. Simple models can then be built up using this information. By comparing the theoretical anomaly of the computed model with the actual anomaly observed an idea of how reasonable the model is can be gauged.

7.2 Determination of Susceptibility and Depth

A number of articles have been written on the problem of obtaining reasonably accurate values of susceptibility and depth of the source of magnetic anomalies. Some of the more important articles which have been used in the present investigation will be briefly reviewed here.

Vacquier et al. (1951) considered the problem in some detail and produced total field and curvature maps over a number of prismatic bodies for comparison with observed anomalies. They discussed a number of depth indices from which the depth of the source can be estimated. The lateral extent of the source can be estimated from the fact that the zero contour on the curvature map tends to outline the top surface of the source. The maps are drawn for a unit susceptibility

so that the actual susceptibility contrast in a particular case can be obtained from the ratio of actual anomaly maximum to that given on the total field map.

Two depth indices which have proved useful in aeromagnetic surveys are "Peters' length" and the "straight slope length". The first, used by Peters (1949), is the horizontal distance between the tangents to the anomaly curve with gradient equal to half the maximum gradient of the anomaly, figure 43. The depth d the source is approximately half this length. The second is based on the fact that the steepest part of the anomaly curve is almost a straight line, figure 43. The horizontal length of this line is approximately equal to the depth of the source. In both cases a multiplication factor which varies somewhat with the direction of polarization of the source is strictly required. These two methods use only the steep portion of the anomaly curve and can therefore be applied to broad sources and cases where the proximity of sources causes some overlapping of anomalies. The second method is particularly useful for obtaining quick estimates of depth from profiles.

Henderson and Zietz (1948) considered the anomalies produced by point and line sources. The case of a line of poles is of importance in the interpretation of oceanic profiles, since over large areas of the ocean the anomaly sources appear to be long narrow structures and therefore approximate to the case of a line of poles. Henderson and Zietz derive and plot a depth factor, k, as a function of the inclination of the earth's field, I, and the angle, β, between the direction of traverse or line of poles, and magnetic north. The depth to the anomaly is $k\eta$, where η is the horizontal distance between the maximum and half maximum amplitude values on the anomaly, figure 43. Smellie (1956) extended the work of Henderson and Zietz to include the cases of the dipole source, and line of dipoles source. Smellie also gives curves for the ratio of half maximum distances η/η', as a function of I and β. This ratio is useful for determining the degree of approximation involved in the model. Provided the approximation is a good one it also enables

an estimate of the direction of magnetization of the body to be made if this is not known, or cannot be assumed equal to that of the earth's field. Smellie does not however point this out.

In all the articles mentioned so far it is assumed that the magnetization of the body arises from induction in the earth's field. In this case the direction of magnetization is known and the susceptibility contrast can be calculated from the amplitude of the anomaly. Sutton and Mumme (1957) consider the effect of remanent magnetization on the shape of the observed anomalies and show that in some cases an estimation of the direction of the remanent magnetization is possible. That the remanent magnetization can be of considerable importance has been shown by a number of workers (Miller and Ewing, 1956; Girdler and Peter, 1960; Hays and Scharon, 1963; Hood, 1964; Mumme, 1964).

Hall (1959) derived equations for the magnetic field over a point dipole, a horizontal line of dipoles, a thin dipping sheet, a thick dipping sheet, and a sloping step, in the case where both the direction of measurement and polarization are arbitrary. He shows that it is possible to develop methods of determining the unknown parameters of the bodies, including the direction of polarization, when magnetic profiles over them are given. Bruckshaw and Kunaratnam (1963) developed a method for the routine interpretation of anomalies arising from uniformly magnetized dykes for the case of arbitrary directions of measurement, polarization, and strike. The theoretical dyke equation has been used in obtaining the calculated profiles presented in the next section.

A basic assumption in all these methods is that the basement rocks are large homogeneous bodies. The fact that large and regular anomalies are observed suggests that in general they do behave as such bodies. The methods also assume that the basement rock bodies approximate to very simple theoretical bodies, generally with flat tops and parallel sides. Steenland (1963) presented a detailed survey of the Peace River country of northwestern Alberta where the calculated depths of the basement rocks were compared with depths found from subsequent

drilling. An average error of 7.4% was obtained, indicating that in general surprisingly good accuracy could be obtained using simple models.

7.3 Analysis of Observed Anomalies

7.3.1 Ocean Basin

Because of the lack of obvious sources for the large anomalies observed over the basin this region has been analysed in some detail. If the correlation discussed in chapter 6.5.2 is accepted, it is clear that the source approximates to a dyke-like structure striking along the lines of correlation. This enables estimates of depth and susceptibility to be determined.

The depth to the top of the source can be quickly estimated from the profiles obtained using the curves of Henderson and Zietz (1949), and Smellie (1956). On all profiles depth values of 2.8 - 3.3 miles were obtained. Values for the susceptibility contrast can also be obtained by comparing the anomalies obtained with the theoretical anomalies plotted by Vacquier et al. (1951). These values ranged from $1\text{-}3 \times 10^{-3}$ c.g.s. units.

It is obvious from the profiles that in a number of cases anomalies from adjacent sources overlap. In such cases it is difficult to obtain accurate depth or susceptibility values from the simple theory. The important facts that emerge from these simple calculations are; (1) the top of the source is very near the surface of the basin floor, and (2) the susceptibility contrast values are of the order of the normal susceptibility of basalts. However, since the parent rock in this case is presumably basalt, this susceptibility contrast represents a considerable magnetization. Part, or even all of this may be due to remanent magnetization.

The next step in investigating the anomaly source is to construct a model basement, the computed anomaly profile of which approximates closely to the observed profile. A reasonable model for a first

approximation would seem to be a series of vertical sided dykes with flat tops at a depth of 3 miles, i.e. just below the basin surface. Since the inclination of the earth's field across the basin is greater than 80°, a vertical magnetization of the dykes would seem reasonable. Using the dyke equation (appendix 3) the anomalies associated with such dykes with depth to width ratios of 1:1, 1:1.5, 1:2, and 1:3 were calculated and plotted. Combinations of these simple models with varying susceptibilities were then used to construct a model basement with the required anomaly profile. The result for part of profile b is given in figure 44. The depth of the base of the dykes was assumed to be 7 miles. This depth gave a slightly better fit than a series of infinite dykes, although the effect of varying the base depth is only minor. The fit obtained with the observed profile is remarkably good, a correlation coefficient of 0.96 being calculated for the two curves. The susceptibility contrast tends to be a minimum over the middle of the profile. This suggests that the basement rock may exhibit a definite concave shape over the basin so that the source of anomalies at the centre is somewhat deeper than along the edges.

Similar profiles have been constructed for the other tracks across the basin. Minor differences in the dyke sources occur. For example, if it is assumed that the depth to the top of the dykes is constant at 3 miles, some variation in susceptibility along a particular dyke is required to fit the observed anomaly amplitudes. Also some variation in width of the dykes occurs across the basin. Such variations are not unreasonable particularly if the sources are in fact intrusive dykes.

Thus the basement structure across the ocean basin appears to consist of stripes of strongly magnetic material within the more normal basement which extend across the basin for considerable distances as indicated in figure 41. The origin of these stripes of magnetic material is uncertain. However because they are aligned in the general direction of the ridge it seems likely that they originate in some way from the ridge. Results off the west coast of North America particularly,

support the idea that the magnetic pattern in the vicinity of the mid-ocean ridge system tends to parallel the ridge. It is therefore logical to assume that the origin of the pattern can be associated with the ridge. It seems that over this region the source is either (1) a system of intrusive dykes presumably arising from fractures in the crust caused by movement away from the ridge, or (2), a series of alternately normal and reversely magnetized blocks of crust as suggested by Vine and Matthews (1963). In the latter case the entire basin crust could be composed of a uniform rock type, the anomalies arising from the changes in remanent magnetization. The fact that on the profiles across the basin two major anomalies do occur which are appreciably more negative than the baseline to the majority of anomalies, figure 31, suggests that reversely magnetized regions do exist but are not the cause of most anomalies.

7.3.2 Campbell Plateau

The large anomalies occurring over the Campbell Plateau are also of considerable interest. We will consider in detail anomaly G occurring on profile b, figure 36.

It is obvious from the steepness of the observed anomalies that the source is very close to the surface of the plateau. Simple calculation of depth indices indicates a depth of around $\frac{1}{2}$ mile. It is therefore clear that the basement has risen considerably across the Subantarctic slope. It is also clear that north of the Campbell Plateau, across the Bounty Trough, the basement depth again increases considerably. Thus the Campbell Plateau appears to be a region of uplifted basement. Because of the shallow depth it is likely that variations in depth of the basement will be reflected in the magnetic record. Thus the broad low portion of anomaly G may well be the topographical effect of a basement ridge. The large sharp anomalies superimposed on this broader anomaly could then be due to dyke-like features intruded along fractures in the ridge and presumably associated with the rise in level of the basement.

The model basement for anomaly G is shown in figure 45. The depth from which the basement ridge has risen cannot be determined from the magnetic data without a knowledge of the susceptibility. In the calculation of figure 45 it has been assumed that the depth of the basement on both sides of the ridge is sufficiently great to be approximated to infinity. This has little effect except on the susceptibility required to fit the anomaly. The fit of the computed and observed anomalies is extremely good, indicating that the basic model is reasonable.

Most of the large anomalies across the plateau are of this form, i.e. a broad anomaly with several sharp peaks superimposed on it. Thus it is likely that all these anomalies have a similar type of source. The small sharp anomalies particularly noticeable on tracks b and d might well be due to local topographical variations over the uplifted basement. Because of the steep gradients of these anomalies they must be associated with a fairly shallow source. A maximum depth of 1 mile is possible for the source of these anomalies.

The good correlation of anomalies along the edge of the plateau is consistent with the idea of a basement ridge running along the edge. The sediments deposited on the plateau have probably built up against this ridge burying the basement across the plateau. The slight concavity of the plateau indicated in the bathymetry records agrees with this idea as also do the steep gradients across the Subantarctic slope. However although there probably is considerable basement relief across the plateau which is reflected in the broad anomalies, the fact that the gradients of all anomalies are steep indicates that in general the basement level is high and not far below the surface of the plateau.

7.3.3 Ridge Anomalies

Across the lower flanks of the ridge the large broad anomalies probably have a similar source to the basin anomalies. The sudden loss of correlation of anomalies between tracks may be partly due to the increased topography over the flanks since, in some cases at least,

this will certainly have some effect on the observed anomalies. If the ridge in this region is in the process of decaying and has already collapsed appreciably, this could also conceivably result in a loss of correlation. The extremely broken topography of the ridge, particularly over the crest, is what would be expected if the ridge had subsided. In the process of subsidence the series of dykes originally paralleling the ridge, and giving rise to a lineated magnetic pattern similar to that across the basin, would become broken and distorted, resulting in the complex magnetic pattern observed. This is in agreement with indications that over young ridges such as the East Pacific Rise (Mason, 1958), and the Juan de Fuca Ridge (Vine and Wilson, 1965), the correlation of anomalies over long distances is particularly striking. Also the axial anomaly observed over this portion of the ridge is smaller than over the East Pacific Rise or even the Pacific-Antarctic Ridge east of 180°E. This is again consistent with the idea that the ridge here is decaying.

The region of subdued anomalies across the upper flanks seems to be a feature of the mid-ocean ridge system (Talwani et al., 1965). A possible reason for the smaller anomaly amplitude is that in this region the susceptibility of the parent rock is appreciably higher than elsewhere, so that the susceptibility contrast of the intrusive sources is reduced. It seems reasonable to expect a higher susceptibility for the crustal rocks over the crest of the ridge because of the upwelling of more basic material.

The large axial anomalies are the result of a highly magnetic source. The axial anomalies of tracks b and h have been considered in detail. The anomaly on track b occurs over the median valley of the ridge, figure 28, and correlates well with the topography. Thus it appears to be caused by a block of highly magnetic material forming the base of the valley and the rift mountains on each side. Figure 46 shows the computed model and anomaly. A number of magnetic intrusions through the main magnetic block are required to obtain a fit between

the observed and computed anomalies.

On track h the major portion of the axial anomaly occurs to the north of the median valley, the large negative anomaly being associated with the rift mountain on the northern side of the valley. There is no correlation of this anomaly with topography. In this case therefore the major source appears to be intrusive. Figure 47 shows the computed model and anomaly. Note that the top of the computed source for the main negative anomaly is at the same depth as the top of the peak it is associated with.

The base of the anomaly sources for both these anomalies is taken as 7 miles. The fact that the large central negative anomaly of track h is missing from track b indicates that the ridge has been active at different times in the two places; in the region of h while the earth's field was reversed, and in the region of b while the field was normal. However a similar negative anomaly occurs on the northern edge of both axial anomalies.

In an attempt to check whether the basement rock dips below the Balleny Plateau, and hence whether the ridge flanks continue south beneath the plateau, 'straight slope' depth indices were calculated for the anomalies of profile b from 67$\frac{1}{2}$° north across the plateau, ridge, and northern flanks to 60°S. The results are shown in table 3. They show that over the northern flanks of the ridge the basement depth increases to 3000 fathoms, while over the Balleny Plateau the basement depth seems little greater than the depth of the plateau. The average values for the depth in the two regions are significantly different - 2.1 for the plateau and 2.7 miles for the northern flanks. The values obtained over the crest of the ridge seem to indicate that the depth indices are reasonably close to the actual source depths. Also over the basin region depth values obtained from this index agree with those obtained from the curves of Henderson and Zietz (1948). Thus these calculations indicate that the southern flanks are not buried by great depths of sediment but that the actual ridge exhibits the asymmetry apparent

from the bathymetry profiles.

Table 3

Region	Latitude	Depth (miles)	Mean Depth
plateau	67 S	3.1	
		2.0	
		1.5	
		2.6	
		2.8	
		1.9	
		1.7	
	66 S	2.9	2.1
		2.2	
		2.0	
		2.2	
		2.1	
		1.5	
	65 S	1.3	
		2.6	
		2.0	
		1.5	
ridge crest		1.0	
	64 S	1.1	
		1.1	
		1.3	
		1.0	1.1
		1.1	
		0.8	
		0.8	
		1.3	
	63 S	1.3	
ridge flanks		2.1	
		2.1	
		2.7	
		2.9	
	62 S	2.9	
		2.9	2.7
		2.9	
	61 S	3.1	
		2.5	
		2.8	
		2.8	
		3.1	

7.3.4 Balleny Seamounts

The two seamounts off the Balleny Islands which were crossed on track j are worth considering in some detail. As already pointed out the first of these produced a single large negative anomaly. It is obviously magnetized in the opposite direction to that of the present earth's field. Figure 48 shows the computed model and anomaly for this seamount. It consists essentially of a reversely magnetized volcanic core which gives rise to the main sharp anomaly and which must continue to considerable depth. The broader flanking anomalies indicate lava flows of considerable thickness which are also reversely magnetized and extend for 4 miles or more from the central core. It is fairly clear that an exact fit could be obtained with the observed anomaly by rounding the sharp corners of the model and extending the flanking flows with gradually decreasing thickness.

The second mount is not so simple, as the observed anomaly contains both positive and negative portions. Figure 49 shows the computed model with its anomaly. It consists of a normally magnetized volcano with a reversely magnetized central core. It has clearly been formed in two stages when the earth's field was in opposite directions. However it should be noted that although the seamount rises to within 50 fathoms of the surface, the minimum depth which will fit the observed anomaly is 500 fathoms. Any shallower source requires considerably steeper anomaly gradients than are in fact observed. It appears that the effect of the upper parts of the mount have been hidden by that of the remainder. This means that the effective susceptibility contrast of the upper parts must be considerably less than that of the body of the mount, possibly because of the effective cancellation of normal and reversely magnetized lava flows.

These two models have been constructed by considering the source to be a dyke-like body as for the earlier cases. In the case of an isolated seamount, as these two mounts presumably are, the dyke model

is not accurate. Prismatic bodies such as were mapped by Vacquier et al. (1951) would be a better representation of the source. However with only a single profile across the mounts no information on lateral extent is available so that it is difficult to choose a suitable model. The fact that such good agreement between computed and observed anomalies can be obtained, particularly for the first mount, indicates that the dimensions of the mount in the direction at right angles to the track are at least as great as those along the track. The fact that there is such a large discrepancy in the depth of the observed mount and computed model in the second case could be partly due to this inadequacy of the model.

CHAPTER 8

SUMMARY and CONCLUSIONS

The work described in this thesis has been largely of an exploratory nature. There are however a number of definite conclusions which can be drawn from the results obtained. These conclusions are summarized in this chapter.

8.1 Equipment

A proton magnetometer has been constructed which can be operated at sea for long periods of time with relatively little maintenance. The adaption of the magnetometer to a direct reading instrument has reduced the work of analysis to a minimum, and, combined with the analogue readout, has enabled on the spot comparisons to be made with existing records.

The seismic reflection profiler has been developed to such a stage that on future trips it should be possible to obtain good reflection profiles in water depths of at least 2,000 fathoms, with the ship travelling at speeds of up to 10 knots. Although the pneumatic gun constructed has not yet been used, results obtained by the Lamont Geological Observatory suggest that excellent records can be obtained with this sound source.

8.2 Regional Field

A total magnetic field map of the region between New Zealand and Antarctica has been constructed for epoch 1964.5. Comparison with other data available for the region indicates a predominantly westward drift of the field at a rate of about 0.25°/year, with a somewhat higher rate in the vicinity of the magnetic pole. This is consistent with present knowledge of the earth's magnetic field in these regions.

A regional anomaly map has also been constructed. This indicates a probable thickening of the magnetic basement just south

of the edge of the New Zealand Plateau, and across the flanks of the Pacific-Antarctic Ridge. The thickening across the flanks of the ridge is probably caused by an increase in the depth of the Curie point isotherm away from the ridge crest. The thickening along the continental margin could also be the result of an increased depth in the Curie point isotherm. One would certainly expect such an increase if the continents are situated over a descending convection current. Dietz's theory of ocean floor spreading would also suggest an increase in the thickness of the crustal material at the ocean-continental margin due to the compression resulting from the ocean floor moving against and under the stationary continent. Certainly these features of the regional anomaly map are consistent with present ideas in which convection in the mantle is a prime force in the evolution of the earth's crust. Measurements of heat flow across these regions of positive regional anomalies should indicate whether or not they are due to differences in level of the Curie point isotherm.

8.3 Campbell Plateau

The Campbell Plateau is completely different to the greater part of the New Zealand Plateau over which small broad anomalies, characteristic of a deep magnetic basement, are usually obtained. The magnetic record here indicates a complex basement structure. Essentially the plateau appears to be a region of uplifted basement over which there is considerable basement relief, the peaks rising to within a short distance of the sea floor. Three major basement ridges are indicated in the records and these contain a number of highly magnetic intrusions suggesting considerable faulting. A more detailed survey, which should include other geophysical measurements, is required over this region. It should be possible to map the basement relief with the seismic profiler described in this thesis. Gravity and seismic refraction measurements would help to clarify the crustal structure.

8.4 Southwest Pacific Basin

The magnetic records across the basin indicate a lineated pattern in a predominantly east-west direction which to the north, closely parallels the edge of the plateau, while to the south, tends more towards the direction of the Pacific-Antarctic Ridge. The Macquarie-Balleny Ridge seems to have had little effect on this pattern, possibly because it is a relatively young offshoot of the main ridge. Correlation of anomalies has been followed across the whole area studied, a distance of some 10° of longitude. An offset in the magnetic pattern is apparent along a line striking 9°E of S and meeting the plateau at $50^{\circ}20'$S 176°E. This corresponds to the sharp change in the direction of the edge of the plateau. The magnetic records indicate that the offset is caused by movement of the ocean crust against the continent. An indication that pressure has been built up by the ocean crust moving against the plateau is given by the difference in length of the magnetic records to the west of the discontinuity as compared with those to the east. Such movement would presumably produce a positive regional anomaly along the continental margin as observed. The fact that there is no evidence of a fracture zone where this discontinuity, if produced south, meets the ridge, that there is a marked decrease in the displacement along the discontinuity towards the south, and that the lineated pattern cannot be followed south of the basin, place considerable doubt on the interpretation of this feature as a transcurrent fault. More measurements in the vicinity of the discontinuity are required, particularly some east-west profiles, before the actual nature of it can be determined. What does appear to be fairly clear is that there is movement of the ocean crust against the continent and that this has resulted in the crustal features tending to become aligned parallel to the continental margin. The differential movement evident across the discontinuity may be due simply to the shape of the continental margin or may be due to a real difference in the rate of growth of the crust on both sides of the line.

The source of the anomalies obtained over the basin cannot be determined uniquely from the data available. The fit of the dyke model (figure 44) to the observed profile indicates the type of source, i.e. long narrow flat-topped source, the top of the source being practically coincident with the ocean floor. The base of the source is at a depth of about 7 miles although this is not well defined by the magnetic record. The actual source could be a system of dykes, or blocks of alternately normal and reversely magnetized rocks. If the latter were the case, a gravity profile across the basin would help to settle the question, since one would not expect to obtain good correlation between gravity and magnetic profiles. On the other hand one would expect some correlation if a system of dykes did in fact exist.

8.5 Pacific-Antarctic Ridge

At the southern edge of the basin the magnetic record changes in character. Whereas to the north across the basin there is good correlation across the tracks, to the south across the ridge flanks there is little correlation between even the closer tracks. There are indications that a detailed survey would reveal some trends paralleling the ridge. It is possible that the increased topography across the ridge flanks is in part the cause of the loss of correlation. However lack of correlation between bathymetric and magnetic profiles indicates that changes in topography are not a major source of anomalies. It seems likely that the lack of correlation indicates a decay of the ridge with a consequent distortion of earlier simple trends.

A division of the ridge into three distinct regions is possible from the magnetic record. (1) The lower flanks, characterised by large, broad anomalies with little or no correlation across widely spaced tracks. (2) The upper flanks, defined by much smaller anomalies. (3) The axial zone, defined by the large, steep-sided axial anomaly. On tracks west of 175°E the axial anomaly appears associated with a rift

valley but to the east, although there still appears to be a rift valley, the axial anomaly is located slightly to the north.

Calculations indicate that the observed anomalies over the ridge are caused mainly by highly magnetic bodies intruded along fractures in the ridge. It is suggested that the region of subdued anomalies is due to a general increase in the susceptibility of the rock forming the ridge, resulting in a decrease in the susceptibility contrast of any intrusions. Such an increase in susceptibility could be the cause of at least part of the positive regional anomaly observed over the flanks. Some of the intrusions are magnetized in the opposite direction to that of the earth's present field. The change from a predominantly positive axial anomaly, observed on tracks west of 175°E, to a negative one on tracks east of 175°E indicates that the main axial source in the two regions was formed at different times.

The main feature emerging from the bathymetric profiles across the ridge is the asymmetry of the ridge in this region. This is due to the proximity of the Antarctic continent to the ridge here. The Balleny Plateau probably forms some sort of link between the two as measurements on basement depth indicate that the basement rock also exhibits a similar asymmetry across the ridge. The northern side of the ridge shows a similar step type formation to that observed in crossings of the Mid-Atlantic Ridge.

8.6 Balleny Plateau

The magnetic records obtained over this region suggest a basement depth of 2000-2500 fathoms. Thus it appears that because of the proximity of Antarctica the southern flanks of the ridge are connected to the continent by the plateau. There is therefore no evidence of the movement of the ridge away from Antarctica suggested by Wilson (1965) in this region. East of Scott Island however the ridge has broken away from the continent and is separated from it by the Pacific-Antarctic Basin. This might be evidence of movement of the

ridge such as suggested by Wilson. There are too few results available at present to determine much about the structure of the Balleny Plateau. The region is certainly volcanic but like the Azores Plateau of the North Atlantic is an anomalous region of the mid-ocean ridge system.

8.7 Ross Sea

There is little doubt that this is part of the Antarctic continental shelf. The unusual depth of the shelf is almost certainly due to ice loading during glacial periods. Lisitzin and Zhivago (1960) state in connection with the continental shelf west of the Balleny Islands, "The regularity in the structure of the shelf could not be accidental and it is, undoubtedly, connected with a comparatively recent regression of the edge of the continental ice; this process is still continuing." The few magnetic anomalies observed over the Ross Sea are consistent with a deep basement as expected over a continental shelf.

8.8 Future Work

In conclusion I am of the opinion that geophysical measurements must be continued in this interesting and little known region of the ocean. Although considerable information can still be obtained from magnetic measurements there is a definite need for correlating these with other measurements. The use of the seismic profiler on future Antarctic trips should provide interesting information, particularly over the Campbell and Balleny Plateaus. It is important also to determine the basement topography across the basin in order to ascertain whether similar topography to that observed over the ridge flanks does occur under the basin sediments. Gravity profiles would yield considerable additional information over the whole region.

There is a definite need for carrying out detailed surveys of each of the three main divisions, Campbell Plateau, Southwest Pacific Basin, Pacific-Antarctic Ridge. Such a survey over the Campbell

Plateau could be accomplished during an oceanographic cruise of H.M.N.Z.S. Endeavour. Detailed surveys of the other regions would be more difficult to arrange with the ships at present available. For such surveys some more reliable navigational system is necessary such as the satellite navigational system at present being investigated at Victoria University. This problem of navigational accuracy will also become more important as more profiles are obtained and the spacing between adjacent profiles decreases.

APPENDIX 1

MODIFICATIONS TO THE MAGNETOMETER

(1) All-transistor Preamplifier

The modified switching of the polarizing current described in chapter 4.3.5 has practically eliminated the large voltage transients which occur during the switch-off of the polarizing field, and which can damage the input circuit of the preamplifier. An all-transistor preamplifier has now been assembled to replace the hybrid circuit described in chapter 4.3.1. The new preamplifier uses the Allison model 660 preamplifier module followed by an emitter follower stage to match it into the low impedance of the cable. The input of the preamplifier is protected by two power diodes connected back to back across the input lead from the relay. These diodes limit the input voltage to 0.5 volt, while having a sufficiently high peak inverse voltage rating to withstand the comparatively small coil transients which still occur should the preamplifier be connected to the coil before these have time to decay. The preamplifier power requirements are 1 mA at 18 V, and this can easily be supplied by batteries in the fish. This leaves a conductor in the cable to be used as an earth return for coil and preamplifier, thus eliminating the need to carry power and signal voltages on the cable screen. In this way cable noise can be considerably reduced without resorting to a special cable.

(2) Locked Oscillator Multiplier

Serson (1961) described a direct reading magnetometer in which the multiplication is achieved by using a local oscillator locked onto a multiple of the precession signal frequency. This method has the advantage that it will discriminate against noise to some extent, thus providing reliable counts even when the signal-to-noise ratio is poor. This improvement is achieved by the use of a phase discriminator to

provide the error signal required to keep the local oscillator on frequency. Since the error signal arises from the averaging of a number of cycles of the two signals fed to the discriminator, random noise pulses have comparatively little effect. The multiplied frequency fed to the counter comes from the local oscillator and is therefore free of noise generated in the amplifiers and cable. A further advantage in some circumstances is that the multiplication factor can be made very large with little increase in complexity.

A similar multiplier to that described by Serson was constructed for trial with the magnetometer described in chapter 4. Tests showed that reliable measurements could be obtained with this circuit when the signal-to-noise ratio was too small for consistent counts to be obtained with the multiplier of chapter 4.3.2. With the preamplifier incorporated in the fish however this improvement was not required. The unit built had the disadvantage that it drifted out of lock because of the drift of the local oscillator. This could presumably be overcome by careful design of the oscillator. For the present use, where a multiplication of eight times is sufficient, the simplicity of the circuit described in chapter 4.3.2 has much to commend it.

APPENDIX 2

SUMMARY OF RESULTS OBTAINED DURING DECEMBER 1965

During the summer of 1965-66 two further trips were made to Antarctica with the magnetometer. The writer was on the first of these (December 10, 1965 - January 8, 1966) during which 4,000 miles of magnetic recordings were made. A brief summary of the results obtained is presented here. A detailed analysis will be presented elsewhere.

On the trip to Antarctica a course of 171° was followed from 45°S, 173°E, until just north of Scott Island. Magnetometer readings were obtained from off Banks' Peninsula until the magnetometer had to be brought in because of ice and fog at 62°14'S, 178°18'E. This was before the crest of the Pacific-Antarctic Ridge was reached. Across the basin the records confirm earlier results the correlation being excellent, particularly over the central portion.

The return trip was along longitude 180°E from 68°S to Bounty Island. From Bounty Island to Wellington a course of 332° was followed. Good magnetic records were obtained from 75°S to 42°S. Two breaks of a few hours occur in the return record, one south of the ridge because of ice conditions, the other on the northern edge of the basin because of flooding of the fish due to an unpredicted stop of the ship. The records across the basin and ridge for this track are shown in figures 50 and 51, together with those of track h (along longitude 178°E) for comparison purposes. Across the basin the anomaly profiles only are given since the topography is essentially flat. Over the ridge the bathymetry and total field records are plotted.

The record across the basin again confirms the correlation of earlier records and indicates that the anomaly pattern east of 178°E again follows an east-west pattern, at least to as far as 180°E. To add this track to the anomaly contour map of figure 40 requires little

more than an extension of the contours already plotted.

Over the ridge a similar pattern to that described for earlier tracks occurs. The axial anomaly here consists of a number of sharp peaks from 500-1000 gamma in amplitude. The axial zone defined by this anomaly is somewhat broader than on earlier tracks. This is in agreement with tracks obtained by the U.S. Navy Hydrographic Office east of 180°E. The anomaly pattern over the crest appears to correlate well with the bathymetry record. There appears to be a rift valley present, but as for track h, the sharpest anomalies occur slightly to the north of the valley.

Over the northern flanks the region of subdued anomalies extends considerably further north than on any other track so far obtained reaching to 60°S, although a few large anomalies do occur over this region. Nor is there evidence of an appreciable regional anomaly over the flank although an anomaly of about 150 gamma amplitude probably does occur between 60°-61°S. The bathymetry record over the ridge shows the same step regions indicated on the earlier tracks.

Scott Island rises out of the southern flanks about 150 miles south of the crest of the ridge. South of Scott Island the track crosses a further 100 miles of the Balleny Plateau, this portion of the plateau being extremely flat at a depth of 2000 fathoms. Depth calculations from the anomalies occurring again suggest that the basement rock is at a depth of 2 - 2.5 miles.

Over the Campbell Plateau a particularly large anomaly is observed at latitude 49°00' - 49°25'S and indicates that the southern basement ridge of figure 37 extends to the east of Antipodes Islands but slightly to the south of how it is extrapolated in this figure. East of Bounty Islands the anomaly is somewhat reduced but probably does run out towards the edge of the plateau.

APPENDIX 3

CALCULATION OF ANOMALY MODELS

The equation for the anomaly due to a dyke of horizontal width t at a depth z below the plane of observation, is given by;

$$T = 2J\sin\theta\left[\sin(\phi - I - \theta)(\alpha_1 - \alpha_2) - \cos(\phi - I - \theta)\log\frac{r_1}{r_2}\right] \quad .....(1)$$

where J is the resultant tranverse intensity of magnetization making an angle ϕ with the horizontal, I the direction lying in the vertical plane containing the magnetic meridian in which the anomaly is measured, θ the geological dip of the dyke and (r_1, α_1), (r_2, α_2) the coordinates of the edges of the dyke referred to the point of observation. This equation applies to a dyke with a strike perpendicular to the magnetic meridian. If the strike direction makes an angle β with the magnetic east-west direction the equation can be written in the same form;

$$T = 2J'\sin\theta\left[\sin(\phi - I' - \theta)(\alpha_1 - \alpha_2) - \cos(\phi - I' - \theta)\log\frac{r_1}{r_2}\right] .....(2)$$

where

$$J' = J(\cos^2 I \cos^2\beta - \sin^2 I)^{\frac{1}{2}}$$

$$I' = \tan^{-1}\left(\frac{\tan I}{\cos\beta}\right)$$

The first term in this equation is an amplitude term while that inside the brackets controls the shape of the anomaly. Of the two terms inside the brackets the first predominates in high latitudes and the second in low latitudes, assuming the magnetization is in the direction of the earth's field. Over the present region the inclination of the earth's field is 80° or more. Assuming this is also the inclination of the magnetization of the dyke we can simplify the equation by assuming a vertical field, and assuming also that $\phi = I$ (as it will for $\beta = 0$) we have as the equation of the anomaly;

$$T = 2J\sin\theta\sin(180 - \theta)(\alpha_1 - \alpha_2) \quad .... (3)$$

For a vertical dyke the equation simplifies even further to;

$$T = 2J(\alpha_1 - \alpha_2) \quad \ldots\ldots\ldots\ldots\ldots\ldots\ldots\ldots\ldots\ldots \quad (4)$$

For most calculations over the region studied equation 4 can be used with good accuracy, particularly for preliminary calculations. Except over the basin region there is little information available to enable a value for β to be determined. Results obtained by other workers suggest that the main sources of anomalies at sea approximate well to a vertical dyke model.

Thus over the region being studied the shape of the anomaly depends on $(\alpha_1 - \alpha_2)$ which in turn depends on the depth to width ratio of the dyke. Using equation 4 it is a simple matter to draw a series of anomaly curves for various depth to width ratios, assuming a unit magnetization for the models. For regions such as the Southwest Pacific Basin, where the profile consists of a series of more or less isolated anomalies, it is then possible to compute a model basement for the profile by selecting the model curve of the right shape for each anomaly and determining the value of magnetization required to obtain the observed amplitude. The magnetization J is equal to $\frac{H}{2T}$ where H is the observed anomaly amplitude and T the theoretical anomaly amplitude for unit magnetization. It is normal practice to define an effective susceptibility contrast for the source defined by $k = \frac{F}{J}$ where F is the value of the earth's total field at the source. If the magnetization is produced by induction in the earth's field this effective susceptibility contrast is the true susceptibility contrast between the source and the surrounding rock. However if appreciable remanence exists, as is likely in most oceanic rocks, then the true susceptibility contrast is less than the effective susceptibility contrast. For the case of negative anomalies produced by a reversely magnetized body, the calculated magnetization is negative. An effective susceptibility, defined as before as $\frac{F}{J}$ has still been quoted for these cases and is of course negative. In this case the whole of the calculated magnetization

is due to the remanent magnetization and in fact the calculated magnetization is somewhat less than the true remanent magnetization since some is required to cancel the induced magnetization of the present field.

Up to now we have been considering dykes of infinite thickness. In fact the base of the magnetic dykes is certainly no deeper than the Curie point isotherm. In deep ocean regions therefore it may not be a good approximation to assume an infinitely thick dyke. The finite thickness of a dyke may be allowed for by subtracting from the original computed anomaly, the anomaly of an infinite dyke with its top surface at a depth equal to the base of the required finite dyke. For example, suppose it is required to calculate the anomaly of a dyke 9 miles wide at a depth of 3 miles and thickness 6 miles. Two anomaly curves are constructed, one for an infinitely thick dyke with depth to width ratio of 1 : 3, and a second for a similar dyke with depth to width ratio of 1 : 1. Subtraction of the second from the first gives the required anomaly.

Calculation of basement models over regions where a number of interacting anomalies occur is more difficult as these regions require the addition of a number of the simple dyke-type models to make up a more complex model. Because of the small interaction between adjacent blocks of material it is possible to build up a quite complex model using a few finite dyke models as building blocks.

APPENDIX 4

COMPARISON OF ANOMALY PROFILES

A figure for the agreement between observed and calculated profiles can be obtained using correlation methods.

The correlation coefficient ρ for two curves X and Y whose average value is zero is defined as;

$$\rho = \frac{\sum x_i y_i}{\sqrt{\sum x_i^2 \sum y_i^2}} \quad \ldots\ldots\ldots\ldots\ldots\ldots\ldots\ldots \quad (1)$$

where x_i and y_i are the ith values of X and Y, and the sums are taken over all values in the required range. If the average values of the two curves are not zero equation 1 can be written in the form;

$$\frac{\sum x_i y_i - N\bar{x}\bar{y}}{\sqrt{(\sum x_i - N(\bar{x})^2)(\sum y_i - N(\bar{y})^2)}} \quad \ldots\ldots\ldots\ldots\ldots \quad (2)$$

where $\bar{x}$ and $\bar{y}$ are the average values of X and Y respectively. A correlation of 1 indicates exact correlation and a coefficient of 0 indicates no correlation.

Correlation coefficients have been calculated for the observed and calculated anomaly profiles over the models of chapter 7. In all cases the coefficients obtained have been in the range 0.95 - 1.00, most of the values being very close to 1.

An attempt has been made to obtain a correlation coefficient to describe the similarity of observed profiles across the Southwest Pacific Basin. Because of the variations in length of profiles, and or parts of profiles, it is difficult to obtain a meaningful coefficient. For example, profiles b and d were taken as one example. A constant scaling factor $k = \frac{y}{x}$ was used in the comparison of the two profiles, where x was the length of profile b being considered and y was the length of the similar portion of d. In this case $y = 0.8x$. A correlation coefficient of 0.26 was obtained. The reason for the small value was

that over the central portion of the basin, because of the constant scaling factor, several anomaly maxima on one profile were occurring over minima on the other even though the anomalies correlated well. This type of variation in distance of anomalies along a profile from profile to profile and also variations in width of the anomalies is quite reasonable and does not invalidate the correlation at all, particularly when it is likely that different parts of the features outlined by the anomalies are under different pressures. Thus it seems unreasonable to expect to be able to calculate a high correlation coefficient for the anomalies shown in figure 38 across the type of discontinuity which is apparent in these results. A correlation coefficient for individual anomalies could of course be obtained. However the visual similarity obvious from figures 38 and 39 appears to be the best guide to whether or not the features are continuous across the region.

REFERENCES

A

Adam, N. V., N. P. Ben'kova, V. P. Orlov and L. O. Tyurmina, 1964. Western drift of the geomagnetic field. Geomagnetism and Aeronomy, 4, 434-441.

Adams, R. D., 1962. Thickness of the earth's crust beneath the Campbell Plateau. N.Z. J. Geol. Geophys., 5, 74-85.

Adams, R. D., 1964. Thickness of the earth's crust beneath the Pacific-Antarctic Ridge. N.Z. J. Geol. Geophys., 7, 529-542.

Adams, R. D. and D. A. Christoffel, 1962. Total magnetic field surveys between New Zealand and the Ross Sea. J. Geophys. Res., 67, 805-813.

Anderson, V. C., 1953. Wide band sound scattering in the deep scattering layer. Scripps Inst. Oceanog. Ref., 53-36. 35 pp.

Arons, A. B. and D. R. Yennie, 1948. Energy partition in underwater explosion phenomena. Rev. Mod. Phys., 20, 519-536.

B

Beckmann, W. C., A. C. Roberts and B. Luskin, 1959. Sub-bottom depth recorder. Geophysics, 24, 749-760.

Bennett, H. F., 1964. A gravity and magnetic survey of the Ross Ice Shelf area Antarctica. Univ. Wisconsin Geophys. and Polar Res. Centre Res. Rep., 64-3.

Bentley, C. R., A. P. Crary, N. A. Ostenso and E. C. Thiel, 1960. Structure of West Antarctica. Science, 131, 131-136.

Bloch, F., 1946. Nuclear Induction. Phys. Rev., 70, 460-474.

Brodie, J. W., 1965. Oceanography. In Antarctica, 101-127, T. Hatherton, ed. Methuen & Co. Ltd., London.

Bruckshaw, J. M. and K. Kunaratnam, 1963. The interpretation of magnetic anomalies due to dykes. Geophys. Prospecting, 11, 509-522.

Bullard, E. C., 1961. Forces and processes in ocean basins. In Oceanography, 39-50. Mary Sears, ed. Amer. Assoc. for the Advancement of Science, Washington, D.C.

Bullard, E. C., 1963. The flow of heat through the floor of the ocean. In The Sea, 3, 218-232. M. N. Hill, ed. Interscience Publishers, London, New York.

Bullard, E. C., C. Freedman, H. Gillman and I. Nixon, 1950. The westward drift of the earth's magnetic field. Phil. Trans. Roy. Soc. London, A243, 67-97.

Bullard, E. C., C. S. Mason, and J. D. Mudie, 1964. Curious behaviour of a proton magnetometer. Proc. Camb. Phil. Soc., 60, 287-293.

Bullard, E. C. and R. G. Mason, 1961. The magnetic field astern of a ship. Deep-Sea Res., 8, 20-27.

Bullard, E. C. and R. G. Mason, 1963. The magnetic field over the oceans. In The Sea 3, 175-217. M. N. Hill, ed. Interscience Publishers, London, New York.

Bullard, E. C., A. E. Maxwell and R. Revelle, 1956. Heat flow through the deep ocean floor. Advances in Geophys., 3, 153-181.

Burrows, A. L., 1963. Location of the South Magnetic Pole. N.Z. J. Geol. Geophys., 6, 454-464.

C

Chadwick, P., 1962. Mountain-building hypotheses. In Continental Drift, 195-234. S. K. Runcorn, ed. Academic Press, New York, London.

Christoffel, D. A., 1961. Total magnetic field measurements between New Zealand and Antarctica. Nature, 190, 776-778.

Christoffel, D. A., 1961. A total magnetic field survey conducted between New Zealand and Antarctica and in the Ross Sea. Univ. British Columbia Rep. 3.

Christoffel, D. A., and D. I. Ross, 1965. Magnetic anomalies south

of the New Zealand Plateau. J. Geophys. Res., 70, 2857-2861.

Cullington, A. W., 1963. The geomagnetic secular variation in the Ross Dependency. N.Z. J. Geol. Geophys., 6, 444-453.

D

Daly, R. A., 1936. Origin of submarine canyons. Amer. J. Sci. 31, 401-420.

Dietz, R. S., 1961. Continent and ocean basin evolution by spreading of the sea floor. Nature, 190, 854-857.

Dorman, J., M. Ewing and J. Oliver, 1960. Study of the shear velocity distribution in the upper mantle by mantle Rayleigh waves. Bull. Seism. Soc. Amer., 50, 87-116.

Drake, C. L., J. Heirtzler and J. Hirshman, 1963. Magnetic anomalies off Eastern North America. J. Geophys. Res., 68, 5259-5275.

Drake, C. L. and R. W. Girdler, 1964. A geophysical study of the Red Sea. Geophys. J., 8, 473-495.

Dunn, S. C., 1951. Twin-T circuits. Wireless Engineer, 28, 162.

E

Edgerton, H. E., 1963. Underwater photography. In The Sea, 3, 473-479. M. N. Hill, ed. Interscience Publishers, London, New York.

Edgerton, H. E. and G. G. Hayward, 1964. The boomer sonar source for seismic profiling. J. Geophys. Res., 69, 3033-3042.

Elsasser, W. M., 1950. The earth's interior and geomagnetism. Rev. Mod. Phys., 22, 1-35.

Evison, F. F., 1960. The growth of continents by plastic flow under gravity. Geophys. J., 3, 155-189.

Evison, F. F., C. E. Ingham, R. H. Orr and J. H. Lefort, 1960. Thickness of the earth's crust in Antarctica and the surrounding oceans. Geophys. J., 3, 289-306.

Ewing, J. I., 1963. Elementary theory of seismic refraction and reflection measurements. In The Sea 3, 3-19. M. N. Hill, ed. Interscience Publishers, London, New York.

Ewing, J. I. and M. Ewing, 1959. Seismic refraction measurements in the Atlantic Ocean basin, in the Mediterranean Sea, on the mid-Atlantic ridge, and in the Norwegian Sea. Bull. Geol. Soc. Amer. 70, 291-318.

Ewing, J. I. and G. B. Tirey, 1961. Seismic profiler. J. Geophys. Res. 69, 2917-2927.

Ewing, J. I. and R. Zaunere, 1964. Seismic profiling with a pneumatic sound source. J. Geophys. Res. 69, 4913-4915.

Ewing, M., B. C. Heezen, D. B. Ericson, J. Northrop and J. Dorman, 1953. Exploration of the Northwest Atlantic mid-ocean canyon. Bull. Geol. Soc. Amer. 64, 865-868.

Ewing, M. and B. C. Heezen, 1956. Some problems of Antarctic submarine geology. In Antarctica in the I.G.Y., 75-81. A Crary et al., ed. Geophys. Mono. 1, Amer. Geophys. Union, Washington D.C.

Ewing, M. and M. Landisman, 1961. Shape and structure of ocean basins. In Oceanography, 3-38. Mary Sears, ed. Amer. Assoc. for Advancement of Science, Washington D.C.

Ewing, M. and F. Press, 1950. Crustal structure and surface wave dispersion. Bull. Seism. Soc. Amer., 40, 271-280.

Ewing, M. and F. Press, 1952. Crustal structure and surface wave dispersion, part 2. Bull. Seism. Soc. Amer. 42, 315-325.

Ewing, M. and F. Press, 1955. Geophysical contrasts between continents and oceans. Geol. Soc. Amer. Spec. Paper, 62, 2917-2927.

F

Fairi, G. and O. Svelto, 1962. Signal to noise considerations in a nuclear magnetometer. Nuovo Cimento Suppl. Series X, 23, 55-65.

Fleming, J. A., 1948. Trans. Assoc. Terr. Mag. a. Electr. Inter. Un. Geod. Geophys., Oslo, 37.

G

Gerard, R., M. G. Langseth and M. Ewing, 1962. Thermal gradient measurements in the water and bottom sediment of the Western Atlantic. J. Geophys. Res. 67, 785-803.

Girdler, R. W. and G. Peter, 1960. An example of the importance of natural remanent magnetization in the interpretation of magnetic anomalies. Geophys. Prospecting, 8, 474-483.

Grant, F., 1957. A problem in the analysis of geophysical data. Geophysics, 22, 309-344.

Green, R., 1960. Remanent magnetization and the interpretation of magnetic anomalies. Geophys. Prospecting, 8, 98-110.

Guilcher, A., 1963. Continental shelf and slope. In The Sea, 3, 281-311, M. N. Hill, ed. Interscience Publishers, London, New York.

Gutenburg, B., 1955. Wave velocities in the earth's crust. Geol. Soc. Amer. Spec. Paper 62, 19-34.

H

Hall, D. H., 1959. Direction of polarization determined from magnetic anomalies. J. Geophys. Res. 64, 1945-1954.

Hamilton, E. L., 1961. Stratigraphy of the deep sea floor. In Oceanography, 51-84. Mary Sears, ed. Amer. Assoc. for Advancement of Science, Washington D.C.

Harrison, J. C., 1959. Tests of the La Coste - Romberg surface-ship gravimeter I. J. Geophys. Res., 64, 1875-1881.

Hays, W. W. and L. Scharon, 1963. An example of the influence of remanent magnetization on magnetic intensity measurements. Geophysics, 28, 1037-1048.

Heezen, B. C., Ewing, M. and D. B. Ericson, 1951. Submarine topography in the North Atlantic. Bull. Geol. Soc. Amer., 62, 1407-1409.

Heezen, B. C. and M. Ewing, 1952. Turbidity currents and submarine slumps, and the Grand Banks earthquake. Amer. J. Sci., 250, 849-873.

Heezen, B. C. and M. Ewing, 1956. Some problems of Antarctic submarine geology. In Antarctica in the I.G.Y., 75-81. Geophys. Mono. I. A. Crary et al., ed. Amer. Geophys. Union, Washington D.C.

Heezen, B. C. and M. Ewing, 1963. The mid-ocean ridge. In The Sea, 3, 388-410. M. N. Hill, ed. Interscience Publishers, London, New York.

Heezen, B. C. and A. S. Laughton, 1963. Abyssal Plains. In The Sea 3, 312-364. M. N. Hill, ed. Interscience Publishers, London, New York.

Heezen, B. C., M. Tharp and M. Ewing, 1959. The floors of the oceans, I. The North Atlantic. Geol. Soc. Amer. Spec. Paper, 65, 125 pp.

Heezen, B. C. and M. Tharp, 1961. Physiographic diagram of the South Atlantic, the Caribbean, the Scotia Sea, and the eastern margin of the South Pacific Ocean. Geol. Soc. Amer.

Heirtzler, J. R. and X. Le Pichon, 1965. Crustal structure of the mid-ocean ridges 3. Magnetic anomalies over the Mid-Atlantic Ridge. J. Geophys. Res. 70, 4013-4033.

Henderson, R. G. and I. Zietz, 1948. Analysis of total magnetic intensity anomalies produced by point and line sources. Geophysics, 13, 428-436.

Herdman, H. F. P., J. D. H. Wiseman, and D. O. Cameron, 1956. Proposed names of features on the deep sea floor, 3. Southern or Antarctic Ocean. Deep-Sea Res., 3, 253-261.

Hersey, J. B., 1963. Continuous reflection profiling. In The Sea, 3, 47-72. M. N. Hill, ed. Interscience Publishers, London, New York.

Hersey, J. B. and S. T. Knott, 1963. Sonar for exploring the sediments and crust beneath the oceans. J. Brit. I.R.E. 26, 245-249.

Hess, H. H., 1954. Geological hypothesis and the earth's crust under the oceans. Proc. Roy. Soc. A222, 341-348.

Hess, H. H., 1955. Serpentines, orogeny and epeirogeny. Geol. Soc. Amer. Spec. Paper, 62, 391-407.

Hill, M. N., 1957. Recent geophysical exploration of the ocean floor. In Physics and Chemistry of the Earth, 2, 129-163. L. E. Ahrens et al., ed. Pergamon Press, London.

Hill, M. N., 1959. A ship-borne nuclear-spin magnetometer. Deep-Sea Res. 5, 309-311.

Hill, M. N., 1960. A median valley of the Mid-Atlantic Ridge. Deep-Sea Res., 6, 193-205.

Hill, M. N., 1963. Single-ship seismic refraction shooting. In The Sea, 3, 39-46. M. N. Hill, ed. Interscience Publishers, London, New York.

Hood, P., 1964. The Konigsberger ratio and the dipping dyke equation. Geophys. Prospecting, 12, 440-456.

Hough, J. L., 1950. Pleistocene Lithology of Antarctic Ocean-bottom sediments. J. Geol., 58, 254-260.

Hvorslev, M. J. and H. C. Stetson, 1946. Free-fall coring tube. A new type of gravity bottom sampler. Bull. Geol. Soc. Amer., 57, 935-950.

K

Knott, S. T. and J. B. Hersey, 1956. Interpretation of high-resolution echo-sounding techniques and their use in bathymetry, marine geophysics, and biology. Deep-Sea Res., 4, 36-44.

Kuenen, P. H., 1953. Origin and classification of submarine canyons. Bull. Geol. Soc. Amer., 64, 1295-1314.

L

La Coste, L., 1959. Surface ship gravity measurements on the Texas A & M College ship the 'Hidalgo'. Geophysics, 24, 309-322.

Langseth, M. G., P. J. Grim and M. Ewing, 1965. Heat flow measurements in the East Pacific Ocean. J. Geophys. Res., 70,

367-380.

Laughton, A. S., 1963. Microphotography. In The Sea, 3, 437-472. M. N. Hill, ed. Interscience Publishers, London, New York.

Le Pichon, X., R. E. Houtz, C. L. Drake and J. E. Nafe, 1965. Crustal structure of the mid-ocean ridges 1. Seismic refraction measurements. J. Geophys. Res., 70, 319-341.

Lepley, L. K., 1964. Submarine geomorphology of Eastern Ross Sea and Sulzerberger Bay, Antarctica. Marine Geol., 2, 253-261.

Lincoln, J. V., 1964. Geomagnetic and solar data. J. Geophys. Res., 69, 1909.

Lincoln, J. V., 1965. Geomagnetic and solar data. J. Geophys. Res., 70, 3228,3763.

Lisitzin, A. P., 1962. Bottom sediments of the Antarctic. In Antarctic Res., 81-88. Geophys. Mono., 7, Amer. Geophys. Union, Washington D.C.

Lisitzin, A. P. and A. V. Zhivago, 1960. Marine geological work of the Soviet Antarctic Expedition, 1955-57. Deep-Sea Res., 6, 77-87.

Luskin, B., B. C. Heezen, M. Ewing and M. Landisman, 1954. Precision measurement of ocean depth. Deep-Sea Res., 1, 131-140.

M

Mason, R. G., 1958. A magnetic survey off the west coast of the United States. Geophys. J., 1, 320-329.

Mason, R. G. and A. D. Raff, 1961. A magnetic survey off the west coast of the United States. Bull. Geol. Soc. Amer., 72, 1259-1265.

Menard, H. W., 1958. Development of median elevations in ocean basins. Bull. Geol. Soc. Amer., 69, 1179-1186.

Menard, H. W., 1960. The East Pacific Rise. Science, 132, 1737-1746.

Menard, H. W., 1964. Marine Geology of the Pacific. McGraw-Hill Co., New York, London.

Miller, E. T. and M. Ewing, 1956. Geomagnetic measurements in the Gulf of Mexico and in the vicinity of Caryn Peak. Geophysics, 21, 406-432.

Mumme, W. G., 1964. Negative total intensity magnetic anomalies in the south east of South Australia. J. Geophys. Res., 69, 309-315.

N

Nagata, T., 1956. Rock Magnetism. Maruzen Company, Tokyo.

Nagata, T., 1962. Morphology and some interpretation of geomagnetic variations in Antarctica. In Antarctic Res. Geophys. Mono., 7, 89-110. Amer. Geophys. Union, Washington D.C.

Nason, R. D. and W. H. Lee, 1962. Preliminary heat-flow profile across the Atlantic. Nature, 196, 975.

Nason, R. D. and W. H. Lee, 1964. Heat flow measurements in the North Atlantic, Caribbean, and Mediterranean. J. Geophys. Res., 69, 4875-4883.

Nature, 1961. Continental and Oceanic Differentiation. A discussion of paper by Dietz (1961) with replies by the author. Nature, 192, 123-128.

O

Officer, C. B., 1955. Southwestern Pacific crustal structure. Trans. Amer. Geophys. Union, 36, 449-459.

Oliver, J. and J. Dorman, 1963. Exploration of sub-oceanic structure by the use of seismic surface waves. In The Sea, 3, 110-133. M. N. Hill, ed. Interscience Publishers, London, New York.

P

Packard, M. and R. Varian, 1954. Proton gyromagnetic ratio. Phys. Rev., 93, 941.

Peters, L. J., 1949. The direct approach to magnetic interpretation and its practical application. Geophysics, 14, 290-320.

Petterson, H. and B. Kullenburg, 1940. A vacuum core sampler for deep sea sediments. Nature, 145, 306.

Piggot, C. S., 1936. Apparatus to secure core samples from the ocean bottom. Bull. Geol. Soc., 47, 675-684.

Piggot, C. S., 1940. Factors involved in submarine core sampling. Bull. Geol. Soc. Amer., 52, 1513-1524.

Raitt, R. W., 1956. Seismic refraction studies of the Pacific Ocean basin, I. Crustal thickness of the central equatorial Pacific. Bull. Geol. Soc. Amer., 67, 1623-1640.

Reitzel, J., 1963. A region of uniform heat flow in the North Atlantic. J. Geophys. Res., 68, 5191-5196.

Robinson, E. S., 1964. Correlation of magnetic anomalies with bedrock geology in the McMurdo Sound area. J. Geophys. Res., 69, 4319-4326.

Roos, S. E., 1937. The submarine topography of the Ross Sea and adjacent waters. Geogr. Rev., 27, 574-583.

Ross, D. I. and B. E. G. Goodger, 1965. A 12V d.c. to 230V a.c. silicon controlled rectifier inverter. Electronic Engineering, 37, 589-591.

Rumbaugh, L. H. and L. R. Alldredge, 1949. Airborne equipment for geomagnetic measurements. Trans. Amer. Geophys. Union, 30, 836-848.

S

Serson, P. H., 1961. Proton precession magnetometer. Canadian Patent No. 618,762.

Shor, G. G., 1963. Refraction and reflection techniques and procedure. In The Sea, 3, 20-38. M. N. Hill, ed. Interscience Publishers, London, New York.

Smellie, D. W., 1956. Elementary approximations in aeromagnetic interpretation. Geophysics, 21, 1021-1039.

Steenland, N. C., 1963. Peace River aeromagnetic interpretation. Geophysics, 28, 745-755.

Sutton, D. J. and W. G. Mumme, 1957. Effect of remanent magnetization on aeromagnetic interpretation. Aust. J. Phys., 10, 547-557.

Sykes, L. R., 1963. Seismicity of the South Pacific Ocean. J. Geophys. Res., 68, 5999-6006.

T

Talwani, M., X. Le Pichon, and M. Ewing, 1965. Crustal structure of the mid-ocean ridges, 2. Computed model from gravity and seismic refraction data. J. Geophys. Res., 70, 341-353.

Taylor, G., 1930. Antarctic adventure and research. Appleton and Co. London, New York.

Thomas, C. W., 1959. Lithology and zoology of an Antarctic ocean bottom core. Deep-Sea Res., 6, 5-15.

Thompson, W. C., 1957. A genetic classification of continental shelves. Proc. 9th Pacific Science Congress, 12, 30-39.

U

U.S. Navy Hydrographic Office, 1955. The total intensity of the earth's magnetic force for the year 1955. Chart No. 1703.

U.S. Navy Hydrographic Office, 1962. Operation Deep Freeze '61. Marine geophysical investigations.

U.S. Navy Hydrographic Office, 1965. Operation Deep Freeze '62.

V

Vacquier, V., A. D. Raff and R. E. Warren, 1961. Horizontal displacements in the floor of the Pacific Ocean. Bull. Geol. Soc. Amer., 72, 1267-1270.

Vacquier, V., N. C. Steenland, R. G. Henderson and I. Zietz, 1951. Interpretation of aeromagnetic maps. Geol. Soc. Amer. Mem. 47, 151 pp.

Vening Meinesz, F. A., 1929. Theory and practice of pendulum observations at sea. Waltman, Delft.

Vening Meinesz, F. A., 1941. Theory and practice of pendulum observations at sea, Part 2. Waltman, Delft.

Vening Meinesz, F. A., 1962. Thermal convection in the earth's mantle. In Continental Drift, 145-176. S. K. Runcorn, ed. Academic Press, London, New York.

Vestine, E. H., 1953. On variations of the geomagnetic field, fluid motions, and the rate of the earth's rotation. J. Geophys. Res., 58, 127-145.

Vine, F. J. and D. H. Matthews, 1963. Magnetic anomalies over oceanic ridges. Nature, 199, 947-949.

Vine, F. J. and J. T. Wilson, 1965. Magnetic anomalies over a young oceanic ridge off Vancouver Island. Science, 150, 485-489.

Von Herzen, R., 1959. Heat flow values from the Southeastern Pacific. Nature, 183, 882.

Von Herzen, R. and S. Uyeda, 1963. Heat flow through the Eastern Pacific Ocean floor. J. Geophys. Res., 68, 4219-4250.

W

Waters, G. S. and P. D. Francis, 1958. A nuclear magnetometer. J. Sci. Instrum., 35, 88-93.

Waters, G. S. and G. Phillips, 1956. A new method of measuring the earth's magnetic field. Geophys. Prospecting, 4, 1-9.

Watford, O. B., W. A. Francis, G. B. Walker and E. B. Fabiano, 1965. Isomagnetic patterns in the regions of the 1965 dip poles. Trans. Amer. Geophys. Union, 46, 661-664.

Wilson, J. T., 1961. Continental and oceanic differentiation. Nature, 192, 125-128.

Wilson, J. T., 1965. A new class of faults and their bearing on continental drift. Nature, 207, 343-347.

Wilson, J. T., 1965. Submarine fracture zones, seismic ridges and the International Council of Scientific Unions Line; proposed western margin of the East Pacific. Nature, 207, 907-911.

Transform faults, oceanic ridges, and magnetic anomalies Southwest of Vancouver Island. Science, 150, 482-485.

Wiseman, J. D. H. and D. C. Ovey, 1954. Proposed names of features on the deep sea floor, 1. The Pacific Ocean. Deep-Sea Res., 2, 93-106.

Worzel, J. L., 1959. Continuous gravity measurements on a surface ship with the Graf Sea Gravimeter. J. Geophys. Res., 64, 1299-1315.

Worzel, J. L. and J. C. Harrison, 1963. Gravity at sea. In The Sea, 3, 134-174. M. N. Hill, ed. Interscience Publishers, London, New York.

Worzel, J. L. and C. L. Shurbet, 1955. Gravity interpretations from standard oceanic and continental sections. Geol. Soc. Amer. Spec. Paper, 62, 87-100.

Z

Zaunere, R. and J. Ewing, 1963. Seismic sound sources. Lamont Geol. Observatory Tech. Rept. 1, cu-1-63, Nonr 266 (79) Tech. Rept. 7, cu-7-63, Nobsr 85077 Geology.

JOURNAL OF GEOPHYSICAL RESEARCH VOL. 70, NO. 12 JUNE 15, 1965

Magnetic Anomalies South of the New Zealand Plateau

D. A. CHRISTOFFEL AND D. I. ROSS

Physics Department, Victoria University of Wellington
Wellington, New Zealand

Abstract. Four total magnetic field profiles between New Zealand and Antarctica are presented, and an attempt is made to analyze these in terms of the ocean floor structure. The magnetic anomaly pattern cannot be completely explained by any current theories on ocean floor formation. Good correlation between the four profiles across the ocean basin is lost where it merges into the foothill region. This suggests that the two regions may have distinctly different magnetic basement structures. The shapes of the observed magnetic anomalies indicate that the remanent magnetization of the basement rocks is important and that reversely magnetized regions occur. Lack of correlation between the magnetic and bathymetric records suggests that topography is not the primary cause of the anomalies.

Introduction. A proton magnetometer was towed from the Antarctic supply ship H.M.N.Z.S. *Endeavour* during her December 1963 supply cruise between New Zealand and McMurdo Sound. Two profiles of the total magnetic field were obtained between New Zealand and Antarctica. These supplement two profiles previously obtained in the summer of 1958–1959 [*Christoffel*, 1961; *Adams and Christoffel*, 1962]. In this communication we describe and give a preliminary interpretation of the pattern of magnetic anomalies found in the region between 54°S and 65°S and 170°E and 180°E.

Results. The track chart is given in Figure 1. Between 54°S and 59°S the tracks cross an ocean basin. South of 59°S the tracks cross part of the mid-oceanic ridge system, the crest of the ridge lying at approximately 63°S and 64°S in these longitudes.

The results are shown in Figures 2 through 6.

Discussion. It is interesting that the change from good to poor correlation across the four tracks corresponds to the boundary between the end of the smooth topography of the basin and the beginning of the more rugged topography of the foothills. This suggests a change in the source of the anomalies in the two regions. This is perhaps not surprising since the basin region is presumably comparatively stable while the whole of the ridge system is more active.

The most acceptable theory at present for the formation of flat ocean basins adjacent to a continental shelf is that they consist of an oceanic basement topography similar to that of the foothill region which has been buried by sediment carried off the continental shelf by

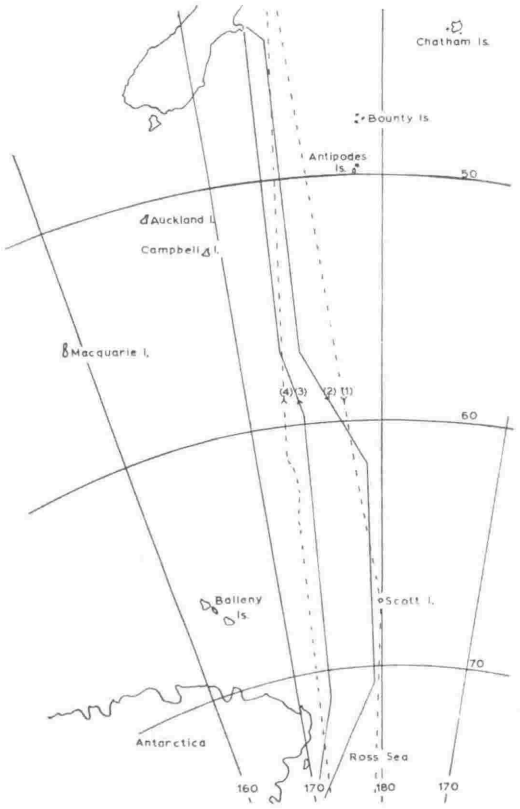

Fig. 1. Track chart. Tracks 1 and 4, summer 1958–1959. Tracks 2 and 3, December 1963.

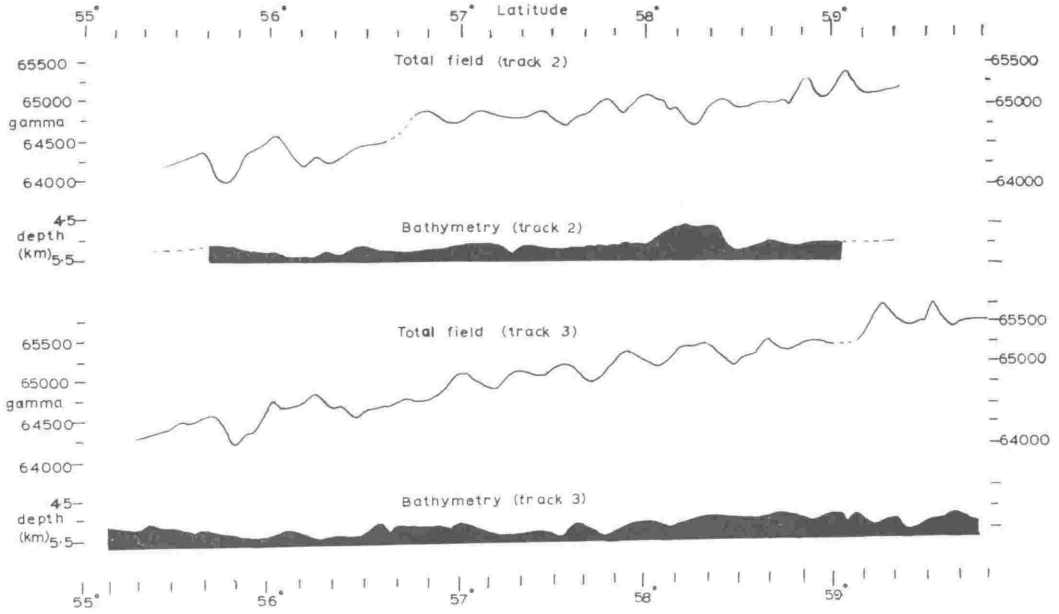

Fig. 2. Total field and bathymetric profiles across the basin for tracks 2 and 3. Despite the smooth topography, the magnetic profile exhibits large anomalies of 200 to 400 γ ($1\ \gamma = 10^{-5}$ gauss). There is no apparent relation between the bathymetry and the magnetic profiles.

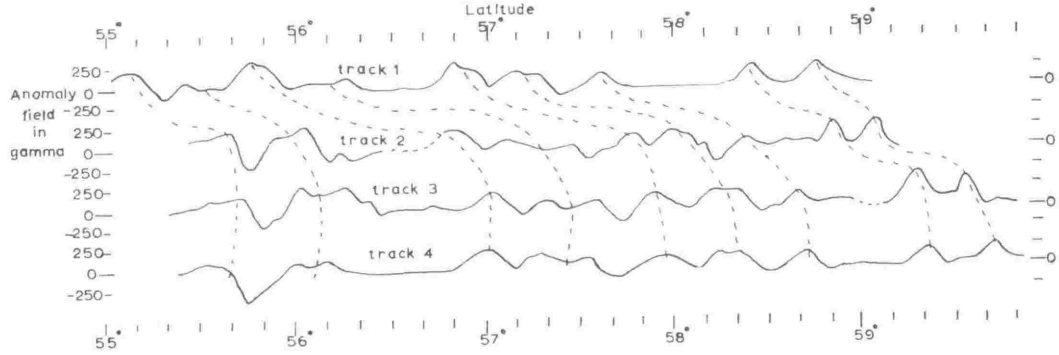

Fig. 3. Magnetic anomaly profiles for all four tracks across the basin. A smooth regional field value has been subtracted from the original profiles. The dotted lines indicate the assumed correlation across the four tracks. The pattern of correlations confirms and extends that suggested by *Christoffel* [1961].

turbidity currents [*Heezen et al.*, 1951; *Ericson et al.*, 1952; *Heezen and Laughton*, 1963]. If this is the case, the magnetic record could well reflect the buried topography. This would imply that the buried topography consisted of a series of approximately parallel ridges running in an east-west direction. However, if the magnetic anomaly pattern does result from the buried topography, one would not expect a sudden change in the correlation at the basin boundary. Rather one would expect a continued correlation across the four tracks for both the magnetic and

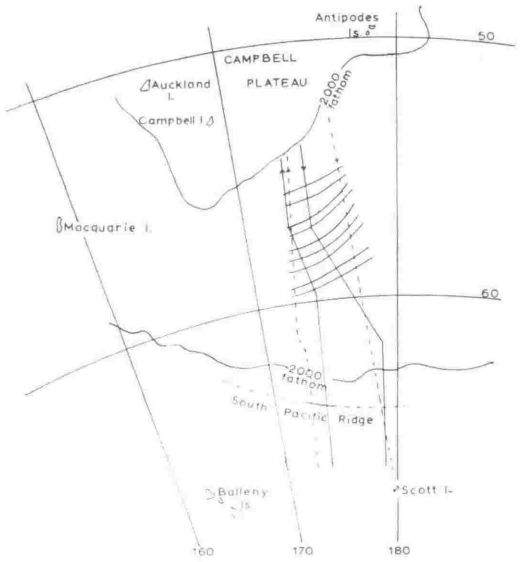

Fig. 4. Assumed correlations of Figure 3 plotted on the track chart. Note that the directions of these lines are intermediate between those of the Campbell rise to the north and the main ocean ridge to the south.

bathymetric records south of the basin, or at least a gradual decline in the correlation as any disturbing effects due to the active ridge system become appreciable. The fact that the good correlation between the magnetic profiles ceases in the region where appreciable variations in topography do occur, and that little correlation exists between the two bathymetric profiles over this region, suggests that the topography may cause confusion in the magnetic pattern rather than being the main cause of the pattern. However, if we assume that the magnetic anomaly pattern across the basin is essentially due to buried topographical variations of the basement rock, there appears to be a marked change in the basement at the southern boundary of the basin.

A second possibility is to assume that variations in topography of the buried basement over the basin have negligible effect on the magnetic record and that the anomalies observed in this region at least have some other source. This is not unreasonable since to produce the observed anomalies by a change in topography of even 1

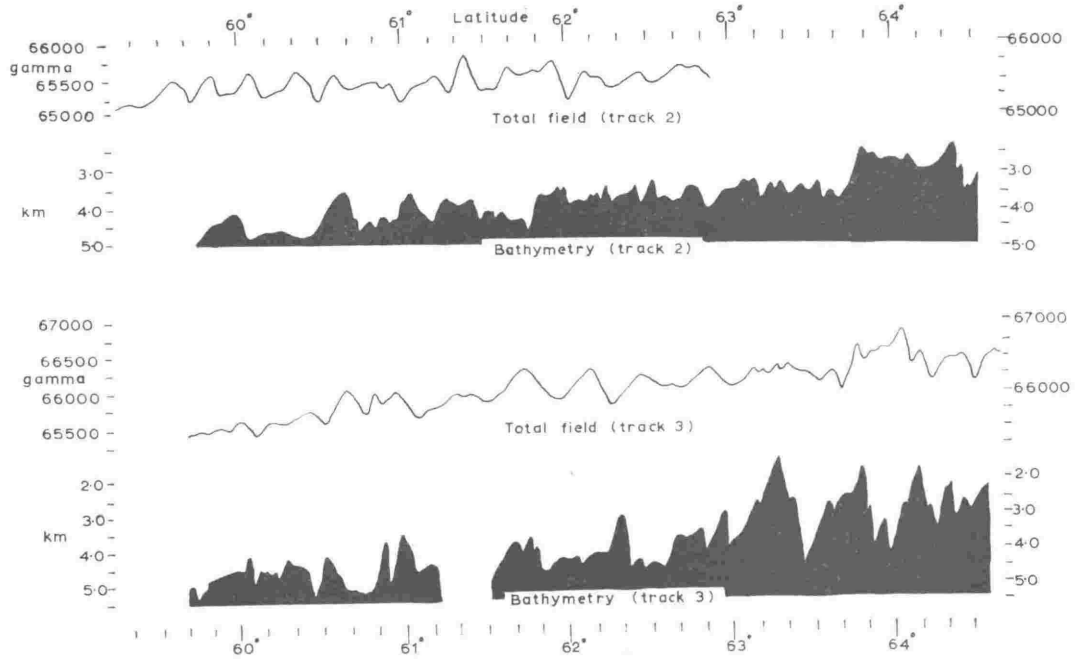

Fig. 5. Total field and bathymetric profiles over the region between 59°S to 65°S for tracks 2 and 3. Note the topography becoming progressively more rugged toward the south and the poor correlation between bathymetric and magnetic records. The crest of the ridge at 63°40′S in track 3 is not obvious from the bathymetric profile but appears as a very characteristic anomaly in the magnetic profile.

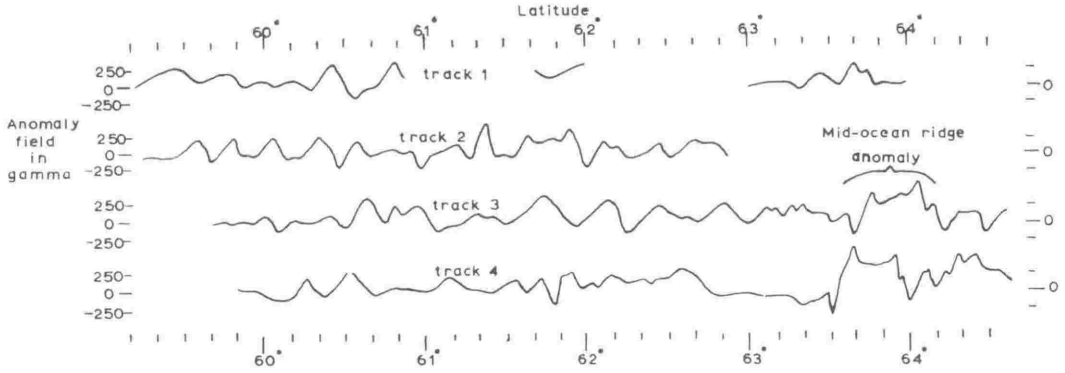

Fig. 6. Magnetic anomaly profiles for all four tracks over the region between 59°S to 65°S. Note that the correlation across the four tracks over the foothills (approximately 59°S to 63°S) is poor. Over the crest of the mid ocean ridge (63°S to 65°S) correlation across the two tracks obtained is excellent with amplitudes of up to 1000 γ occurring.

to 2 km at this depth (5 km) requires a highly magnetic basement. An attempt was therefore made to explain the anomaly pattern by changes in lithology of the basement. Because of the lineation of the anomalies a series of parallel, infinitely thick dike-type structures was taken as the assumed model. Using this model we estimated the depth to the source of the more regular anomalies following the methods given by *Henderson and Zeitz* [1948] and by *Smellie* [1956]. In all cases a depth of approximately 5 km was obtained; i.e., the source appears to practically coincide with the sea floor. Thus the peaks at least of the source appear to have very little sediment covering. An estimation of the susceptibility contrast of the source was also determined. Values obtained lay within the range 1 to 2 $\times$ 10^{-3} cgs units.

An examination of Figures 3 and 6 reveals that appreciable negative anomalies occur in the records. At these latitudes, assuming normal magnetization, the sharp negative anomalies are unexpected. Some of these could possibly be explained by sediment-filled trenches. For example, the large negative anomaly at the northern extremity of the basin could be attributed to a marginal trench now filled with sediment at the base of the continental rise.

If the effect of basement topography on the magnetic record over the basin is discounted and the apparent negative anomalies are accepted, it must be assumed that the remanent magnetization of the rocks is at least of the order of the induced magnetization and that the direction of magnetization may be different from that of the present field. This is in fact quite feasible. *Nagata* [1956], for example, gives the ratio of remanent to induced magnetization for basalts as 2 to 10, and there is no reason to suppose that the present resultant direction of magnetization of the rock coincides with that of the earth's present field, even if it did originally coincide. The simple dike model, assuming only induced magnetization in the direction of the earth's field, was therefore extended to one in which the

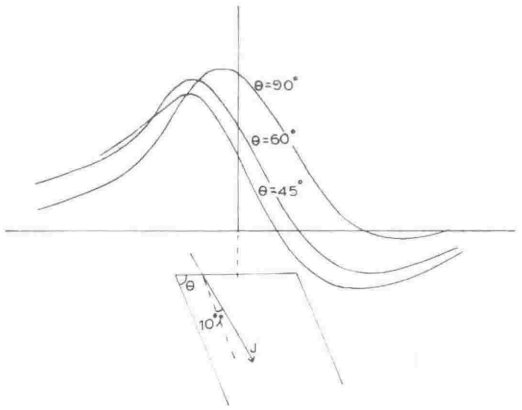

Fig. 7. Calculated total magnetic field anomaly profiles across a dipping dike using the equations of *Bruckshaw and Kunaratnam* [1963]. The profiles shown in this figure correspond to a dike magnetized in the direction of J which has been tilted since it was magnetized. Such a model gave the most pronounced negative anomaly.

direction of magnetization was different from that of the present field.

Calculated anomaly patterns were drawn for various directions of magnetization and for a number of dikes dipping at different angles. Three representative profiles are shown in Figure 7. Although negative values do occur for small dip angles of the magnetization vector and the dike, the negative portions are broad and flat whereas the associated positive portion is relatively steep and sharp. To obtain the sharp negative anomalies actually observed requires a complete reversal of the magnetization vector.

Vine and Matthews [1963] have postulated a mechanism for the explanation of the anomaly pattern associated with ocean ridge systems which includes such a reversed direction of magnetization. Their basic assumptions are, first, a periodic reversal of the earth's magnetic field and, second, an impermanent ocean floor as postulated by *Dietz* [1961]. Such a mechanism could be used to explain the anomaly pattern observed here, particularly over the basin region. South of the basin the lack of correlation across the tracks could then be attributed to basement topography effects.

Acknowledgments. We are grateful to the Royal New Zealand Navy and officers and men of H.M.N.Z.S. *Endeavour* for their cooperation and help with the project.

Financial assistance for the project was obtained through a grant-in-aid from the University Grants Committee.

References

Adams, R. D., and D. A. Christoffel, Total magnetic field surveys between New Zealand and the Ross Sea, *J. Geophys. Res., 67*, 805–813, 1962.

Bruckshaw, J. M., and K. Kunaratnam, The interpretation of magnetic anomalies due to dikes, *Geophys. Prospecting, 11*, 509–522, 1963.

Christoffel, D. A., Total magnetic field measurements between New Zealand and Antarctica, *Nature, 190*, 776–778, 1961.

Dietz, R. S., Continent and ocean basin evolution by spreading of the sea floor, *Nature, 190*, 854–857, 1961.

Ericson, D. B., M. Ewing, and B. C. Heezen, Turbidity currents and sediments in the North Atlantic, *Bull. Am. Assoc. Petrol. Geologists, 36*, 489–511, 1952.

Heezen, B. C., M. Ewing, and D. B. Ericson, Submarine topography in the North Atlantic, *Bull. Geol. Soc. Am., 62*, 1407–1409, 1951.

Heezen, B. C., and A. S. Laughton, Abyssal plains, in *The Sea*, vol. 3, pp. 312–364, edited by M. N. Hill, Interscience Publishers, New York, 1963.

Henderson, R. G., and I. Zeitz, Analysis of total magnetic intensity anomalies produced by point and line sources, *Geophysics, 13*, 428–436, 1948.

Nagata, T., *Rock Magnetism*, Maruzen Company, Tokyo, 1956.

Smellie, D. W., Elementary approximations in aeromagnetic interpretation, *Geophysics, 21*, 1021–1040, 1956.

Vine, F. J., and D. H. Matthews, Magnetic anomalies over oceanic ridges, *Nature, 199*, 947–949, 1963.

(Manuscript received February 26, 1965; revised March 26, 1965.)

Reprinted from ELECTRONIC ENGINEERING, *September 1965.*

A 12V d.c. to 230V a.c. Silicon Controlled Rectifier Invertor

By D. I. Ross* and B. E. G. Goodger*

A 12V d.c. to 230V a.c. silicon controlled rectifier (s.c.r.) invertor is described. The frequency of the invertor is controlled by a 1kc/s fork oscillator to produce a stable 50c/s output. The circuit works efficiently under loads varying from zero to 70W. A safety circuit is incorporated to protect the s.c.r.'s from accidental overload.

A NUMBER of d.c. to a.c. invertors using silicon controlled rectifiers and operating at frequencies in the vicinity of 400c/s have been described in the literature[1–4]. However at frequencies around 50c/s difficulties in commutation are experienced and the efficiency of the invertor drops. This article describes an s.c.r. invertor which will operate very efficiently at 50c/s under loads varying from zero to its full operating load of 70W.

The S.C.R. Invertor

The basic invertor circuit[1–3] is shown in Fig. 1. Operation is as follows. When SCR_1 is switched on current flows through half the primary of the output transformer

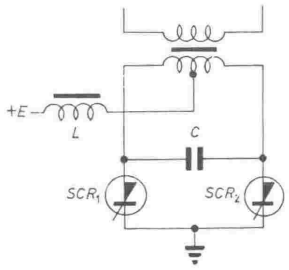

Fig. 1. Basic s.c.r. invertor circuit

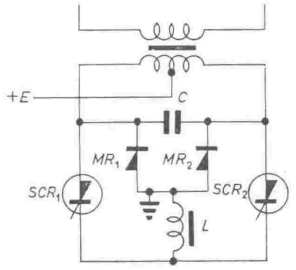

Fig. 2. Improved s.c.r. invertor circuit

charging the capacitor C to $2E$ by auto-transformer action. If now SCR_2 is switched on C will discharge through the two s.c.r.'s producing a reverse voltage across SCR_1 thus cutting it off. C then charges in the opposite direction ready for the next switching cycle. The inductance L in the positive supply line limits the capacitor charging current during the switching period. The time-constant of L and C should be an appreciable fraction of one cycle of the operating frequency. This circuit is very sensitive to the load it is supplying, the required commutation capacitance varying considerably with the load. An improved circuit is shown in Fig. 2. The feedback diodes MR_1, MR_2 compensate for inductive loads and reduce the peak voltage across the s.c.r.'s. The inductance L is in the cathode circuit of the s.c.r. and forms an oscillatory circuit with C thus producing the required reverse voltage across an s.c.r. during the switching period. The value of L is appreciably less in this case since the resonant period of L and C is of the order of the switch-off time of the s.c.r. This circuit is not so sensitive to varying load conditions as the first and appears to work satisfactorily above about 100c/s.

However at lower frequencies the circuit becomes critical, design of the output transformer particularly being important in this region. The reason for this is that during the interval between switching periods (an interval of practically half a cycle) the commutating capacitor C must hold sufficient of its charge to produce the reverse voltage required to cut the conducting s.c.r. off when the other is switched on by the next trigger pulse. At frequencies of 50c/s this means that either C must be large or the transformer primary impedance must be kept high so that no appreciable charge is lost through the transformer primary. In converting 12V to 230V the transformer primary impedance is necessarily limited so that C must be large to obtain reliable commutation. In the prototype built a capacitance of around $80\mu F$ was required, the actual value being very dependent on the load the invertor was driving. With such capacitances the charging time becomes long, and the increased losses reduce the efficiency considerably. This problem could be overcome if after having been charged to its full voltage $2E$, the commutating capacitor could be isolated from the rest of the circuit until the next switching pulse fires the second s.c.r. Ward[5] has done this by inserting series diodes between each side of the transformer primary and the commutating capacitor as shown in Fig. 3. In this circuit the only discharge path for the capacitor is through the s.c.r.'s so no appreciable loss can occur between switching periods. By incorporating series diodes in the circuit, leaving in the shunt diodes of Fig. 2 to limit the peak voltage across the s.c.r.'s, the required commutating capacitance was reduced to $7\mu F$ and the invertor functioned satisfactorily under all load conditions from zero to full load whether resistive or inductive. In the case of inductive

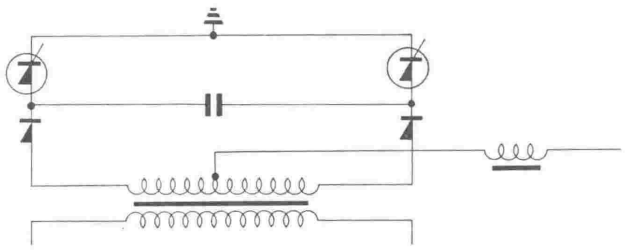

Fig. 3. Low frequency s.c.r. invertor circuit as given by Ward

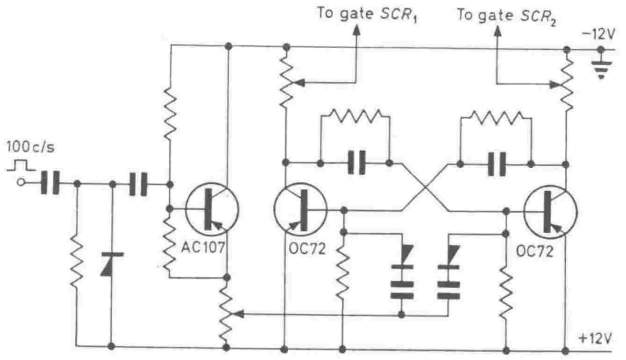

Fig. 4. S.C.R. trigger circuit

* *Victoria University of Wellington, New Zealand.*

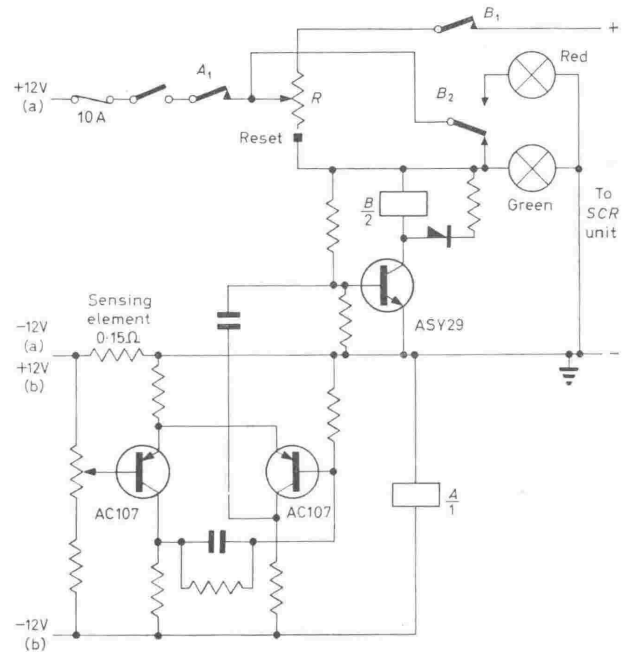

Fig. 5. S.C.R. safety circuit

loads some compensating capacitance was required across the load to reduce harmonic distortion of the output waveform.

S.C.R. Trigger Circuit

Transistorized firing circuits for s.c.r.'s have been published in the literature[6]. In this particular application a standard 50c/s a.c. supply was required to run seismic recorder motors. A stable 50c/s trigger pulse was therefore required to drive the s.c.r. supply.

A 1kc/s fork oscillator was used as the signal source since this was available and had the required stability. The 1kc/s signal was passed through a pulse shaper and decade counter to obtain 100c/s pulses. Further decade counters supplied 1sec, 1min, and 10min pulses for calibration of other equipment. Philips circuit blocks were used for the pulse shaper and decade units. The 100c/s pulses from the first decade were then fed into the trigger circuit shown in Fig. 4. This consists of an emitter-follower, to avoid loading of the decade counter, followed by a flip-flop unit which divides by two and supplies the required 50c/s gate pulses for the s.c.r.'s. The s.c.r. gates are direct coupled to the 250Ω potentiometers in the collector circuits of the OC72's. The use of potentiometers allows individual adjustment of the voltages required by each s.c.r. gate.

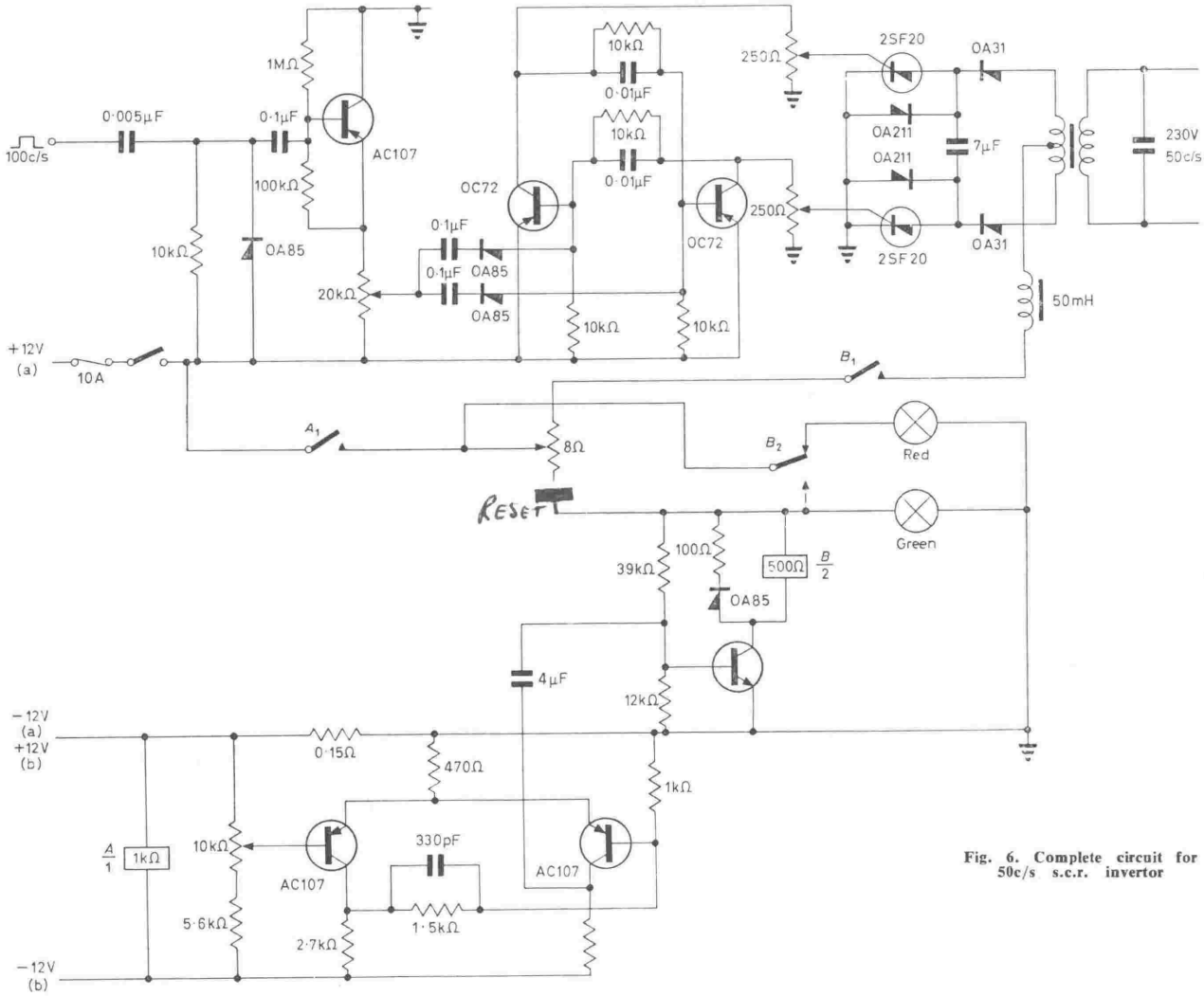

Fig. 6. Complete circuit for 50c/s s.c.r. invertor

S.C.R. Safety Circuit

The current through the s.c.r.'s will rise rapidly if triggering or commutation fail for any reason. Some form of safety circuit is therefore necessary to safeguard the s.c.r.'s if this were to happen. The circuit used in this particular case is shown in Fig. 5 and consists of a Schmidt trigger feeding a power transistor and relay. The Schmidt trigger is tied across a sensing element in the negative line to the invertor. If the current through this element rises above a specified level the Schmidt trigger switches, cutting off the power transistor and hence opening the relay *B* and breaking the power to the s.c.r.'s. The use of a relay instead of a transistor in the power line to the invertor eliminates the possibility of damage to the safety circuit by transients while still being sufficiently fast to safeguard the s.c.r.'s. Relay *A* cuts the power to the invertor should the power to the Schmidt trigger be cut off for any reason. Resistance *R* was used to adjust the supply current to the invertor and was arranged to act as a manual reset should the safety circuit cut the supply voltage. In this way the invertor could not be started until *R* was returned to its maximum position. The lights indicate the state of the relay *B*.

Conclusions

A reliable 12V d.c. to 230V a.c. invertor working at 50c/s has been constructed which functions satisfactorily under a wide variety of load conditions, the maximum output power with the s.c.r.'s used being 70W. The use of series diodes between the primary of the output transformer and the commutating capacitor allows a considerable reduction in the required commutating capacitor and makes the design of the transformer much less critical.

The complete circuit of the invertor is shown in Fig. 6. As already mentioned the invertor was constructed to run the synchronous motors of two seismic recorders. The circuit was sufficiently insensitive to load conditions that switching either or both the motors had no effect on the operation of the invertor. With the values shown the safety circuit was designed to open the s.c.r. supply line when the current rose above 7A. The efficiency of the invertor was very high, the only appreciable losses occurring in the choke, output transformer and safety circuit sensing element.

REFERENCES

1. Silicon Controlled Rectifier Manual. G.E.C. New York (1961).
2. NOWICKI, J. R. *S.C.R. Invertor for Fluorescent Lamp.* Mullard Tech. *Commun. (GB) 7,* 22 (1962).
3. THOMPSON, R. High Frequency Silicon-Controlled-Rectifier Sinusoidal Invertor. *Proc. Instn. Elect. Engrs. 110,* 647 (1963).
4. PAYNE, R. A., REEVES, E. S. Switch Off Circuits for S.C.R.'s Operating on D.C. *Mullard Tech. Commun. (GB) 7,* 162 (1963).
5. WARD, E. E. Invertor Suitable for Operation over a Range of Frequency. *Proc. Instn. Elect. Engrs. 111,* 1423 (1964).
6. JARRATT, T. J. Transistorized S.C.R. Firing Circuits. *Mullard Tech. Commun. (GB) 7,* 141 (1963).

Printed in England by The Press at Coombelands Ltd., Addlestone, Surrey.

A MAGNETIC SURVEY OF THE SOUTHWEST PACIFIC OCEAN

Volume 2

by

DAVID IRWIN ROSS

Submitted for the Degree of

Doctor of Philosophy in Physics

at

Victoria University of Wellington

Wellington

New Zealand

April 1966

DIAGRAMS.

LIST OF DIAGRAMS

FIGURE 1.

Standard crustal sections for continental and oceanic crust.

(After Worzel and Shurbet, 1955.)

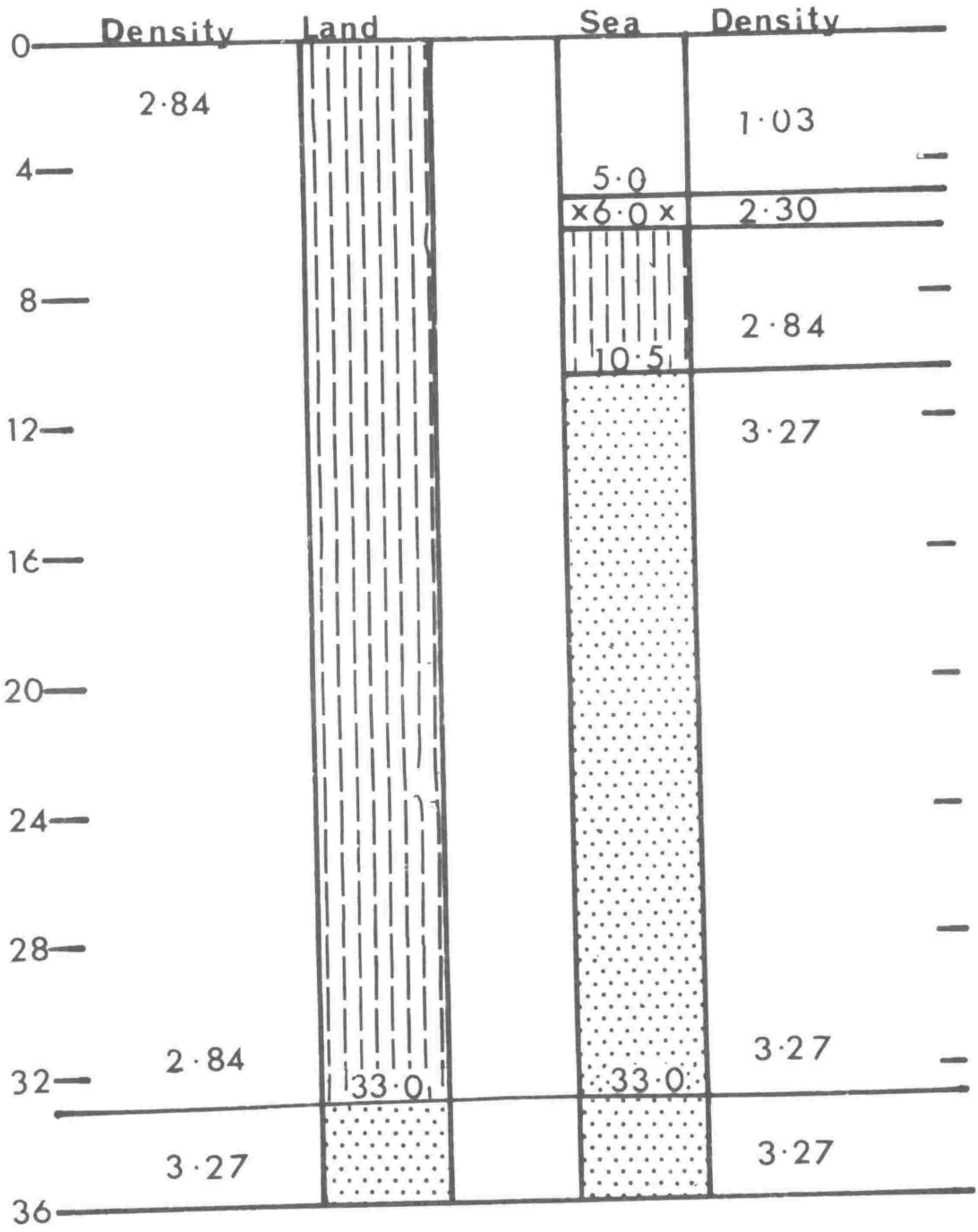
Density
Land
Sea
Density
0
4
8
12
16
20
24
28
32
36
2·84
1·03
5·0
×6·0×
2·30
2·84
10·5
3·27
2·84
33·0
33·0
3·27
3·27
3·27

FIGURE 2.

Chart of the area studied showing its division into the three main morphologic divisions; continental margin, ocean basin, and mid-ocean ridge. The contour interval is 500 fathoms, contours from 1000 - 2500 fathoms being shown on the chart.

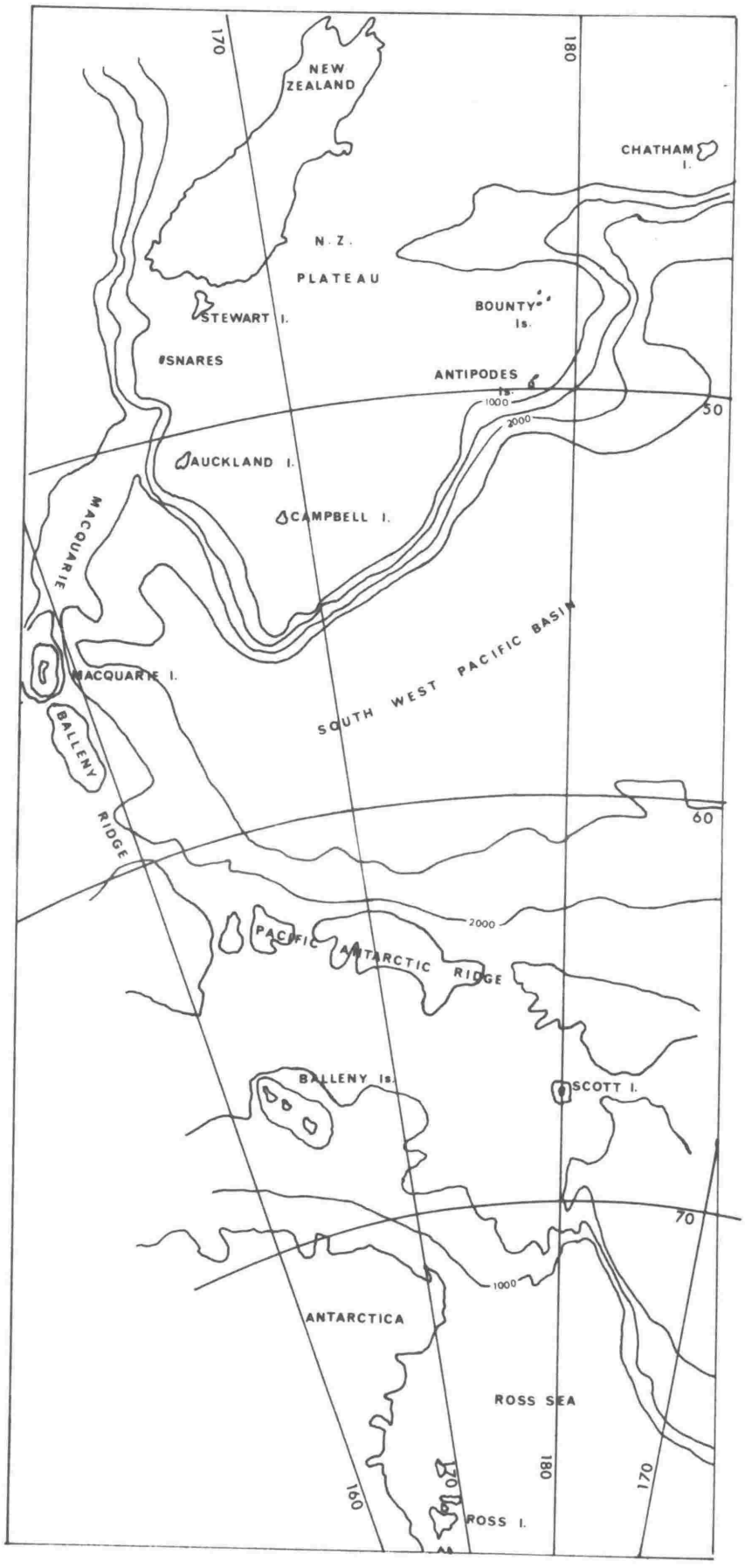
170
180
NEW ZEALAND
CHATHAM I.
N.Z. PLATEAU
STEWART I.
BOUNTY Is.
SNARES
ANTIPODES Is.
1000
2000
50
AUCKLAND I.
CAMPBELL I.
MACQUARIE
MACQUARIE I.
SOUTH WEST PACIFIC BASIN
BALLENY RIDGE
60
2000
PACIFIC ANTARCTIC RIDGE
BALLENY Is.
SCOTT I.
70
1000
ANTARCTICA
ROSS SEA
160
180
170
ROSS I.

FIGURE 3.

Block diagram of the proton magnetometer.

Note: In the circuit diagrams which follow resistor values are in kilohms and capacitance values in microfarads unless otherwise stated.

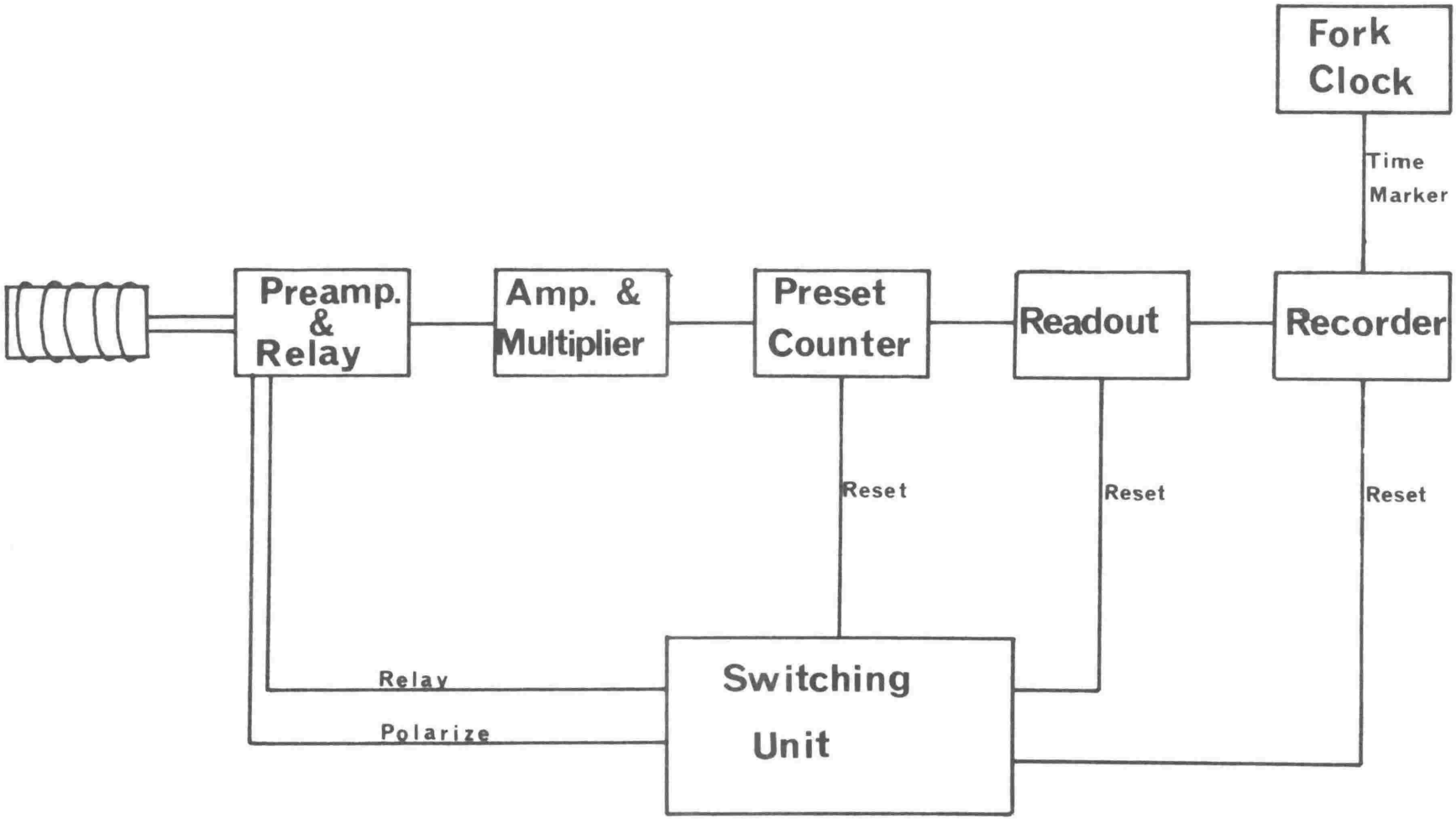
Fork
Clock
Time
Marker
Preamp.
&
Relay
Amp. &
Multiplier
Preset
Counter
Readout
Recorder
Reset
Reset
Reset
Relay
Polarize
Switching
Unit

FIGURE 4.

Cricuit diagram of the hybrid amplifier for incorporation in the fish.

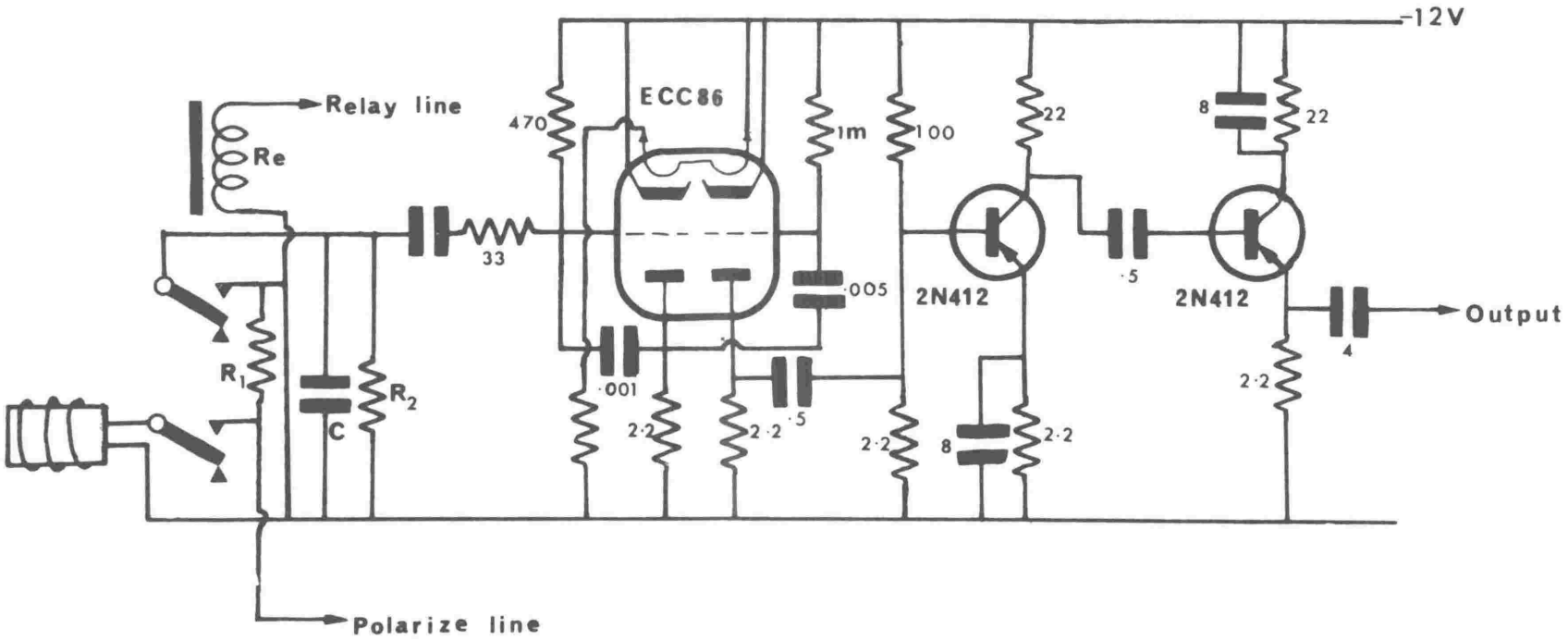
-12V
Relay line
Re
470
ECC86
1m
100
22
8
22
33
·005
2N412
·5
2N412
Output
4
R1
R2
C
·001
2·2
2·2
·5
2·2
8
2·2
2·2
Polarize line

FIGURE 5.

Photograph of preamplifier and input circuitry ready for mounting in the fish.

FIGURE 6.

(a) First two stages of the frequency multiplier using two cascade stages of full-wave rectifier circuit.

(b) Third stage of the frequency multiplier using a differentiator and inverter amplifier circuit.

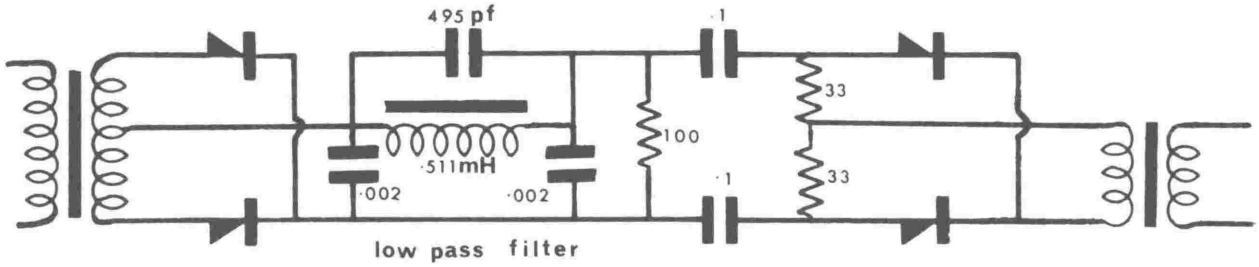
495 pf
·1
33
100
·511mH
·002
·002
·1
33
low pass filter

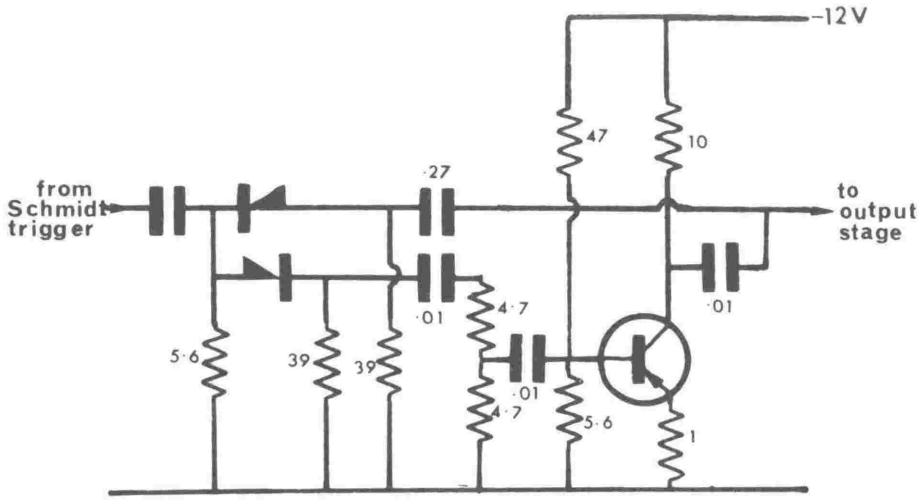
-12V
47
10
from Schmidt trigger
·27
to output stage
·01
·01
4·7
5·6
39
39
·01
4·7
5·6
1

FIGURE 7.

Circuit diagram of the main amplifier. A total gain of 10^4 is obtained and a frequency multiplication of 8 times. The frequency is variable from 1.8 - 3.0 kc/s and the bandwidth from 0.1 - 1 kc/s.

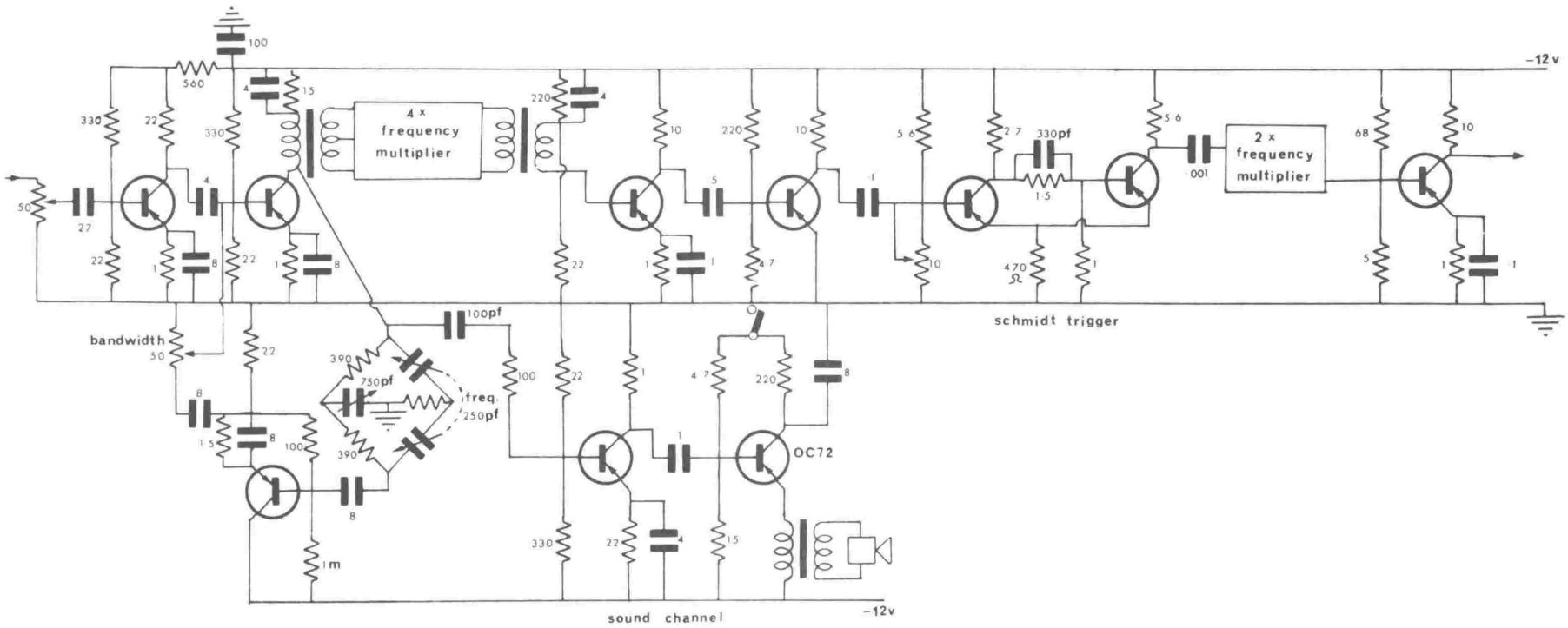
-12 v
4 x
frequency
multiplier
2 x
frequency
multiplier
schmidt trigger
bandwidth
freq.
OC72
sound channel
-12v

FIGURE 8.

Block diagram of the frequency counter for obtaining a direct reading of the field. The preset timing counter B is set to count 29362 cycles of the 100 kc/s oscillator.

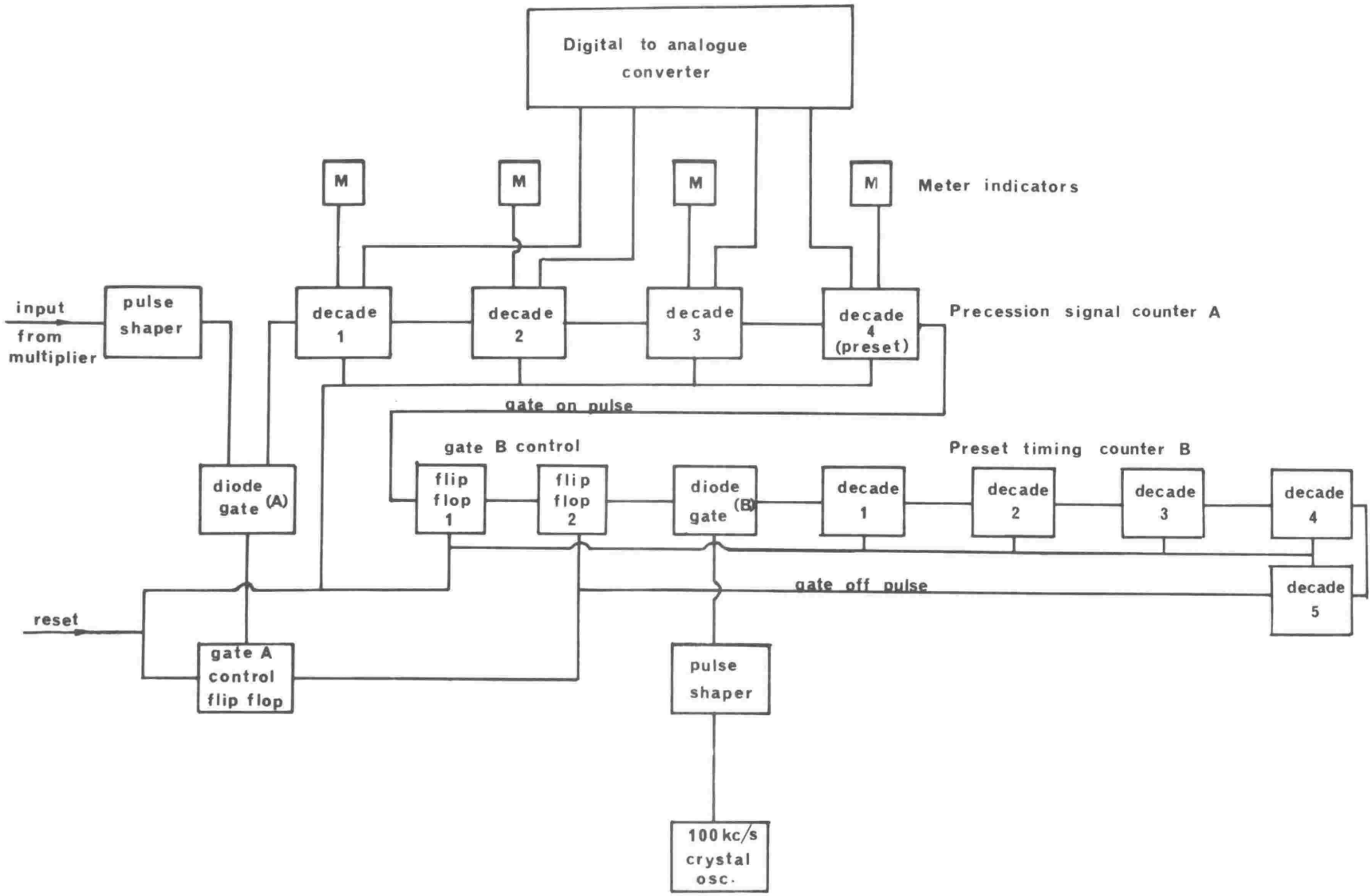
Digital to analogue converter
M
M
M
M
Meter indicators
input from multiplier
pulse shaper
decade 1
decade 2
decade 3
decade 4 (preset)
Precession signal counter A
gate on pulse
gate B control
Preset timing counter B
diode gate (A)
flip flop 1
flip flop 2
diode gate (B)
decade 1
decade 2
decade 3
decade 4
decade 5
gate off pulse
reset
gate A control flip flop
pulse shaper
100 kc/s crystal osc.

FIGURE 9.

Circuit of the 100 kc/s crystal oscillator. This is a conventional Colpitt's oscillator followed by an emitter follower.

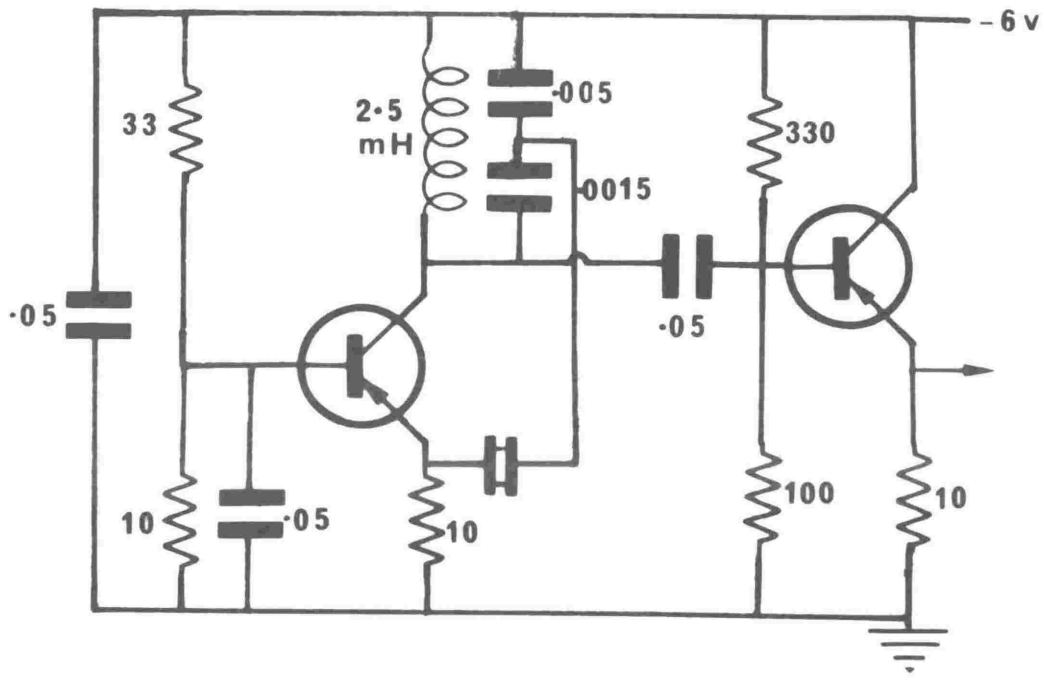
-6 v
33
2·5
mH
·005
·0015
330
·05
·05
10
·05
10
100
10

FIGURE 10.

(a) Basic potentiometer readout circuit. Switches S_1- S_4 are operated by the binary units of the first decade and S_5- S_8 by the binary units of the second decade.

(b) Circuit of the transistor readout unit. Each binary unit of the first two decades is connected to one transistor switch. The current through the transistor is adjusted to give the required voltage reading across R.

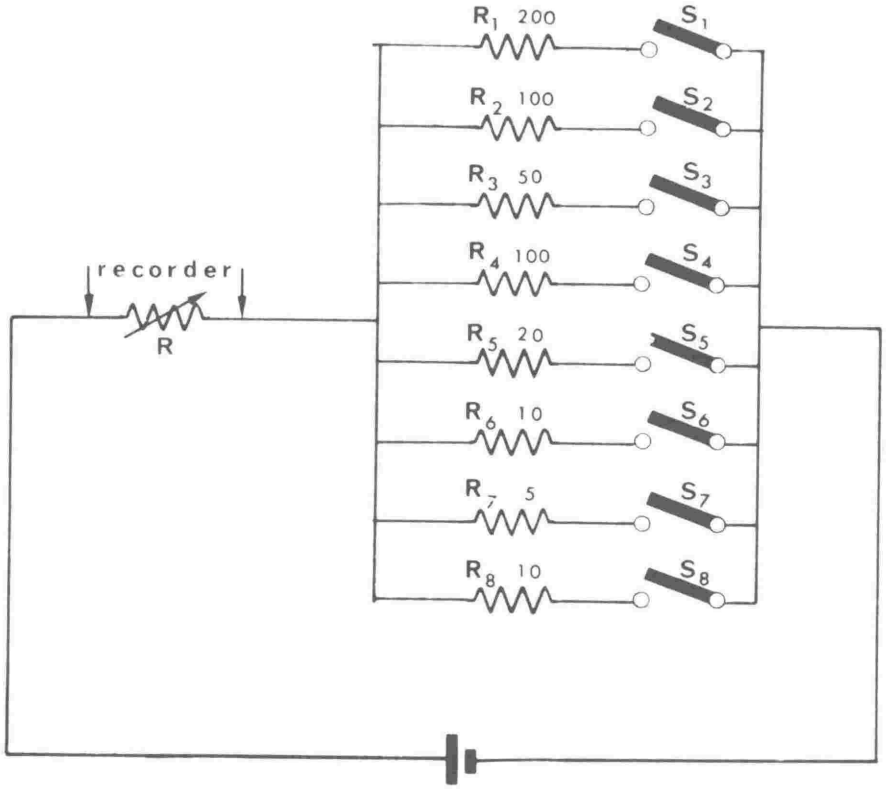
R1 200
S1
R2 100
S2
R3 50
S3
R4 100
S4
R5 20
S5
R6 10
S6
R7 5
S7
R8 10
S8
recorder
R

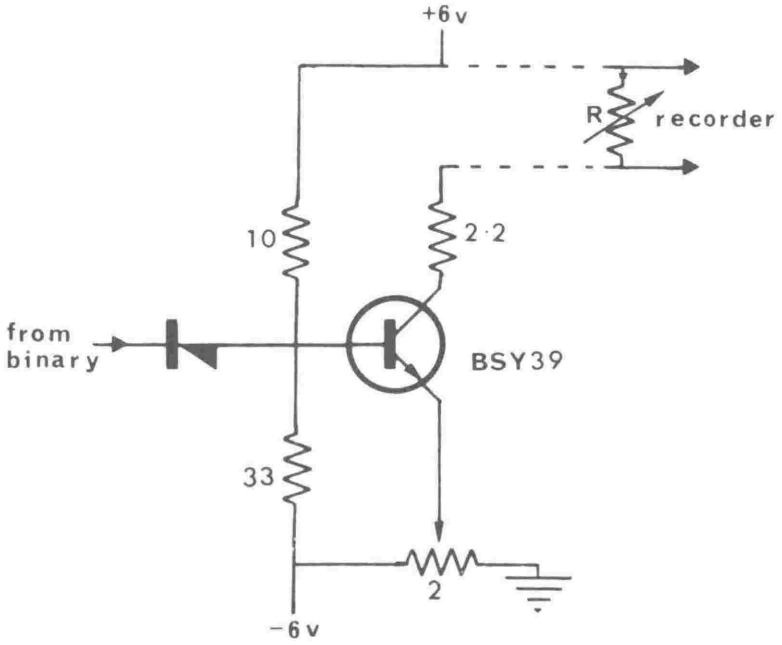
+6v
R
recorder
10
2·2
from
binary
BSY39
33
2
-6v

FIGURE 11.

Magnetometer switching unit controlling the polarizing of the magnetometer bottle and the resetting of the counter and recorder.

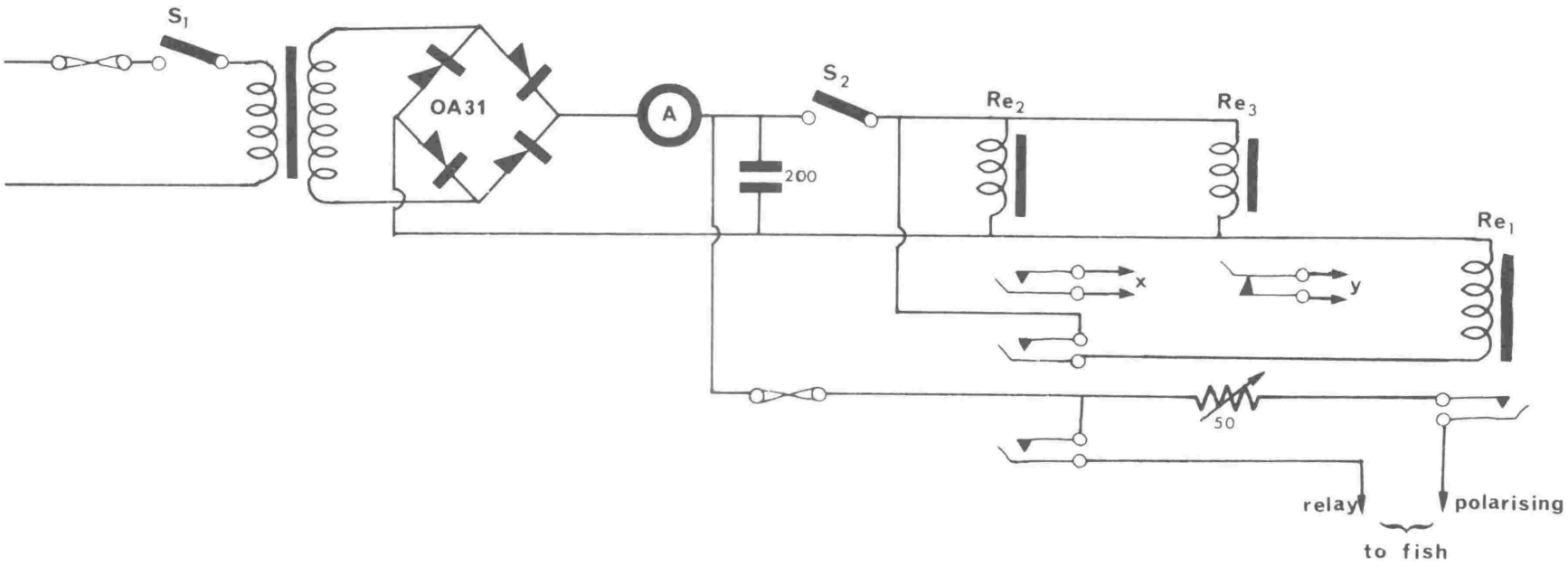

x — counter reset

y — recorder or readout reset

FIGURE 12.

Circuit of the power supply for the electronics. The +6v,0,-6v supply is required for the Philips circuit blocks used in the counter.

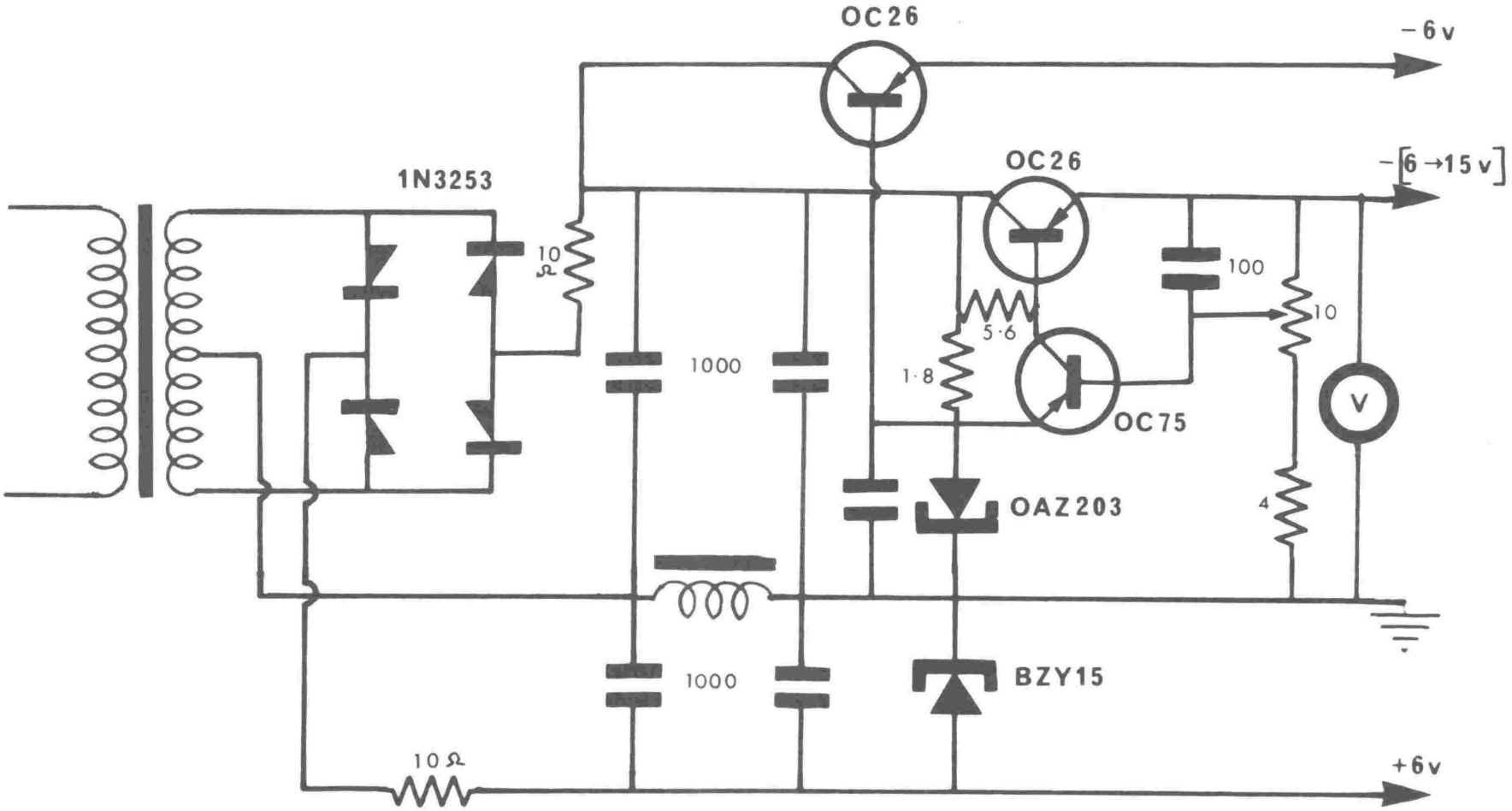
OC26
−6v
OC26
−[6→15v]
1N3253
10Ω
1000
100
10
5·6
1·8
OC75
V
OAZ203
4
1000
BZY15
10Ω
+6v

FIGURE 13.

Diagram of fish showing details of construction, seals and assembly.

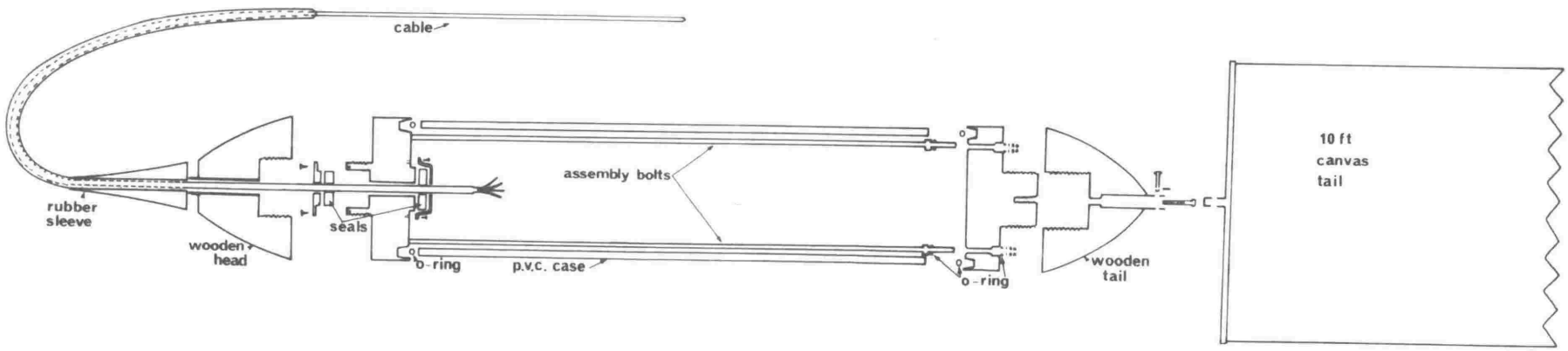
cable
rubber sleeve
wooden head
seals
o-ring
p.v.c. case
assembly bolts
o-ring
wooden tail
10 ft canvas tail

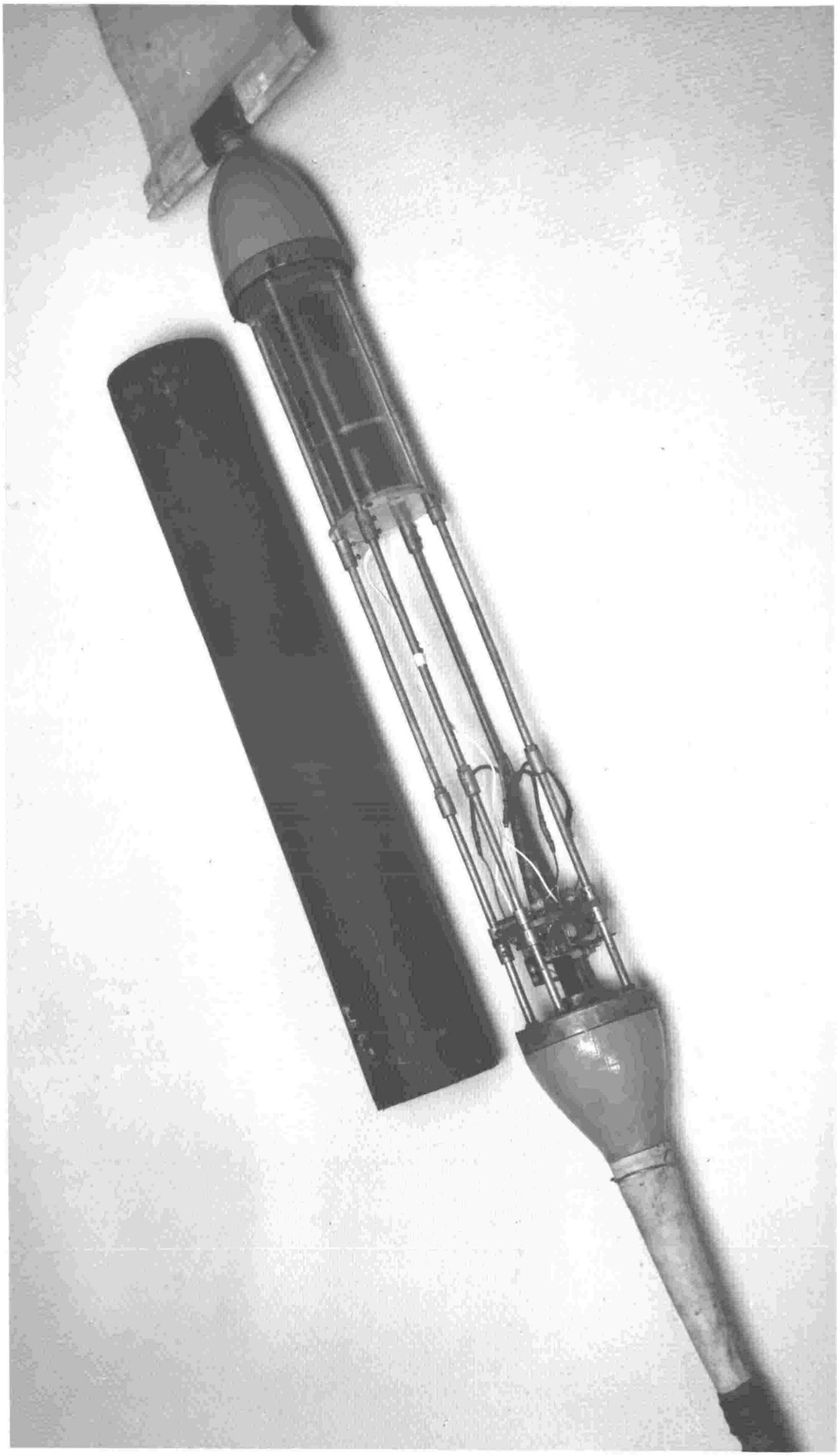

FIGURE 15.

Oscilloscope photograph of a recorded precession signal obtained with the magnetometer constructed.

8 seconds.

FIGURE 16.

Photograph of a portion of the magnetometer record obtained on the return trip from Antarctica in February 1965.

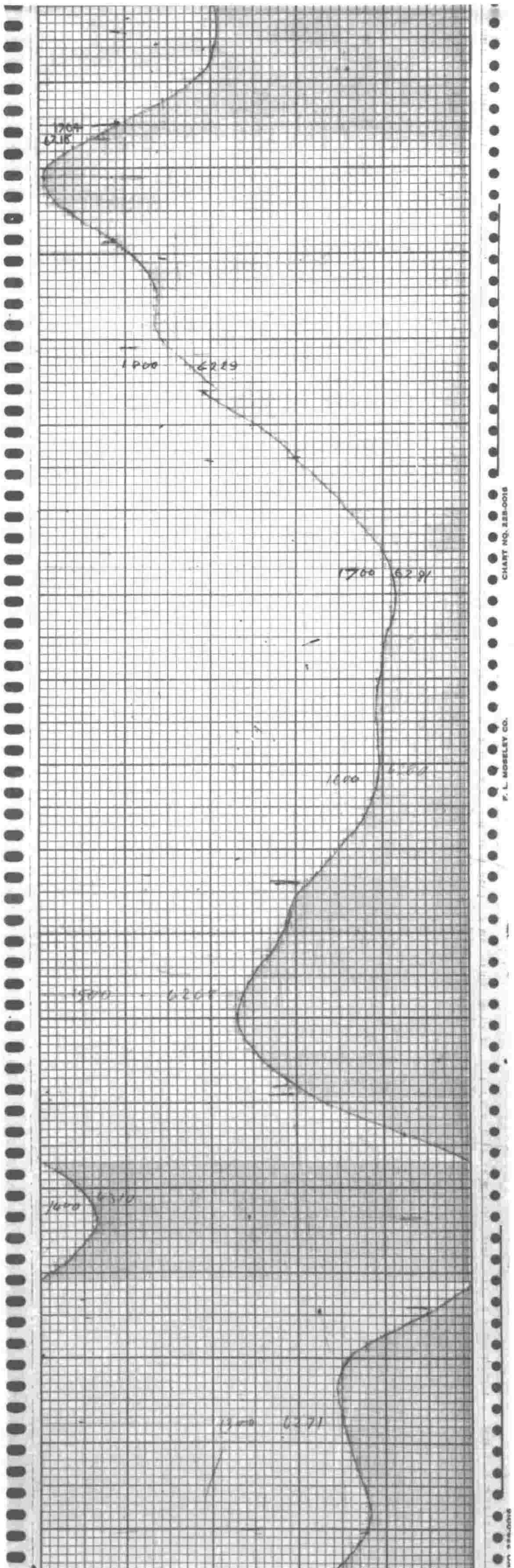
CHART NO. 225-0015
F. L. MOSELEY CO.

FIGURE 17.

Oscilloscope photograph of a recorded grenade shot as received by the hydrophone array. Note the three main groups of waves.

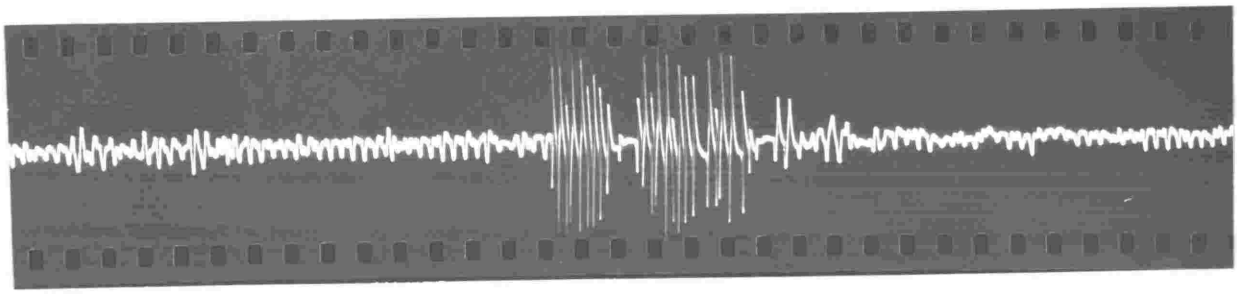

0.2 seconds.

FIGURE 18.

Diagram of the pneumatic gun constructed from drawings supplied by Lamont Geological Observatory.

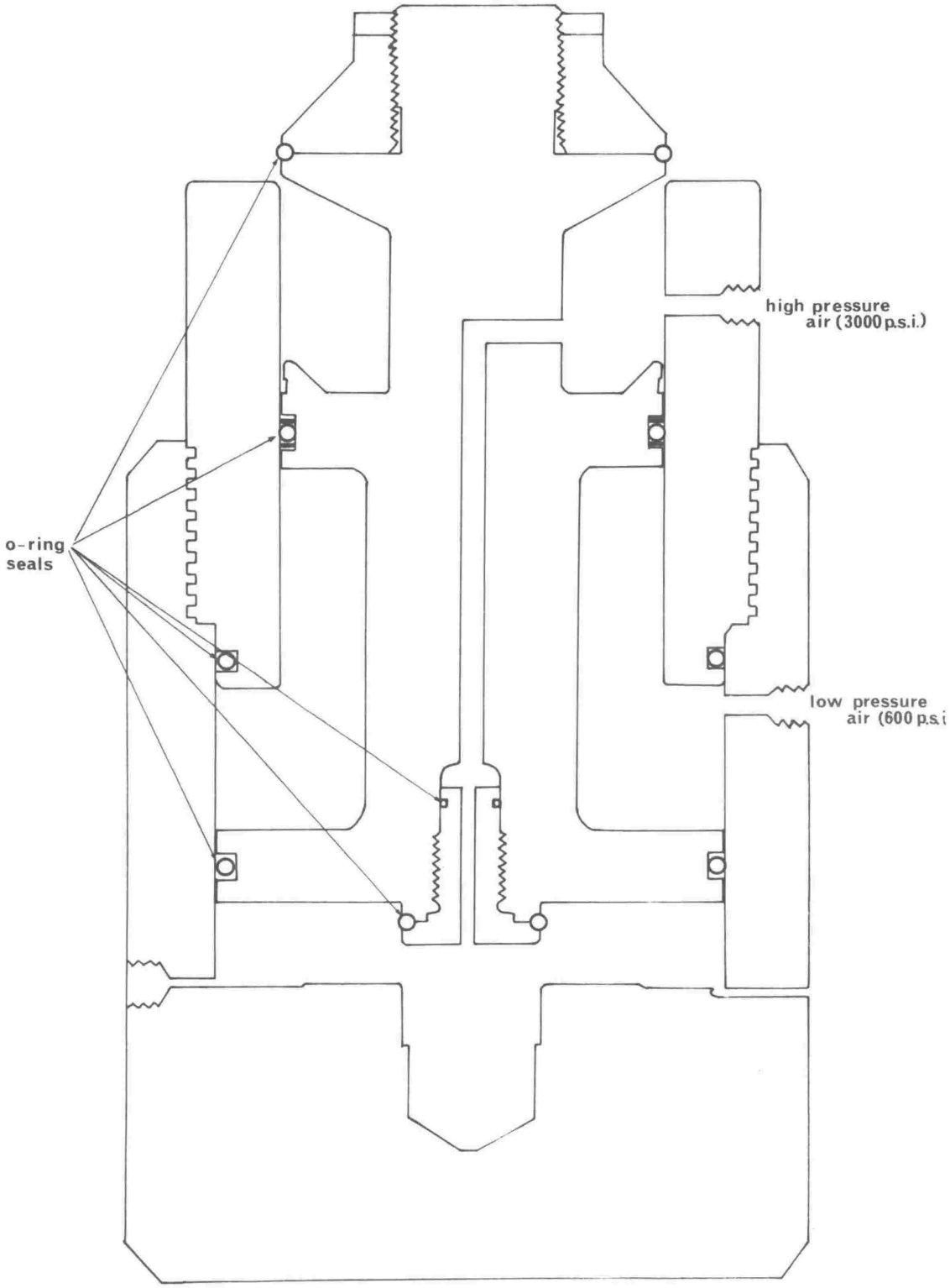
high pressure
air (3000 p.s.i.)
o-ring
seals
low pressure
air (600 p.s.i

FIGURE 19.

Photograph of the MP-4 and smaller MP-7 hydrophones showing their relative sizes. (Approximately actual size.)

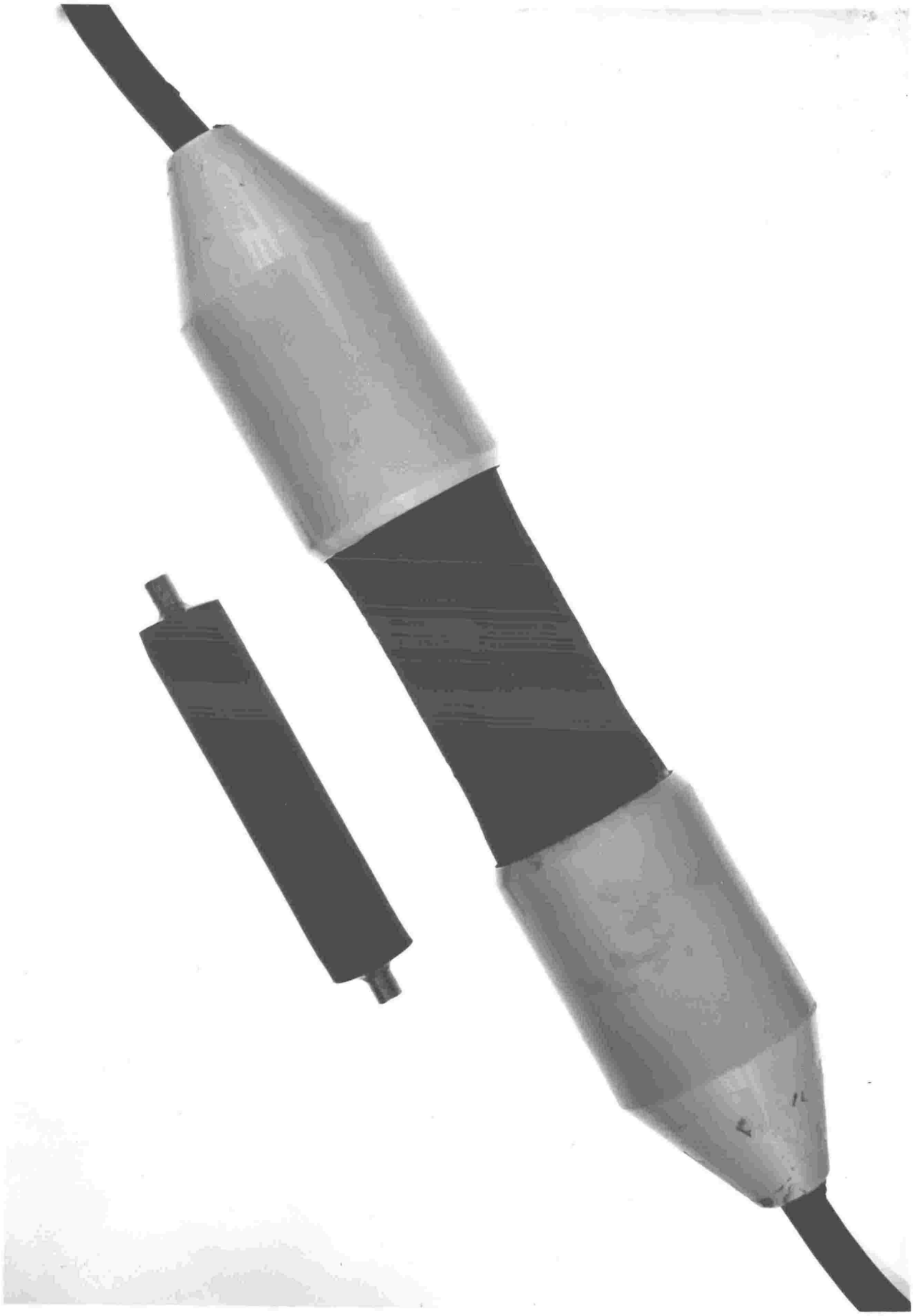

FIGURE 20.

Block diagram of the seismic profiler.

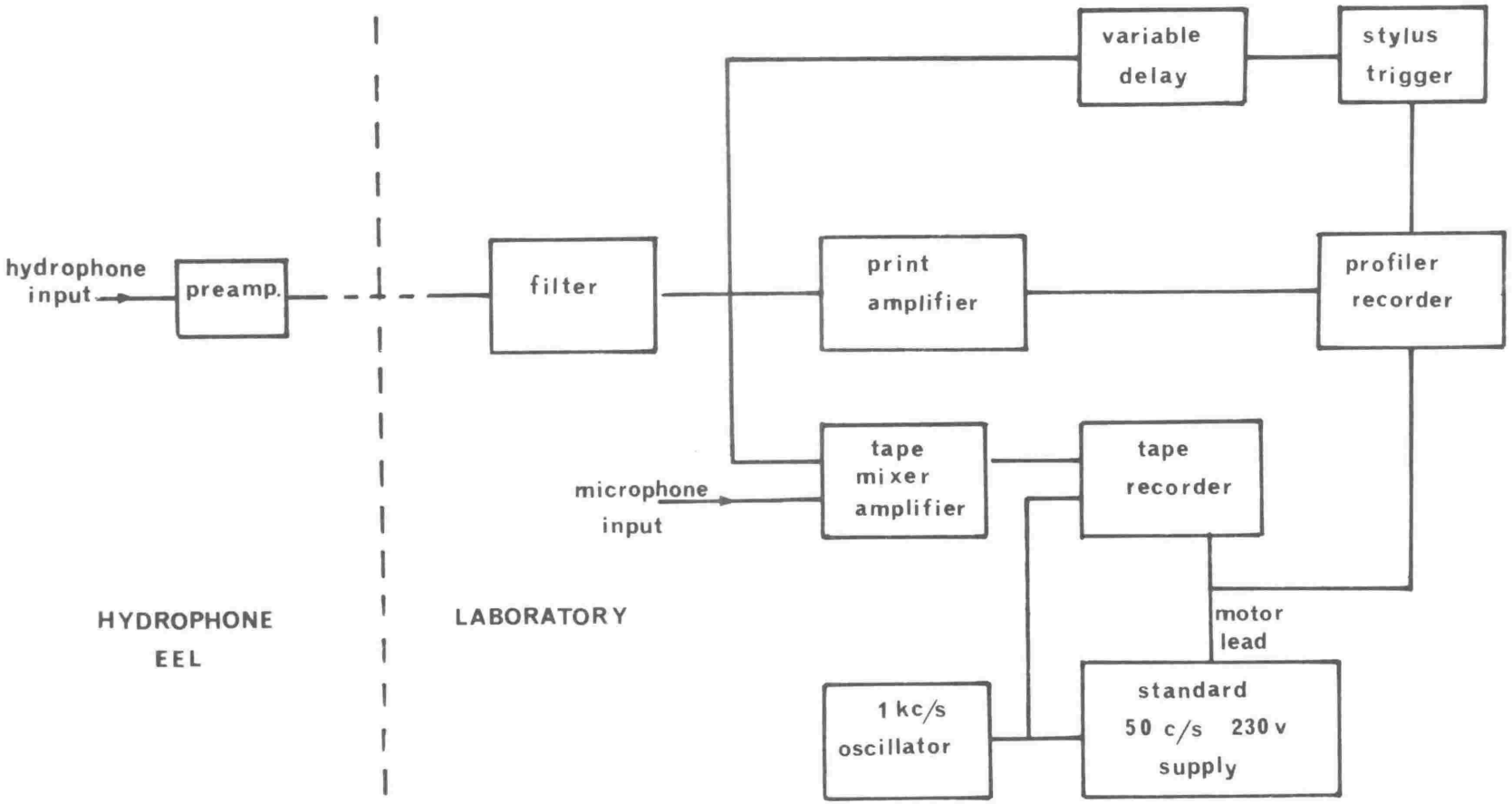
variable delay
stylus trigger
hydrophone input
preamp.
filter
print amplifier
profiler recorder
tape mixer amplifier
tape recorder
microphone input
motor lead
HYDROPHONE EEL
LABORATORY
1 kc/s oscillator
standard 50 c/s 230 v supply

FIGURE 21.

Circuit diagram of the main amplifier and trigger for the seismic profiler. A separate hydrophone close to the gun supplies the shot-instant signal for the trigger.

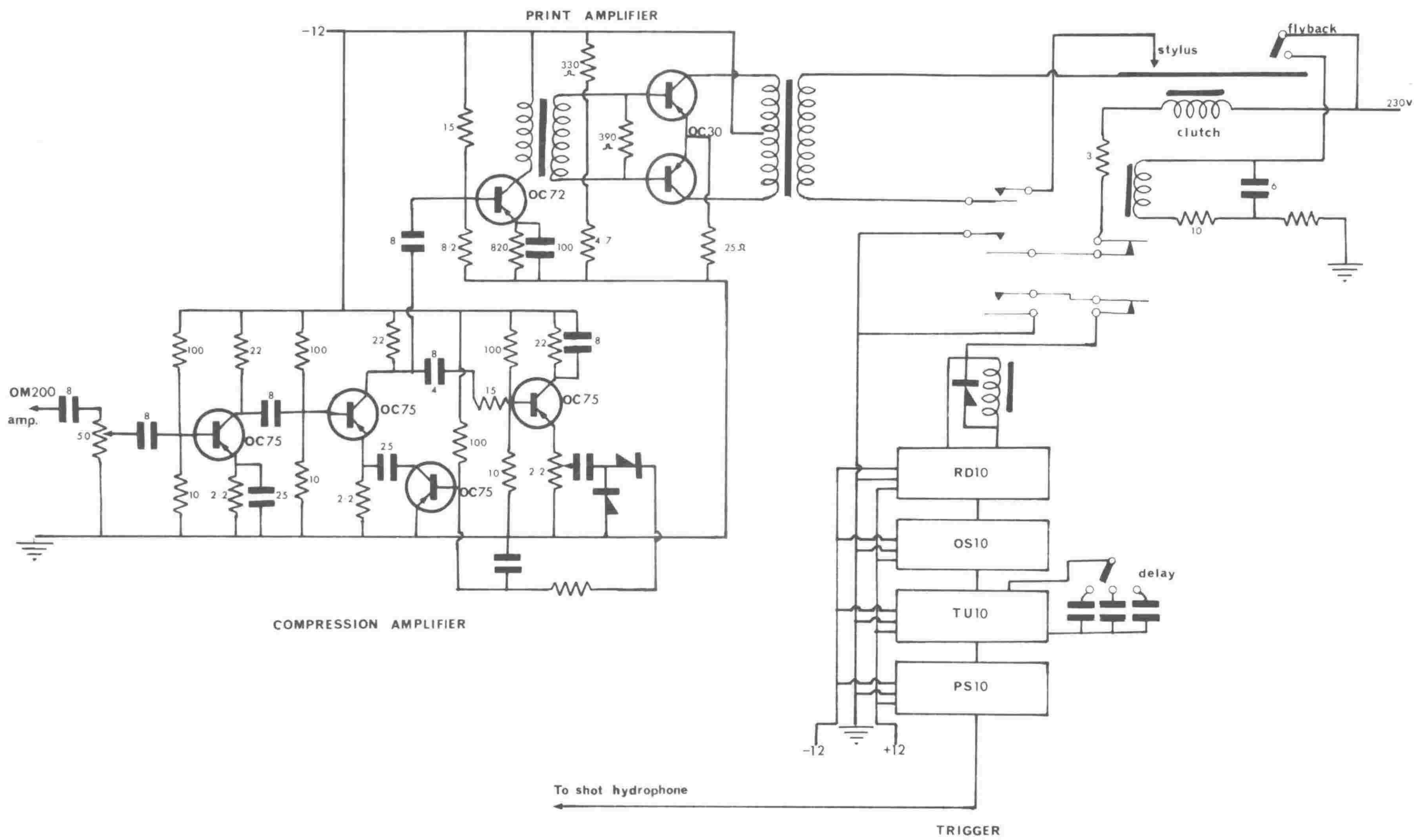
PRINT AMPLIFIER
COMPRESSION AMPLIFIER
OM200 amp.
OC75
OC72
OC30
stylus
flyback
clutch
230v
RD10
OS10
TU10
PS10
delay
-12
+12
To shot hydrophone
TRIGGER

FIGURE 22.

Oscilloscope photographs of two successive reflections recorded over the Campbell Plateau. The bottom echo bagins at R. Note that the strong sub-bottom echo at X on (a) is absent from (b). The time interval between the two shots was 5 minutes.

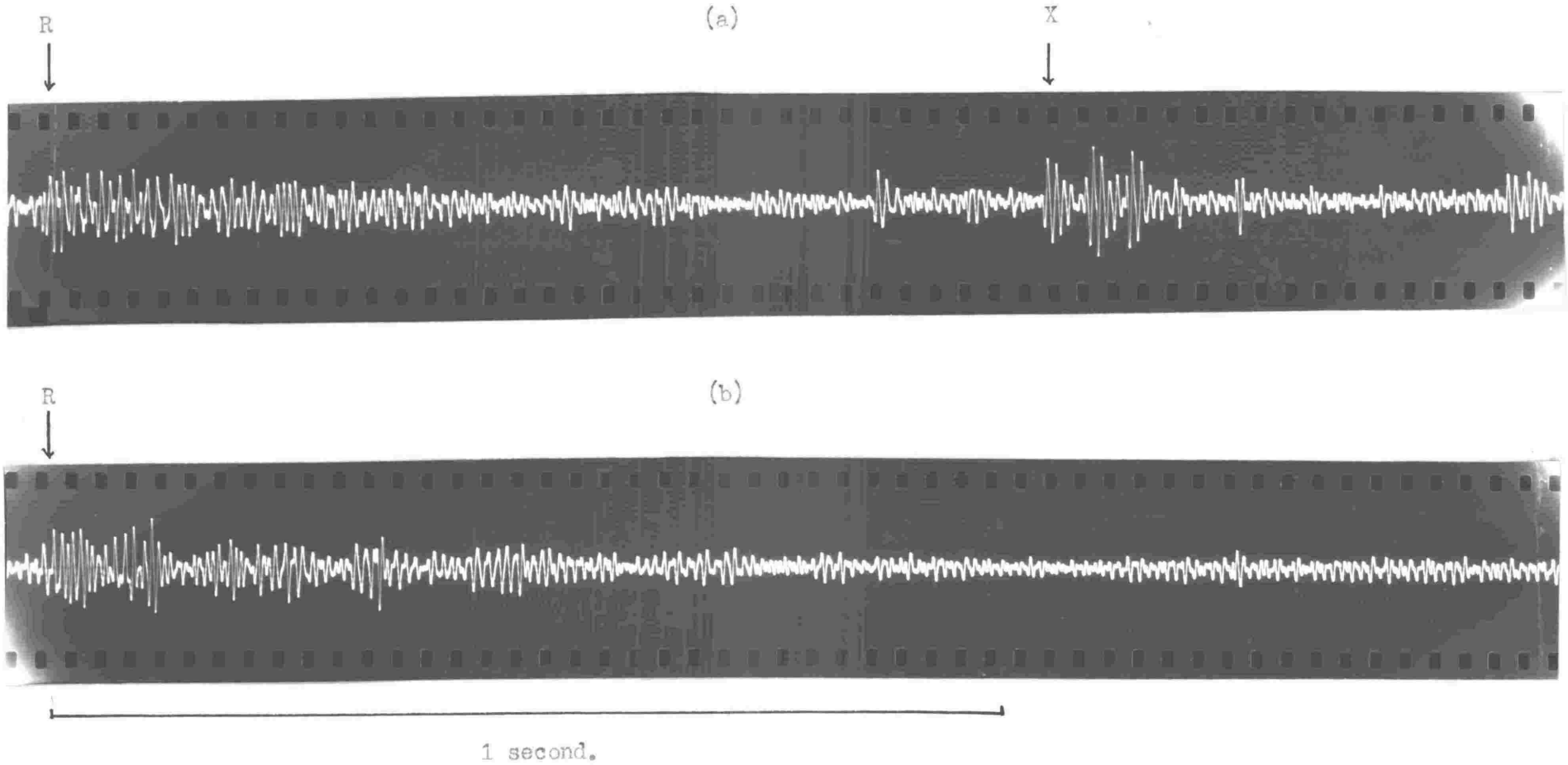
R
(a)
X
R
(b)
1 second.

FIGURE 24.

Bathymetry profiles between New Zealand and Antarctica (tracks d - e) and between New Zealand and Balleny Islands (track j). Vertical exageration 75:1.

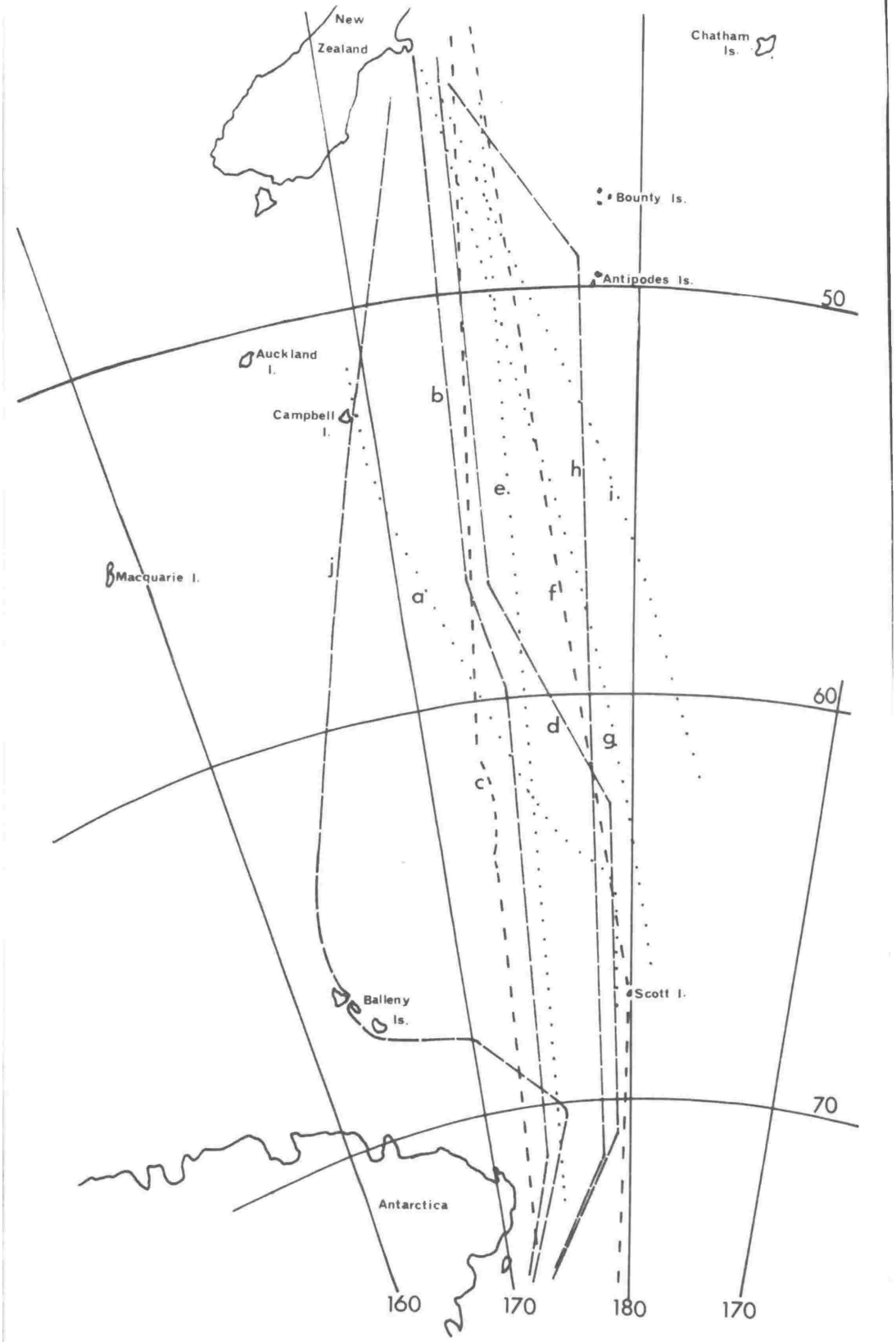
New
Zealand
Chatham
Is.
Bounty Is.
Antipodes Is.
50
Auckland
I.
Campbell
I.
b
e
h
i
j
a
f
Macquarie I.
60
d
g
c
Balleny
Is.
Scott I.
70
Antarctica
160
170
180
170

FIGURE 23.

Chart of the area studied showing the tracks over which the results which follow were obtained. Results on tracks b,d,h and j were obtained by the author. Those on tracks c and f were obtained by Christoffel (1961), those on tracks g and i were obtained by U.S.N.S. Staten Island (U.S. Navy Hydrographic Office, 1962), and those on tracks a and e are unpublished results obtained by D.S.I.R. personnel.

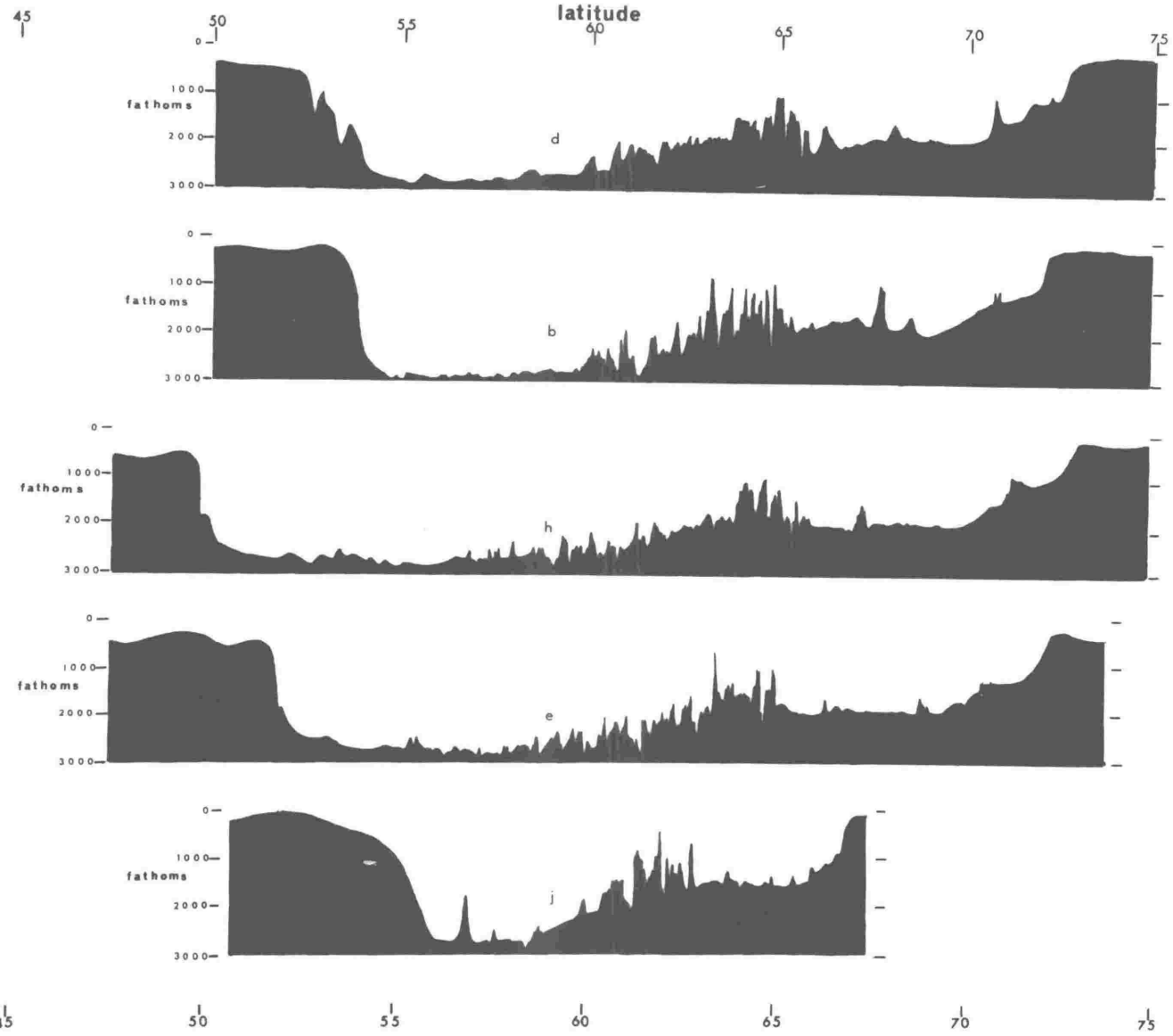
latitude
45
50
55
60
65
70
75
0
1000
2000
3000
fathoms
d
b
h
e
j

FIGURE 25.

Bathymetry profiles across the northern flanks and crest of the Pacific -Antarctic Ridge showing the division of the ridge into step provinces similar to those described by Heezen et al. (1959) for the Mid-Atlantic Ridge. At the edge of each step the average depth changes abruptly by 200 or more fathoms, remaining practically constant across each step. Vertical exageration 15:1.

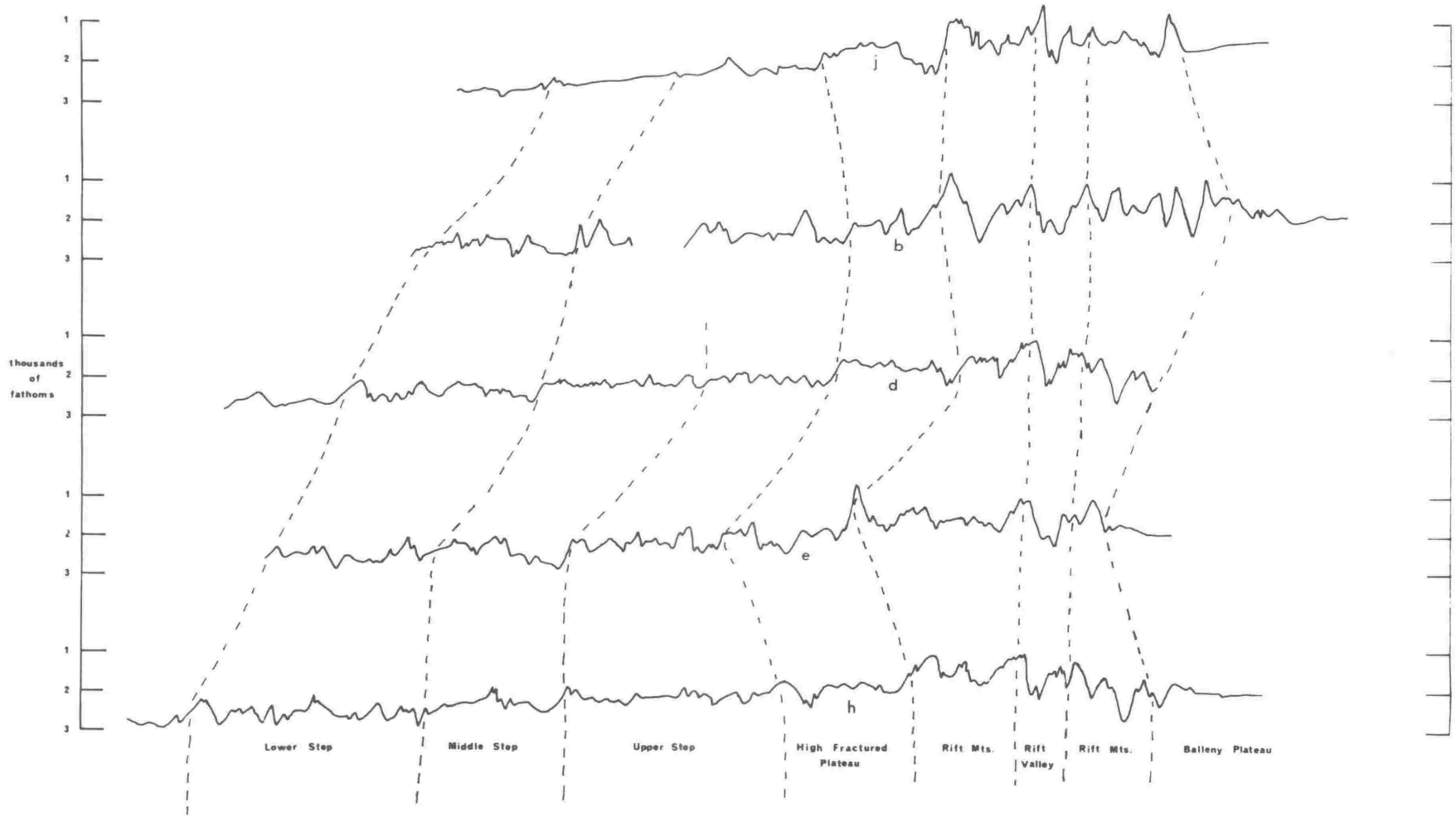
thousands of fathoms
1
2
3
j
b
d
e
h
Lower Step
Middle Step
Upper Step
High Fractured Plateau
Rift Mts.
Rift Valley
Rift Mts.
Balleny Plateau

FIGURE 26.

Total field and bathymetry profiles across the Campbell Plateau and the Bounty Trough. Vertical exageration of bathymetry profiles 15:1.

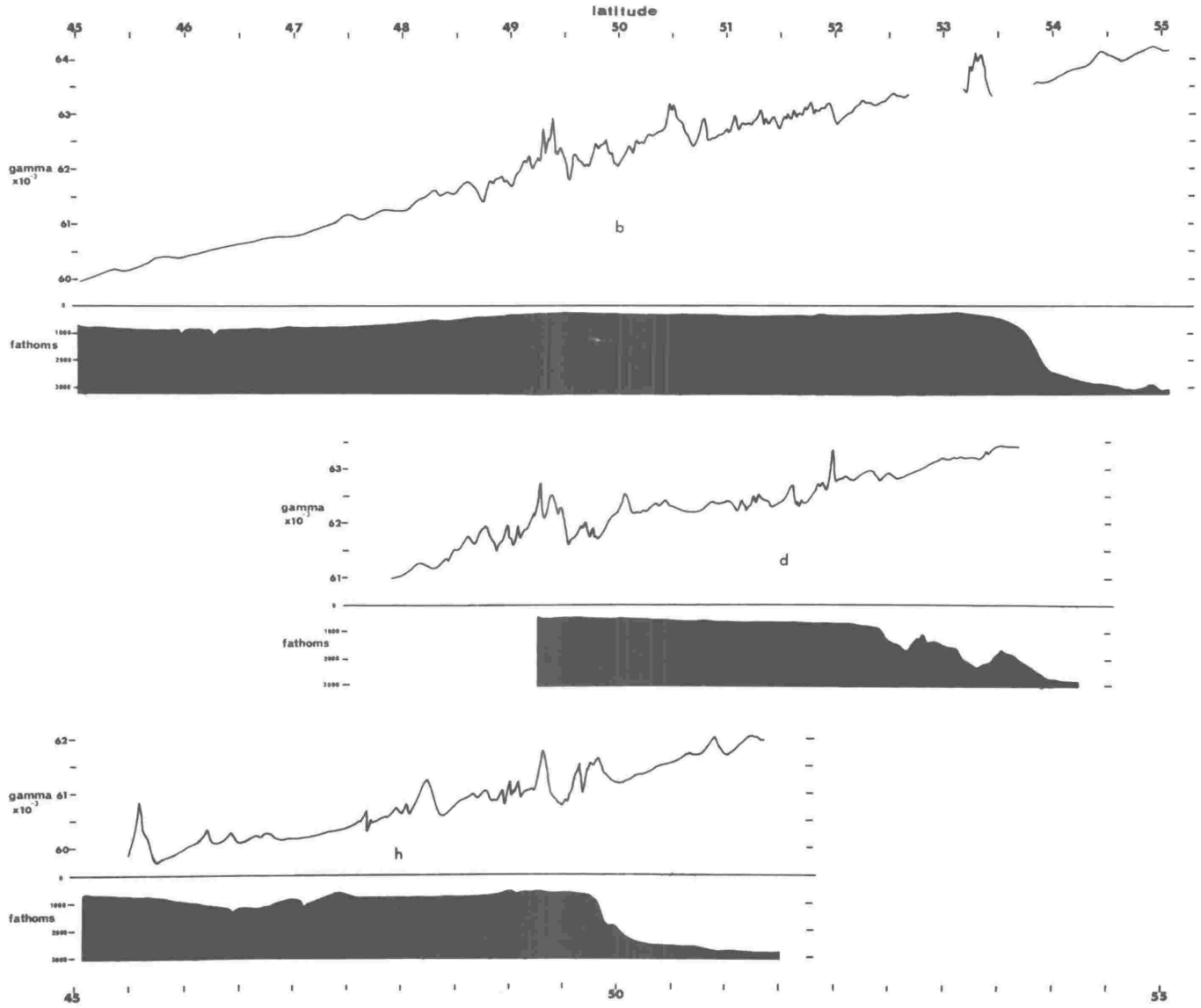
latitude
45
46
47
48
49
50
51
52
53
54
55
gamma x10⁻³
64
63
62
61
60
b
fathoms
1000
2000
3000
gamma x10⁻³
63
62
61
d
fathoms
1000
2000
3000
gamma x10⁻³
62
61
60
h
fathoms
1000
2000
3000
45
50
55

FIGURE 27.

Total field and bathymetry profiles across the Southwest Pacific Basin. Vertical exageration of the bathymetry profiles 15:1.

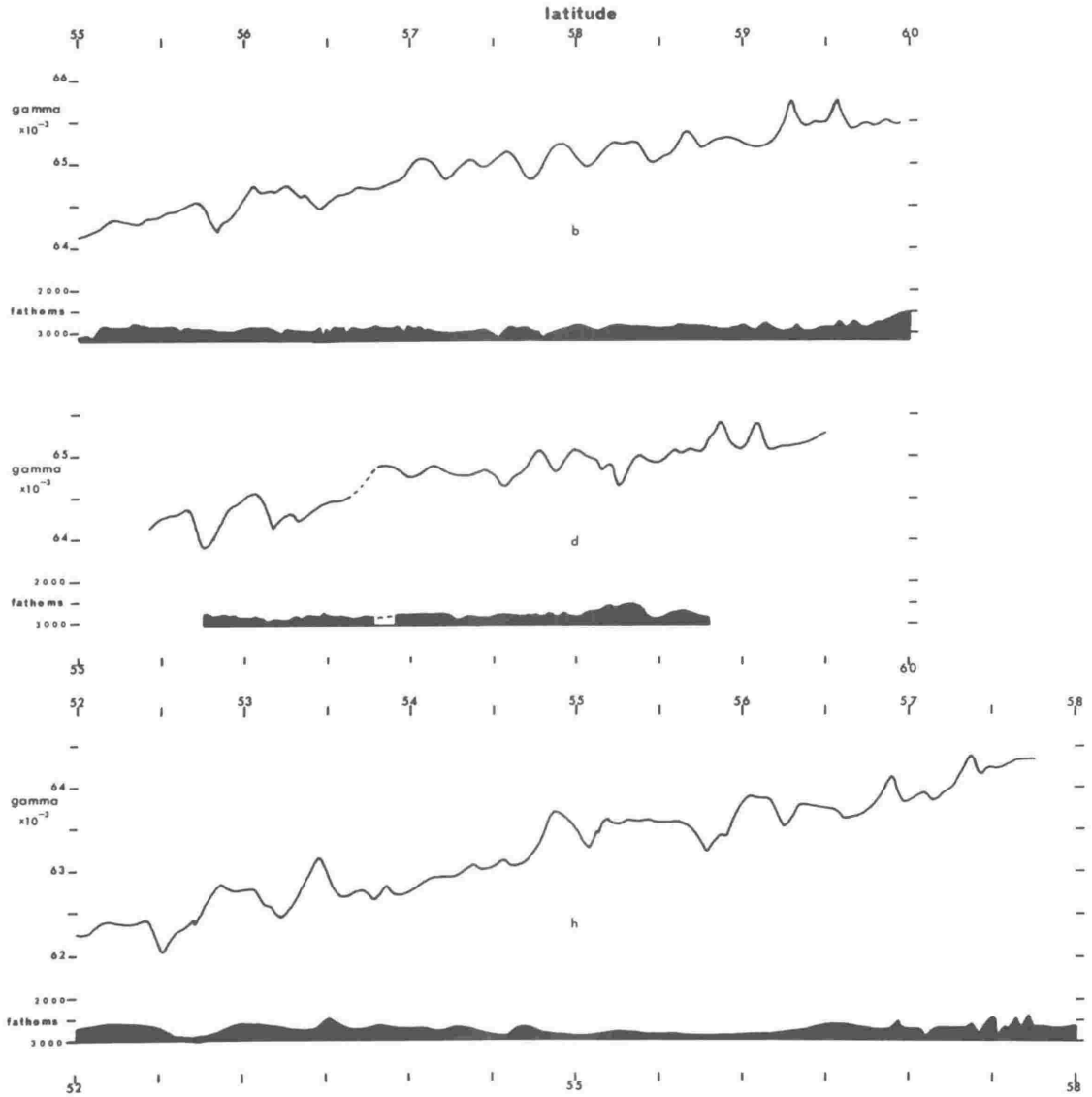
latitude
55
56
57
58
59
60
66
gamma
x10⁻³
65
64
b
2000
fathoms
3000
65
gamma
x10⁻³
64
d
2000
fathoms
3000
55
60
52
53
54
55
56
57
58
64
gamma
x10⁻³
63
62
h
2000
fathoms
3000
52
55
58

FIGURE 28.

Total field and bathymetry profiles across the Pacific-Antarctic Ridge. Vertical exageration of bathymetry profiles 15:1.

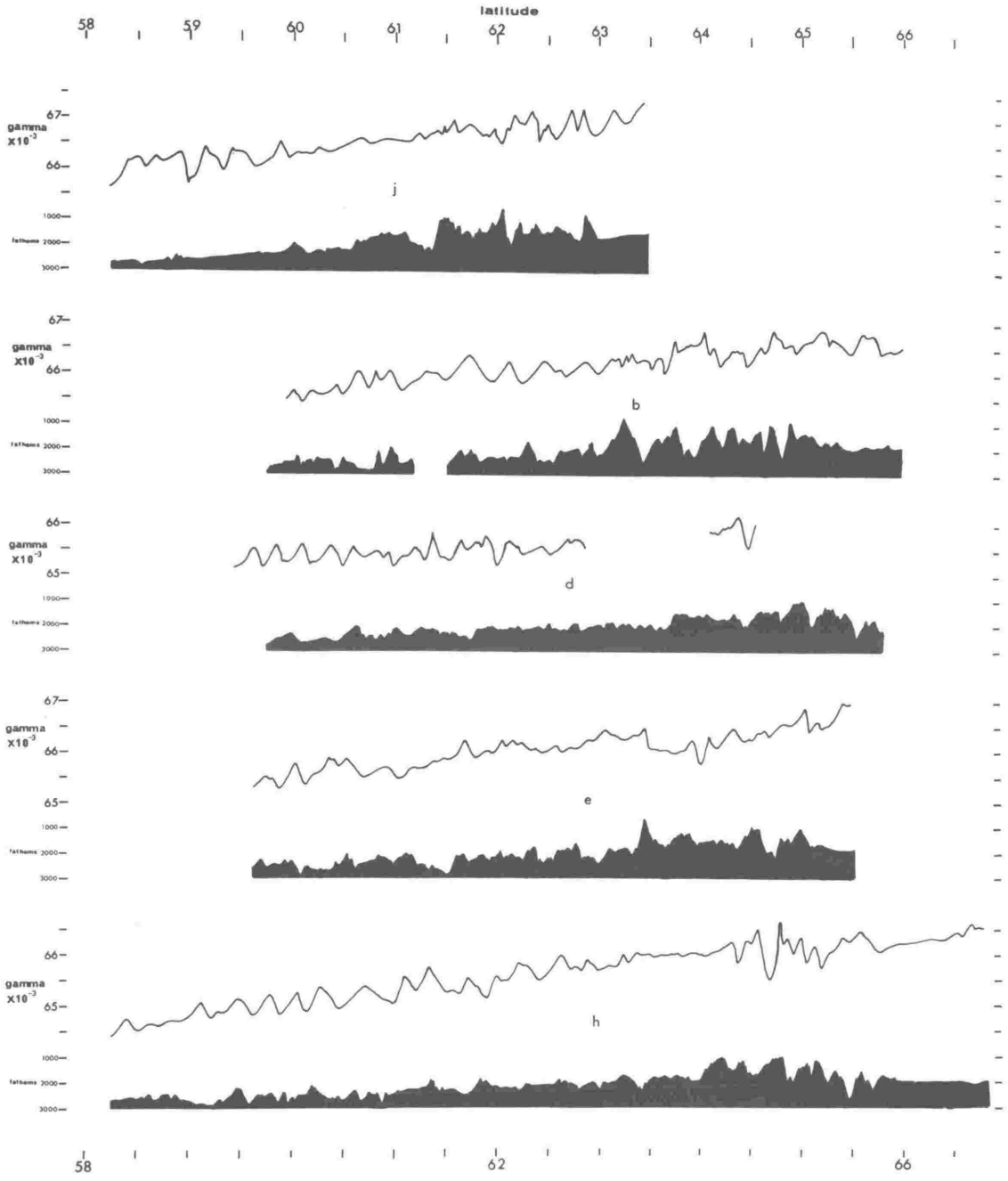
latitude
58
59
60
61
62
63
64
65
66
gamma
X10-3
67
66
65
fathoms
1000
2000
3000
j
b
d
e
h
58
62
66

FIGURE 29.

Total field and bathymetry profiles across the Balleny Plateau. Note the two seamounts near the beginning of the upper profile and the negative anomalies associated with them. Vertical exaggeration of bathymetry profiles 15:1.

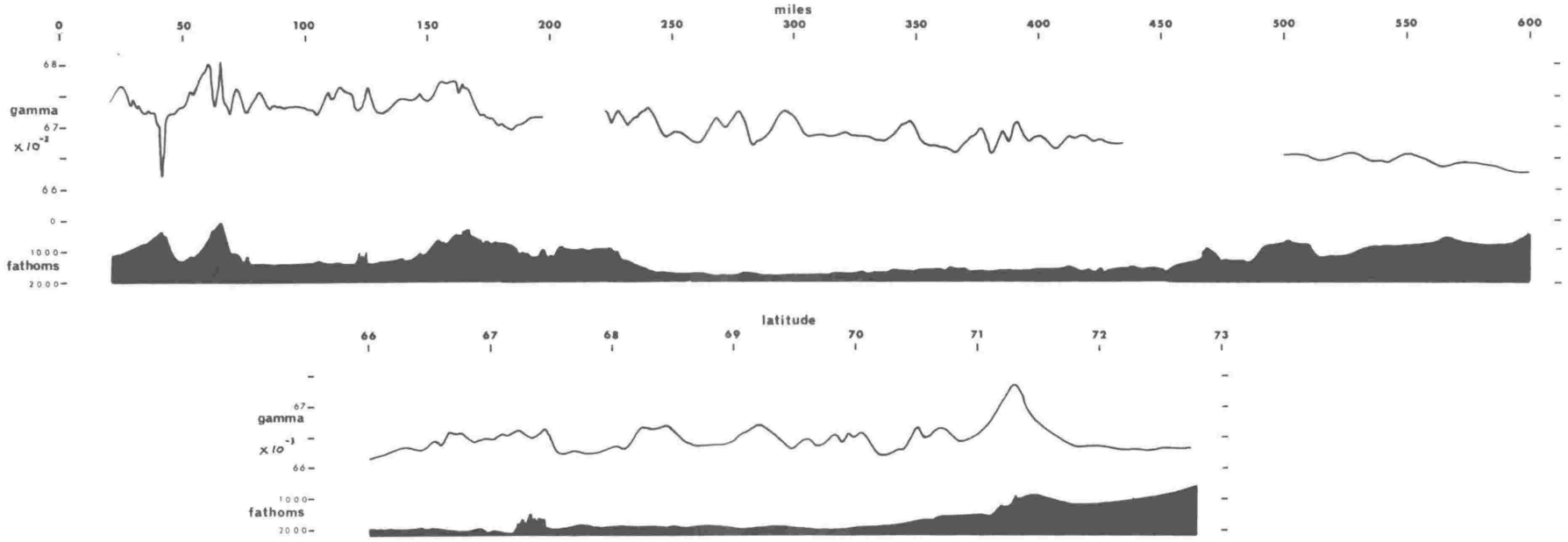
miles
0
50
100
150
200
250
300
350
400
450
500
550
600
68
gamma
67
x 10^-2
66
0
1000
fathoms
2000
latitude
66
67
68
69
70
71
72
73
67
gamma
x 10^-1
66
1000
fathoms
2000

FIGURE 30.

Total field and bathymetry profiles across the Antarctic slope and the Ross Sea (track b). Vertical exageration of the bathymetry profile 15:1.

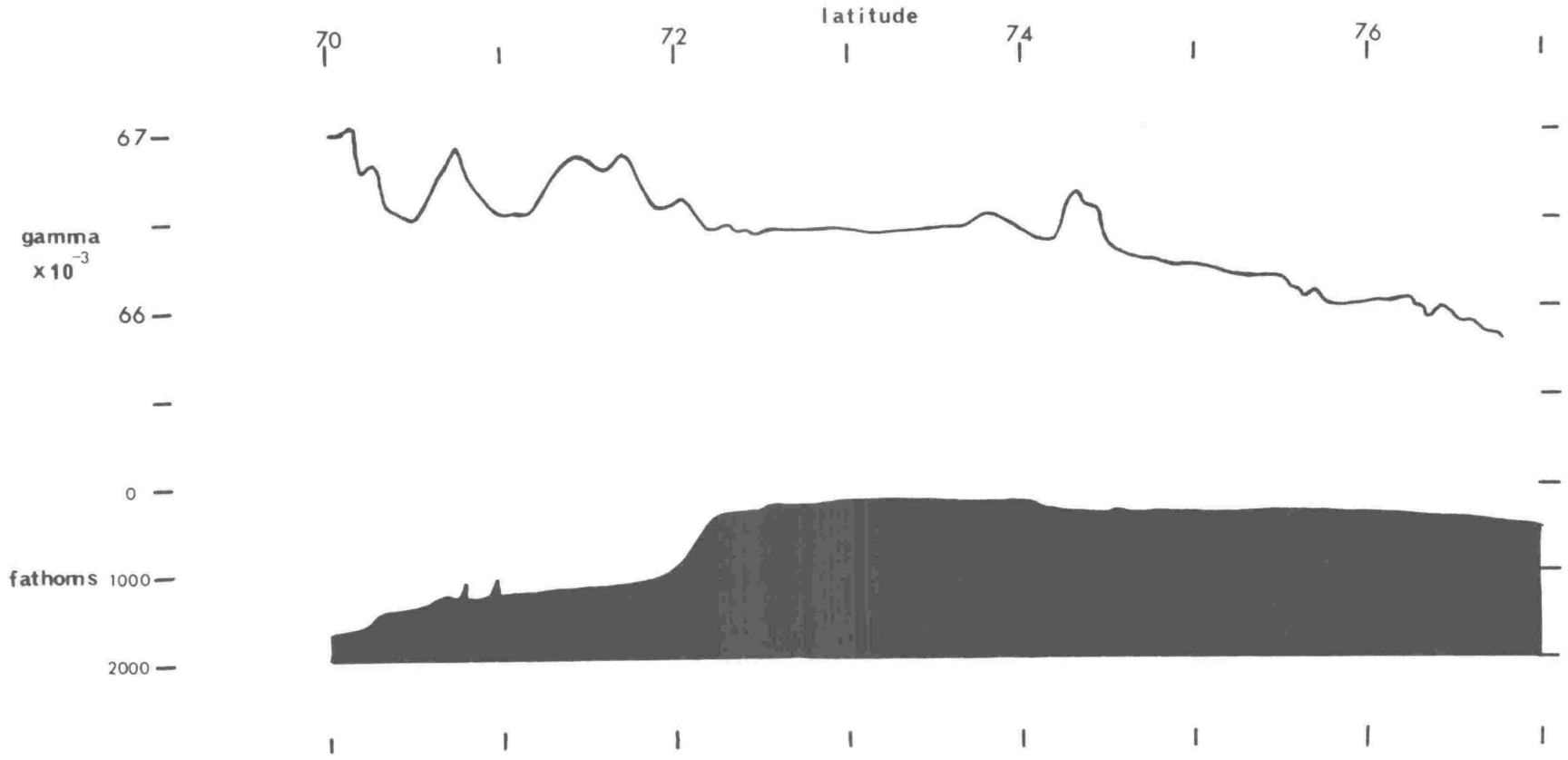
latitude
70
72
74
76
67
gamma
x10^-3
66
0
fathoms
1000
2000

FIGURE 31.

Total field profile across the Southwest Pacific Basin with the regional field drawn in.

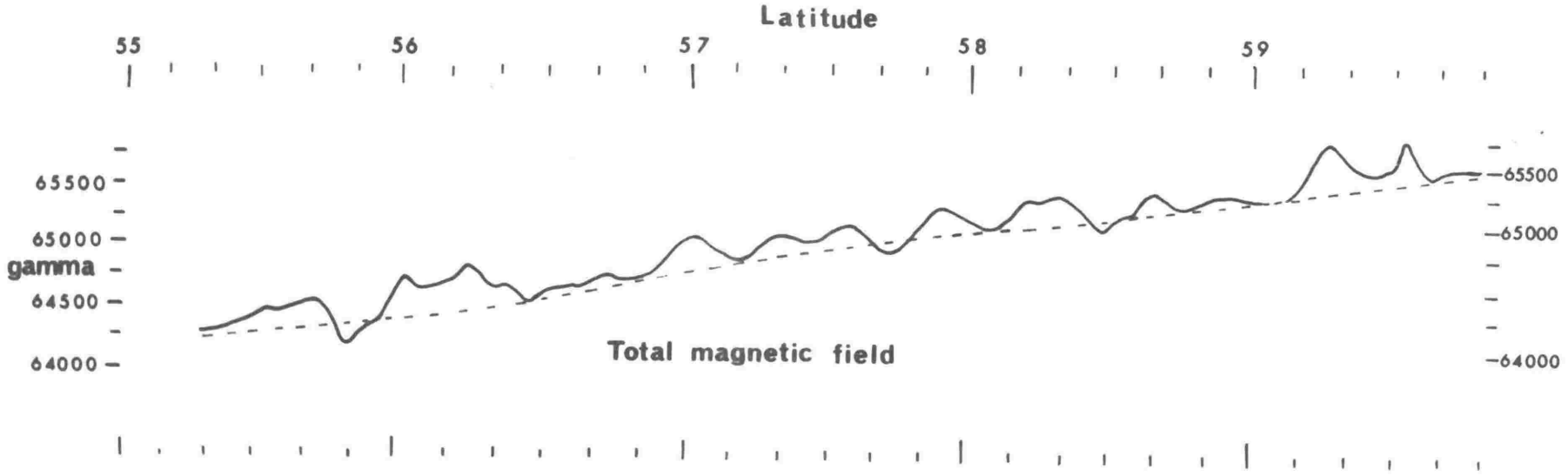
Latitude
55
56
57
58
59
65500
65000
gamma
64500
64000
Total magnetic field
65500
65000
64000

FIGURE 32.

Regional magnetic field map of the area studied showing the tracks over which the magnetic results used for drawing the map were obtained.

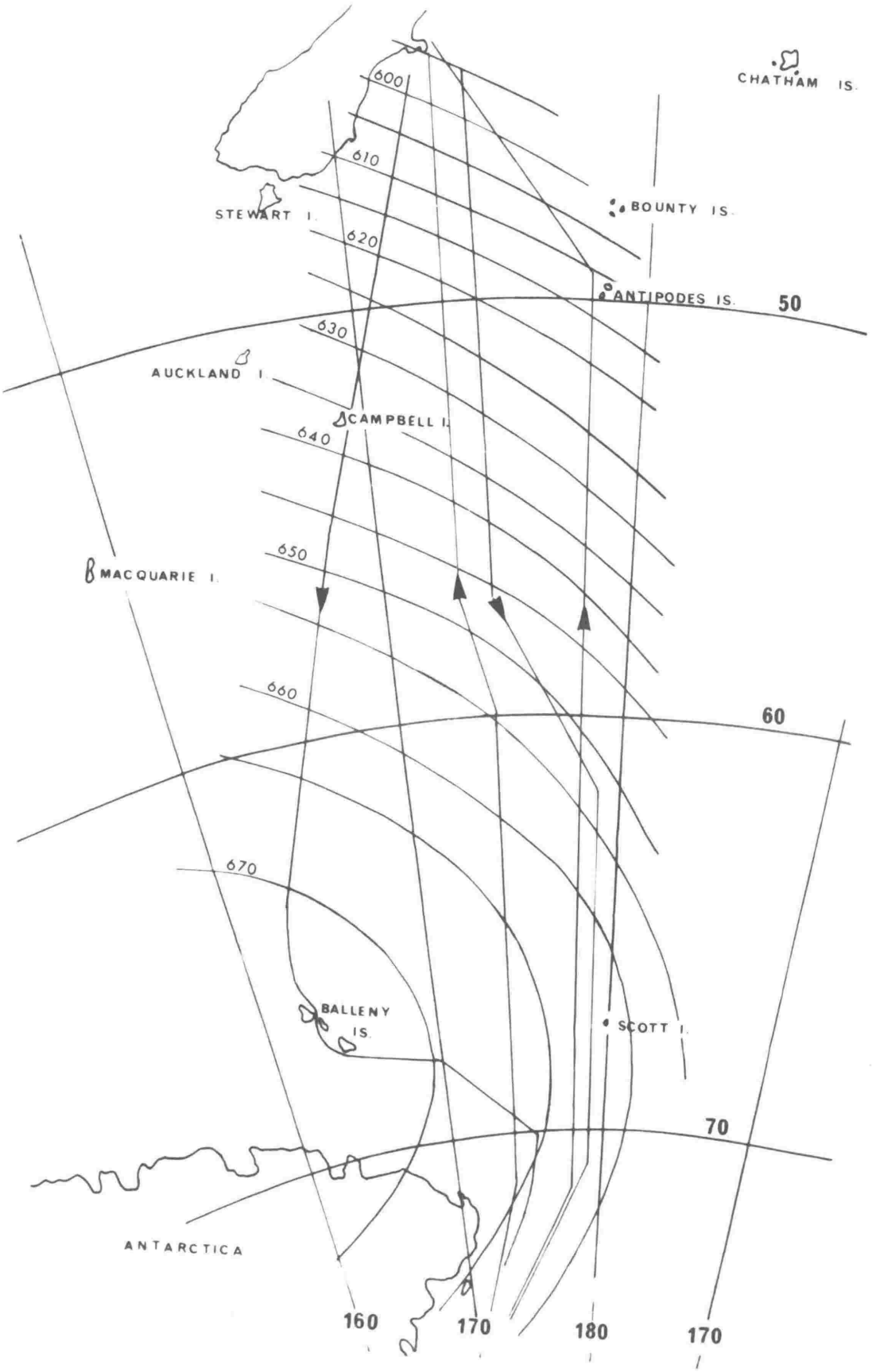
CHATHAM IS.
600
610
STEWART I.
BOUNTY IS.
620
ANTIPODES IS.
50
630
AUCKLAND I.
CAMPBELL I.
640
650
MACQUARIE I.
660
60
670
BALLENY IS.
SCOTT I.
70
ANTARCTICA
160
170
180
170

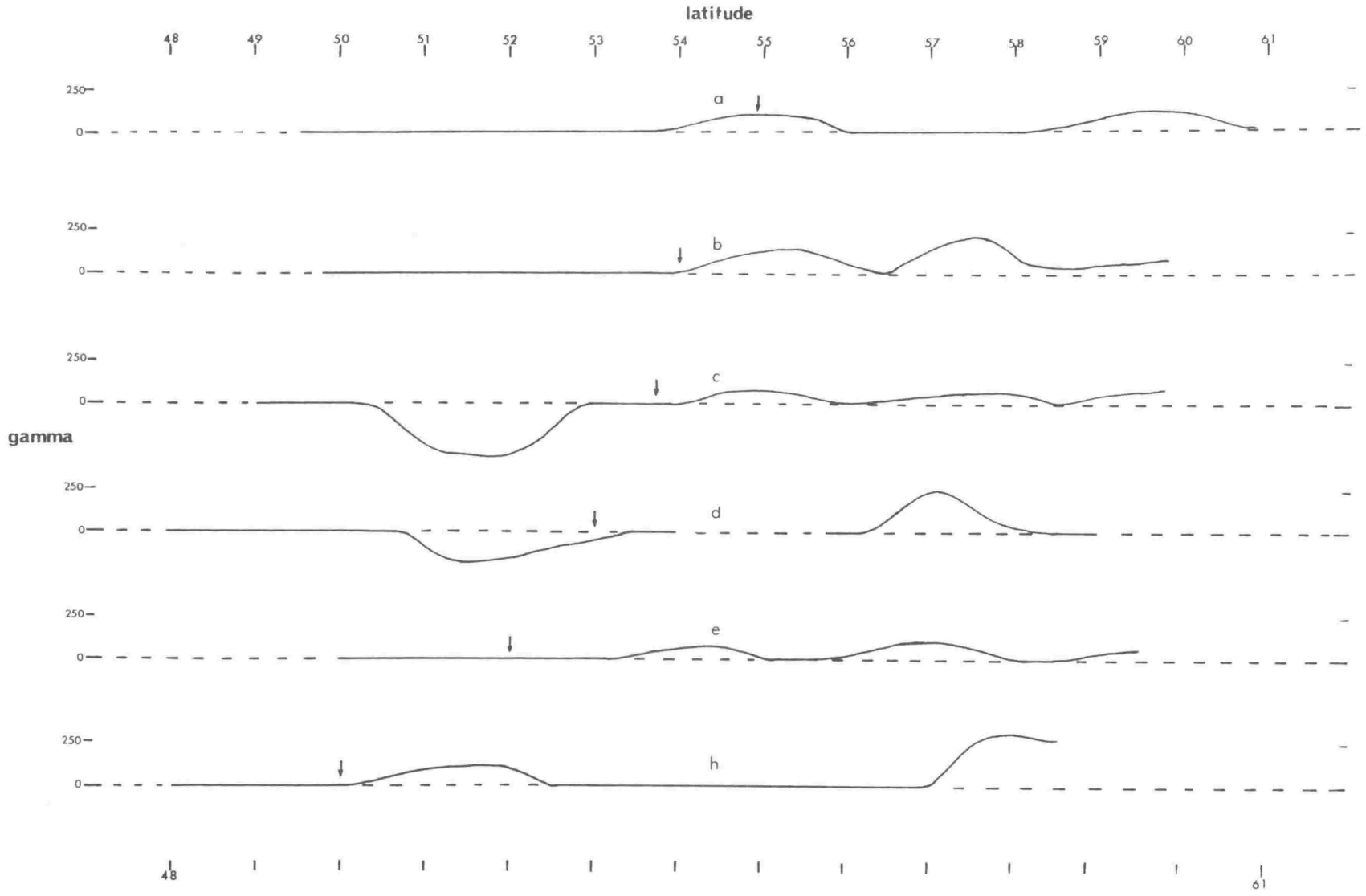
latitude
48
49
50
51
52
53
54
55
56
57
58
59
60
61
250
0
a
b
c
gamma
d
e
h

FIGURE 34.

Regional magnetic anomalies across the Pacific-Antarctic Ridge. The two arrows indicate the extent of the axial zone.

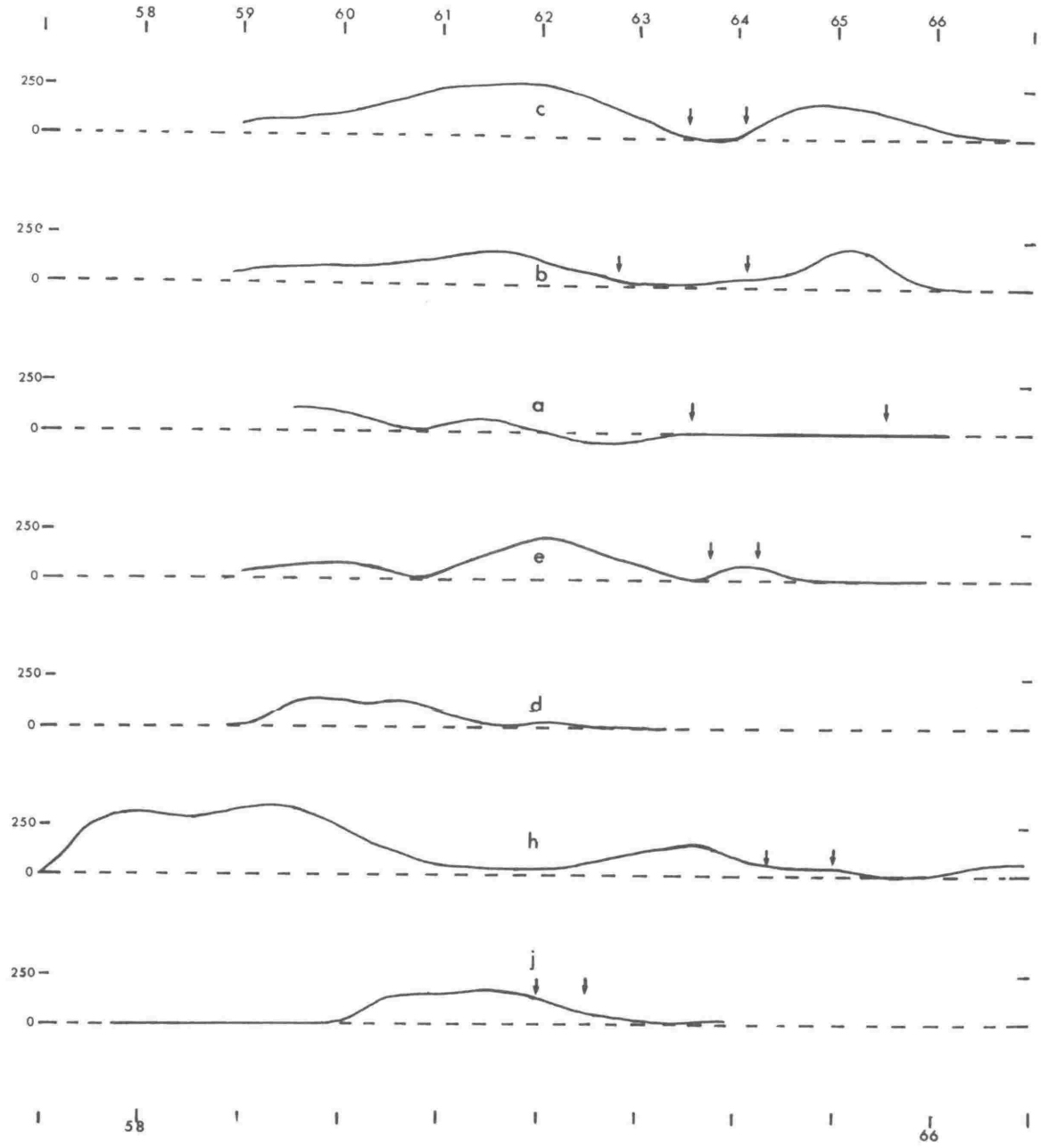
58
59
60
61
62
63
64
65
66
250
0
c
b
a
e
d
h
j
58
66

FIGURE 35.

Regional anomaly map. The contour interval is 100 gamma and the shaded areas indicate regional anomalies greater than 100 gamma. Only one negative anomaly occurs, to the east of Auckland and Campbell Islands on the Campbell Plateau.

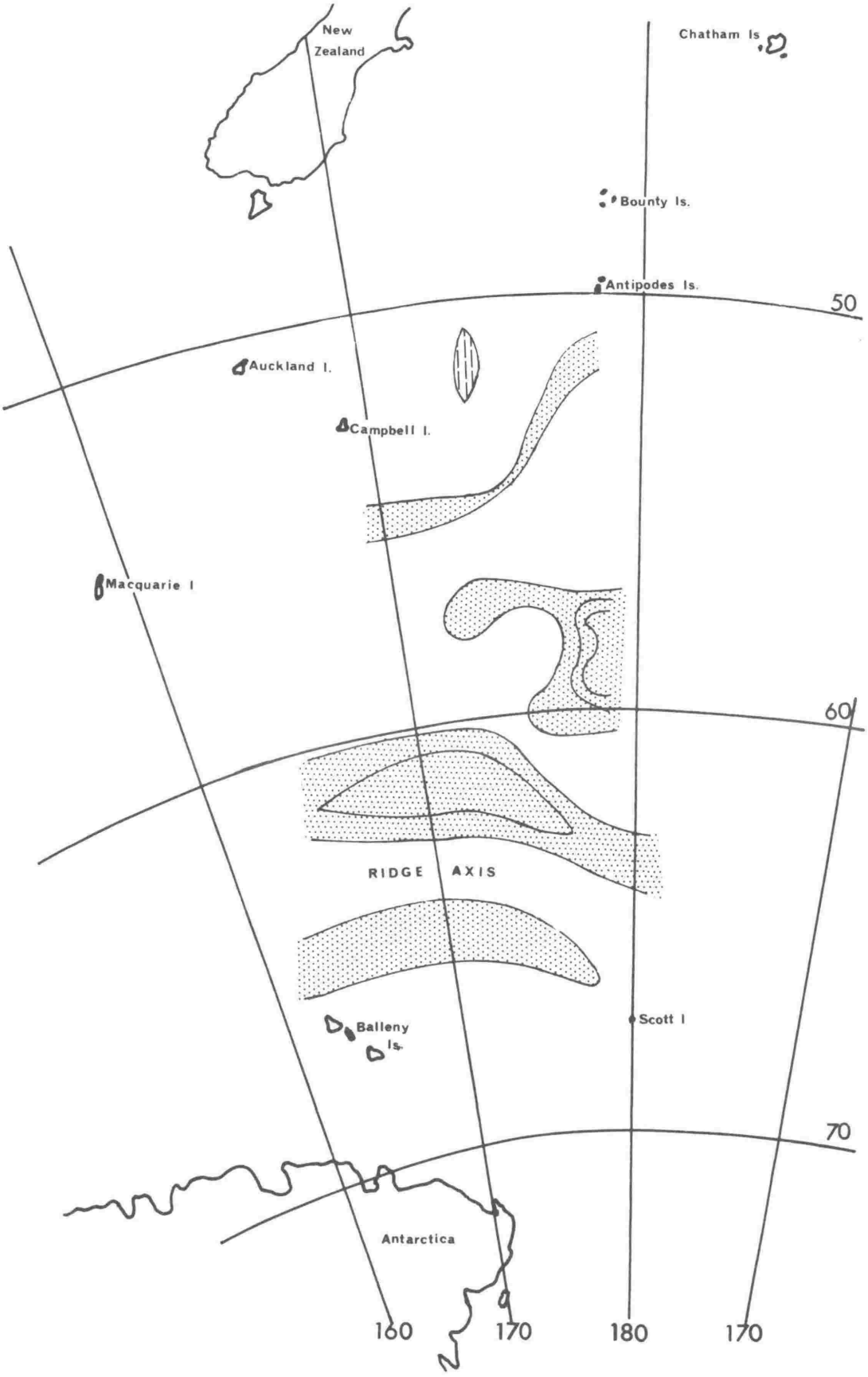
New
Zealand
Chatham Is
Bounty Is.
Antipodes Is.
50
Auckland I.
Campbell I.
Macquarie I
60
RIDGE AXIS
Balleny
Is.
Scott I
70
Antarctica
160
170
180
170

FIGURE 36.

Magnetic anomaly profiles across the southeast New Zealand Plateau.

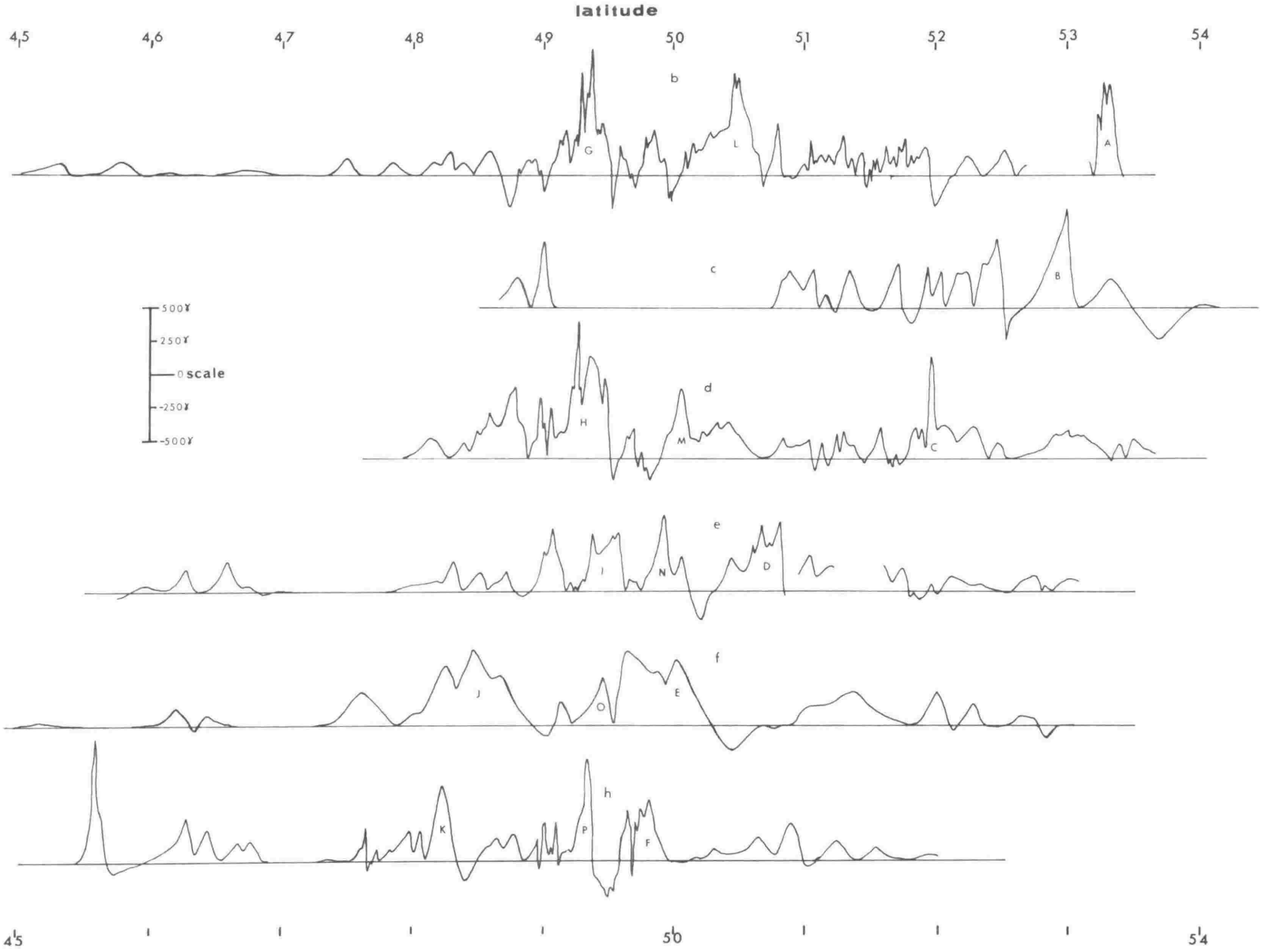
latitude
4,5
4,6
4,7
4,8
4,9
5,0
5,1
5,2
5,3
5,4
b
G
L
A
c
B
500γ
250γ
0 scale
-250γ
-500γ
d
H
M
C
e
I
N
D
f
J
O
E
h
K
P
F
4'5
5'0
5'4

FIGURE 37.

Chart of the Campbell Plateau showing the relation between the three main magnetic ridges and the bathymetry contours. The dashed portion of the solid lines is the assumed continuation of the ridges east of Bounty and Antipodes Islands.

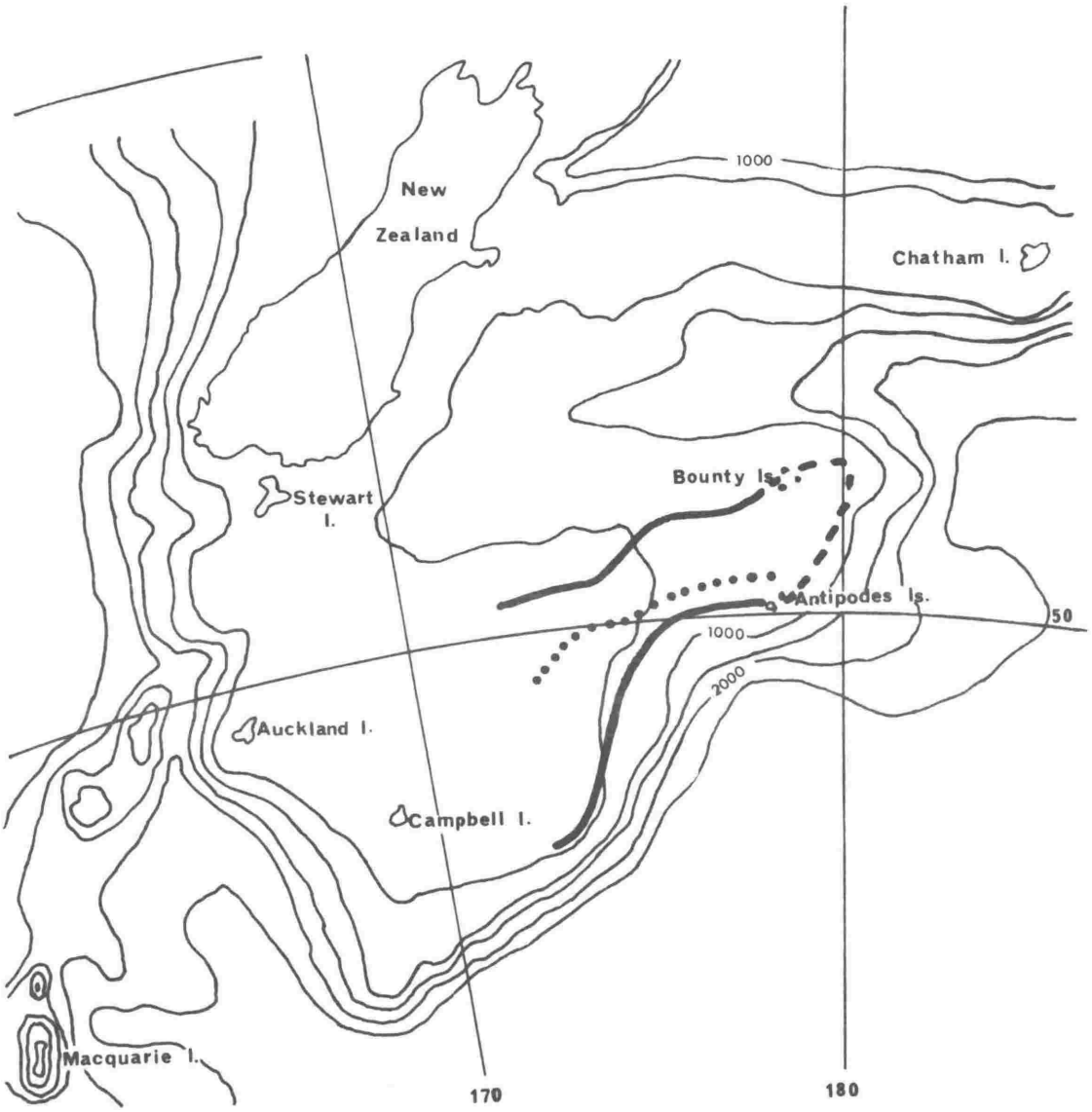
New
Zealand
1000
Chatham I.
Bounty Is.
Stewart
I.
Antipodes Is.
50
1000
2000
Auckland I.
Campbell I.
Macquarie I.
170
180

FIGURE 38.

Magnetic anomaly profiles across the Southwest Pacific Basin. Profiles g and i are only approximate copies of the profiles published by the U.S. Navy Hydrographic Office (1962). They are included to show the general agreement of these records with those presented in this thesis.

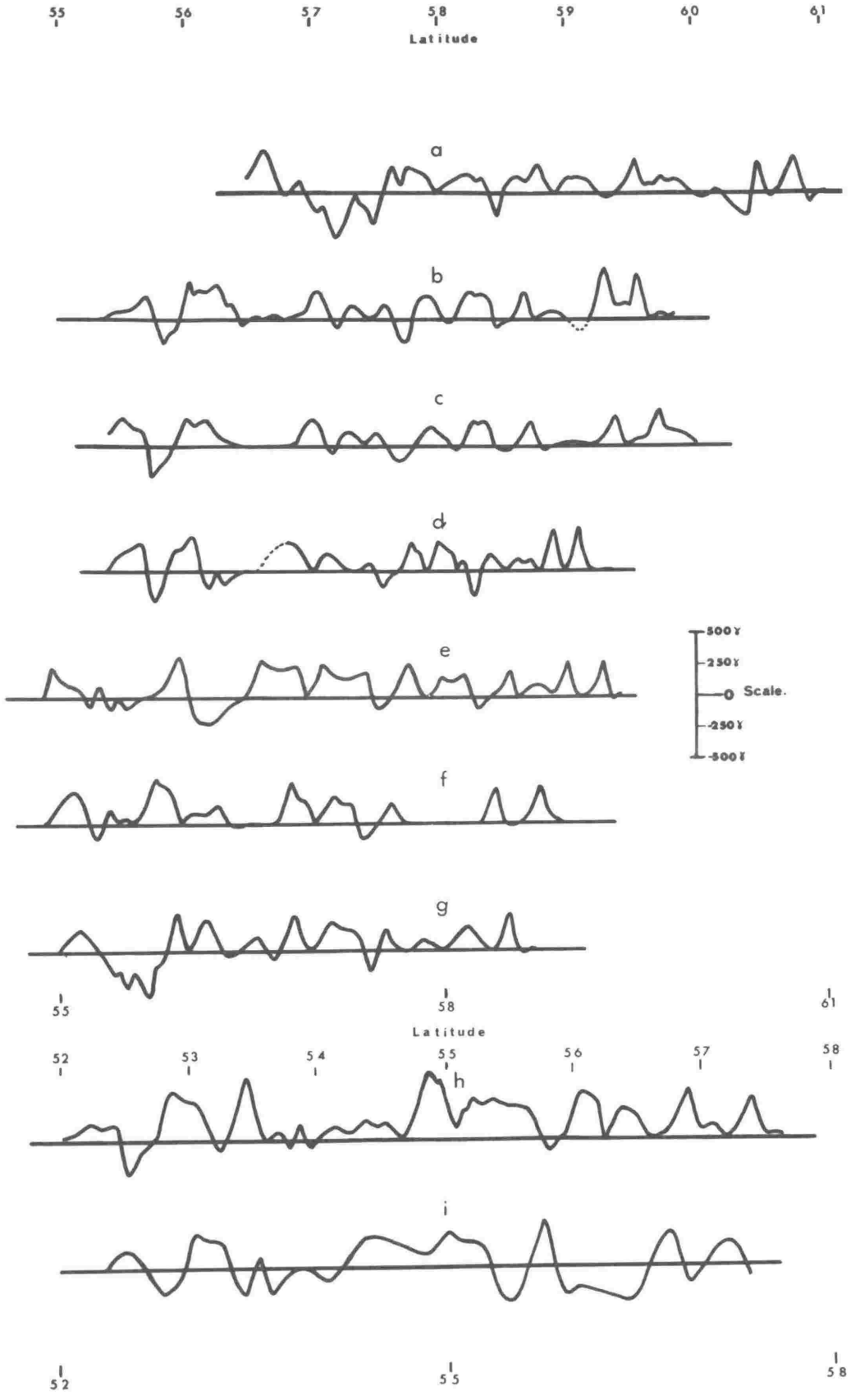
55
56
57
58
59
60
61
Latitude
a
b
c
d
e
f
g
500γ
250γ
0 Scale.
-250γ
-500γ
55
58
61
Latitude
52
53
54
55
56
57
58
h
i
52
55
58

FIGURE 39.

Four magnetic anomaly profiles across the Southwest Pacific Basin with the assumed correlation drawn in (after Christoffel and Ross, 1965). Tracks 1 - 4 of this paper correspond to tracks f,d,b,c, respectively in this thesis.

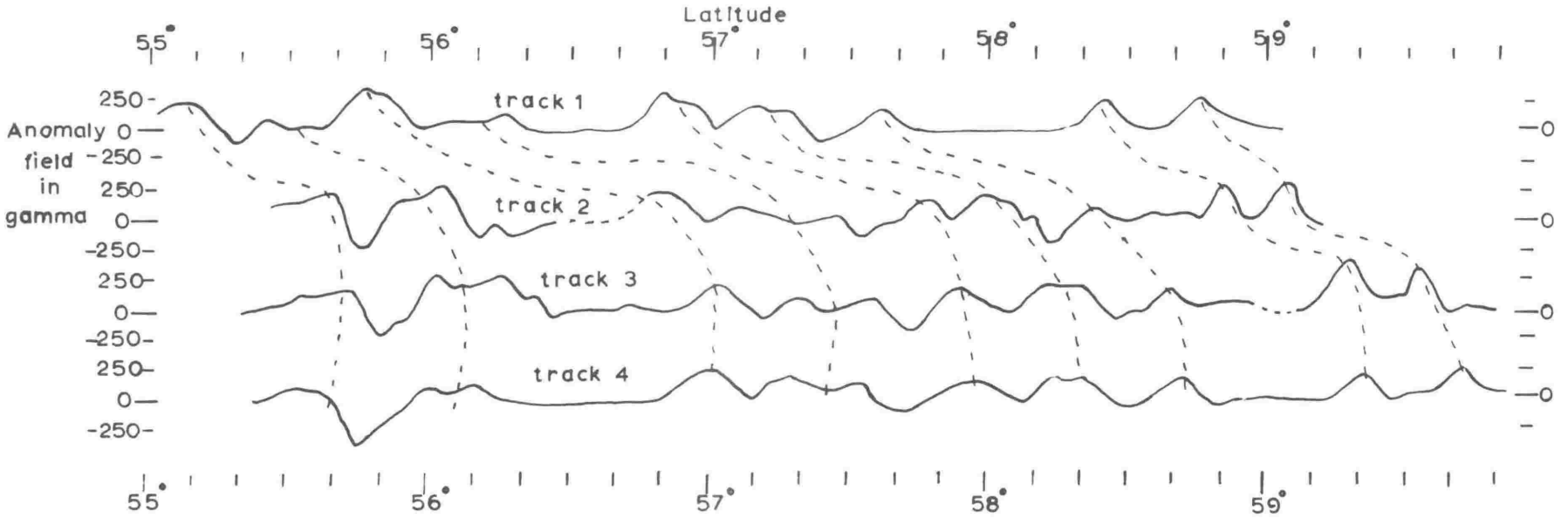
Latitude
55°
56°
57°
58°
59°
Anomaly field in gamma
250
0
-250
track 1
track 2
track 3
track 4

FIGURE 40.

Magnetic anomaly contour map of the Southwestern Pacific Basin.

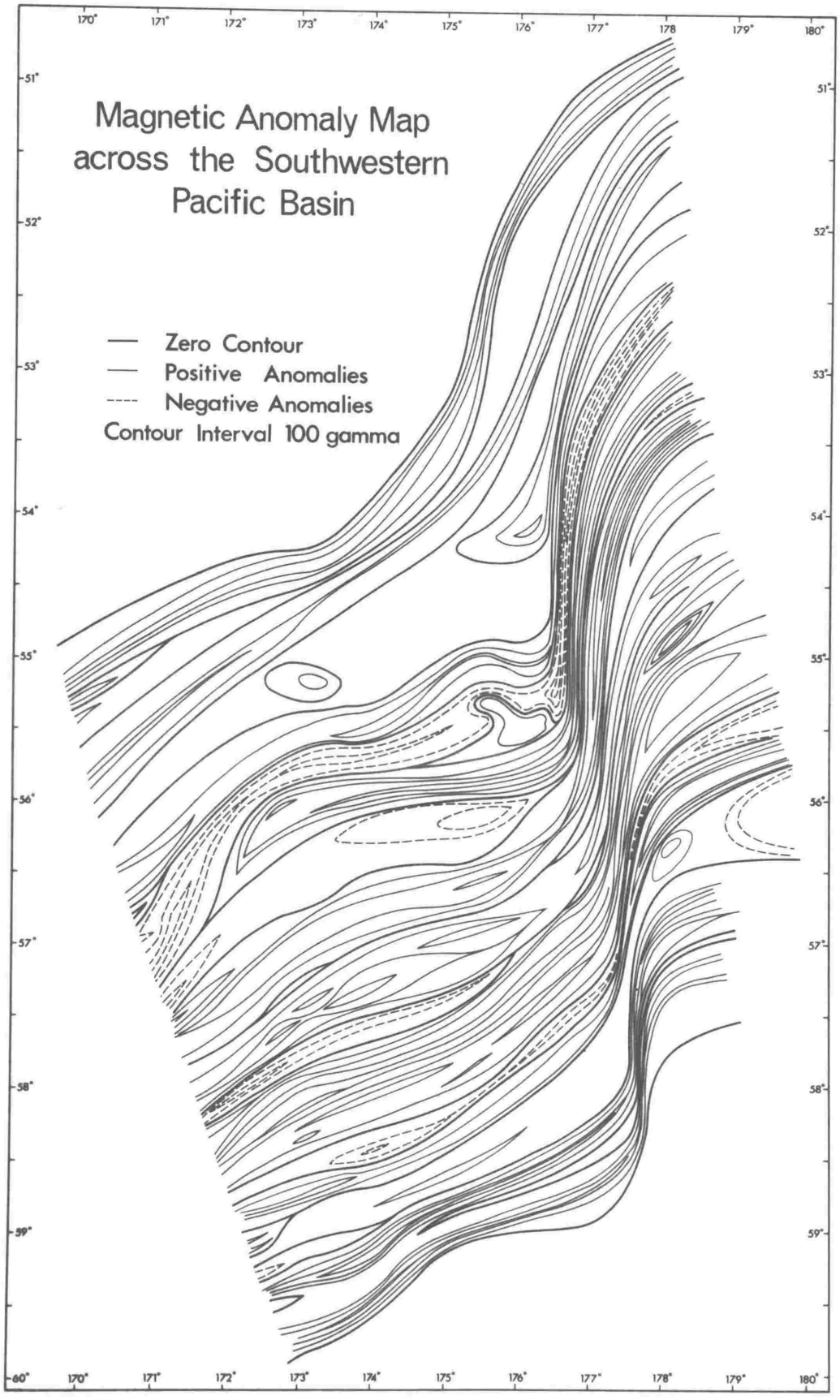
Magnetic Anomaly Map
across the Southwestern
Pacific Basin
Zero Contour
Positive Anomalies
Negative Anomalies
Contour Interval 100 gamma
170°
171°
172°
173°
174°
175°
176°
177°
178
179°
180°
51°
52°
53°
54°
55°
56°
57°
58°
59°
60°

FIGURE 41.

Magnetic features and bathymetry across the Southwestern Pacific Basin.

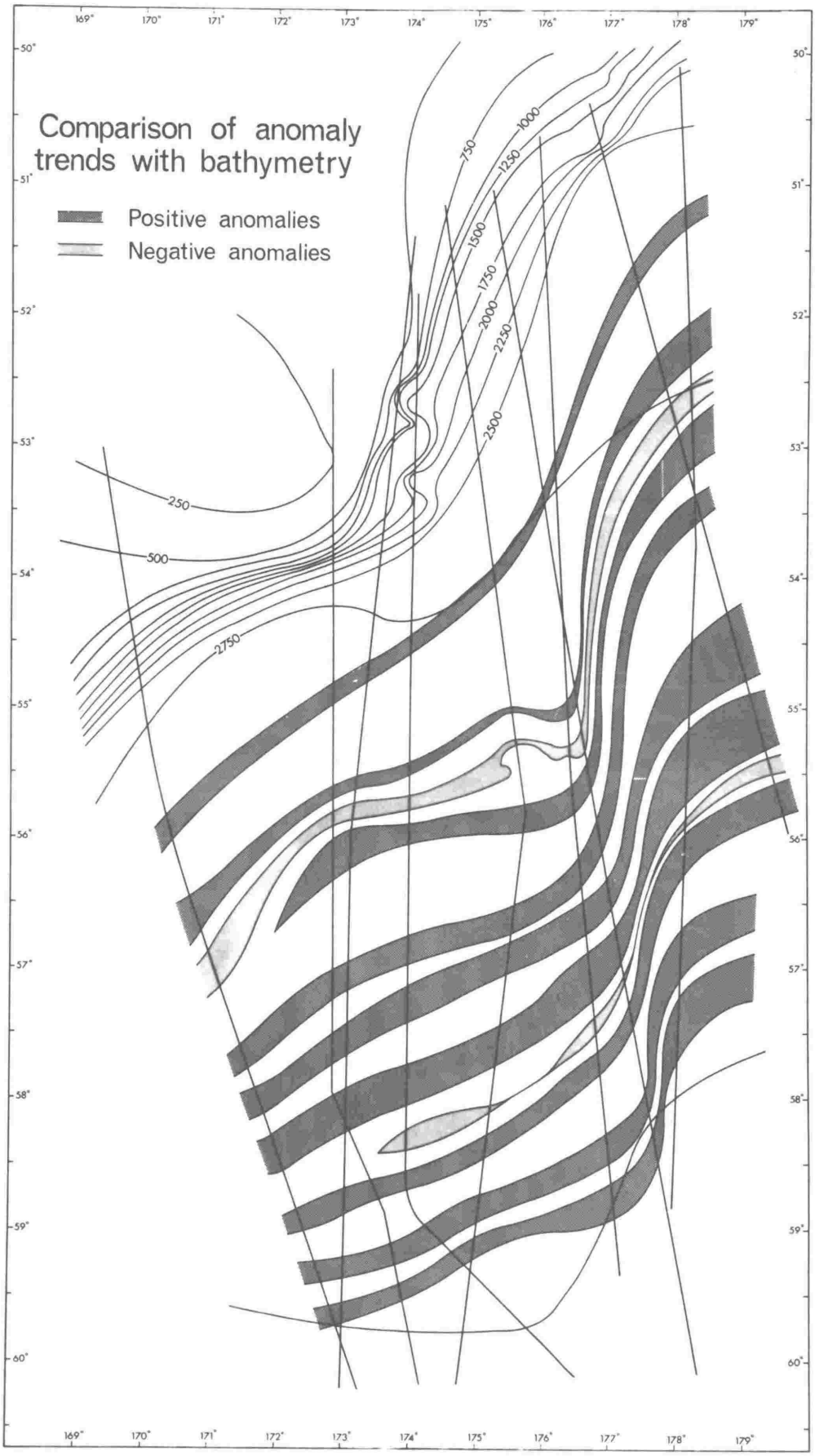
Comparison of anomaly trends with bathymetry
Positive anomalies
Negative anomalies
250
500
750
1000
1250
1500
1750
2000
2250
2500
2750
169°
170°
171°
172°
173°
174°
175°
176°
177°
178°
179°
50°
51°
52°
53°
54°
55°
56°
57°
58°
59°
60°

FIGURE 42.

Magnetic anomaly profiles across the Pacific-Antarctic Ridge. R.C. denotes the ridge crest as determined from the bathymetry profiles.

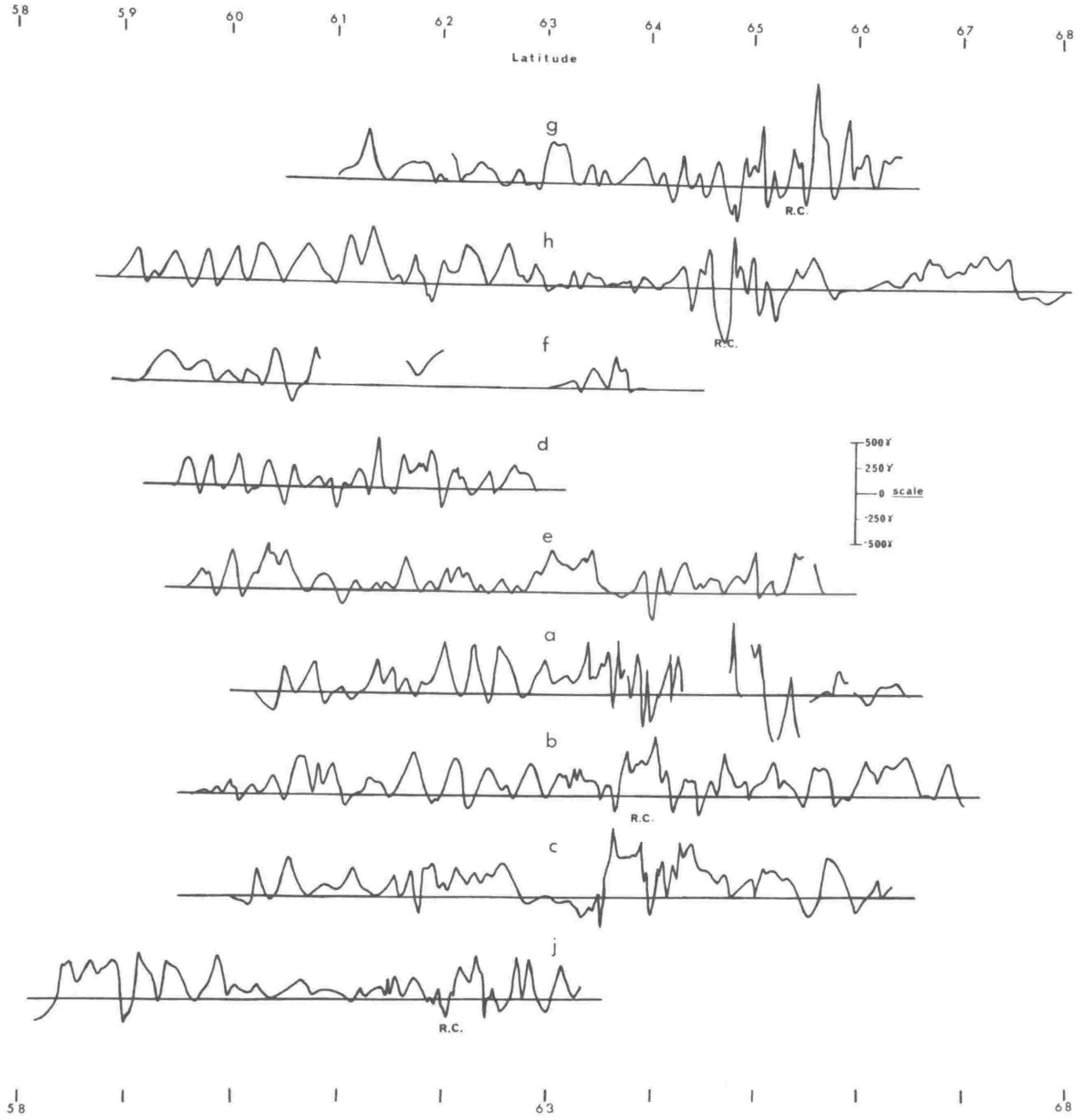
58
59
60
61
62
63
64
65
66
67
68
Latitude
g
R.C.
h
R.C.
f
d
500γ
250γ
0 scale
250γ
500γ
e
a
b
R.C.
c
j
R.C.
58
63
68

FIGURE 43.

Magnetic anomaly over a vertical dyke showing the depth indices mentioned in the script.

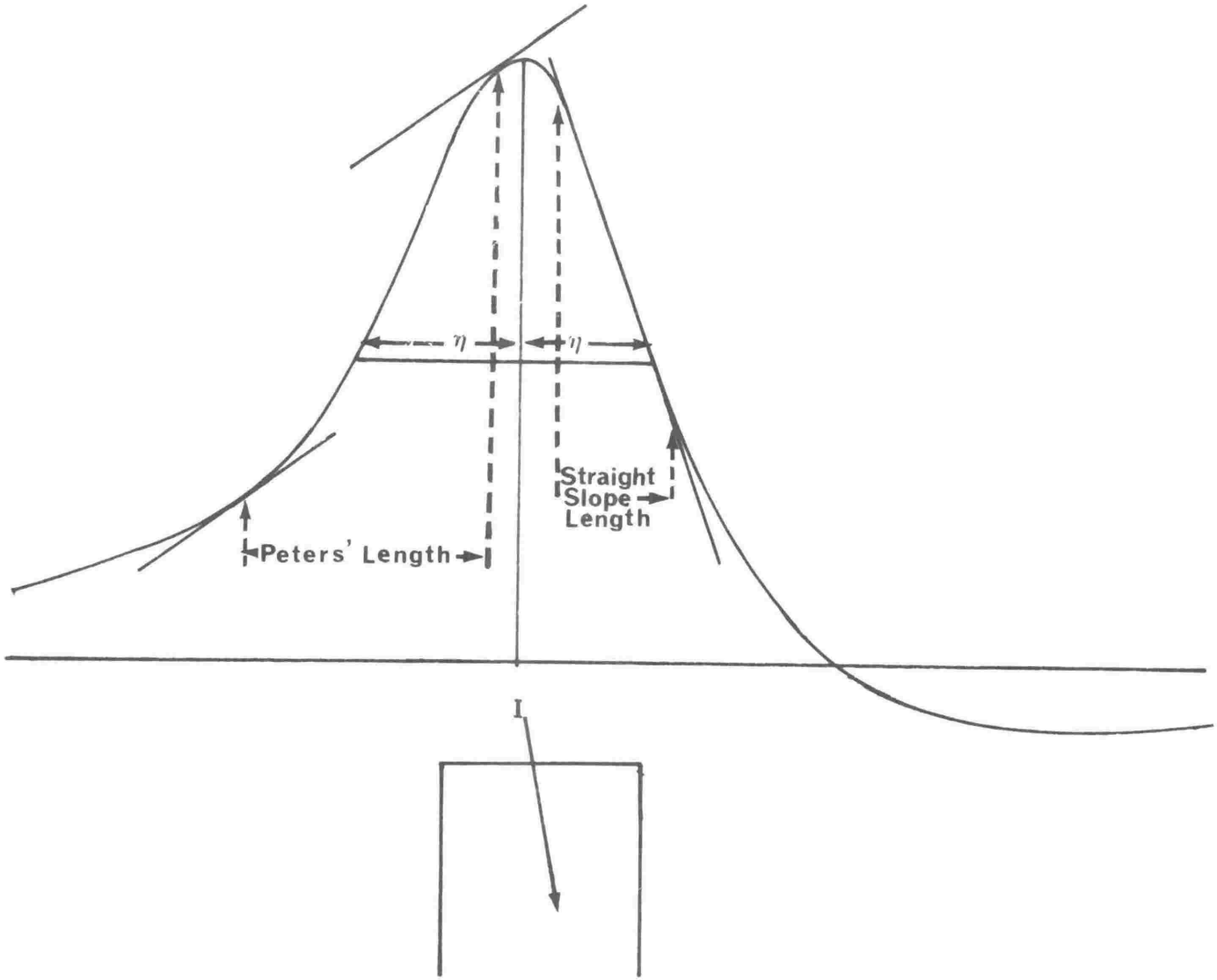
η
η
Straight
Slope
Length
Peters' Length
I

FIGURE 44.

Model basement across part of the Southwest Pacific Basin with the calculated and observed anomaly profiles.

Note: In this and all following models the horizontal and vertical scales are equal.

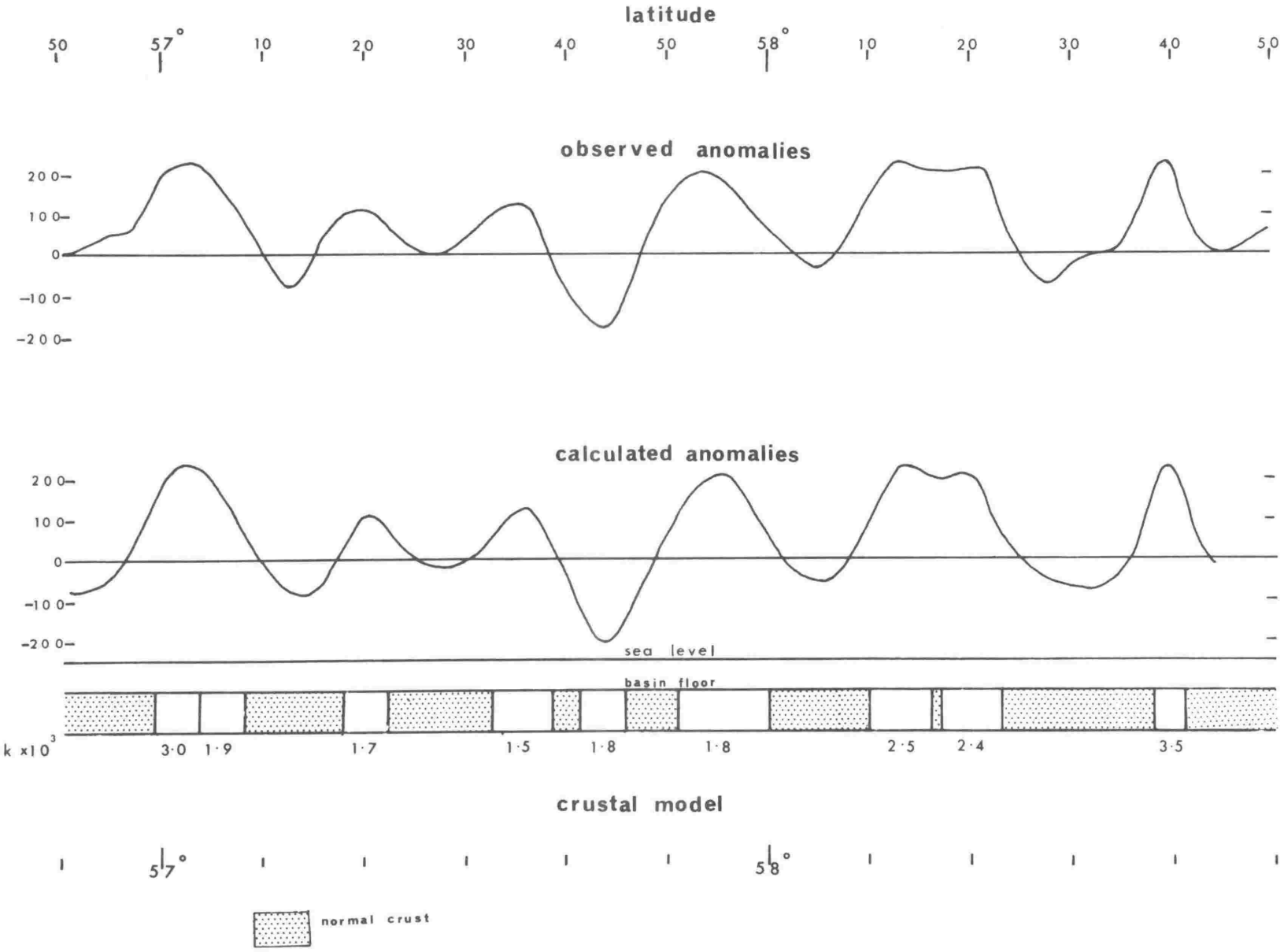
latitude
50
57°
10
20
30
40
50
58°
10
20
30
40
50
observed anomalies
200
100
0
-100
-200
calculated anomalies
200
100
0
-100
-200
sea level
basin floor
k x10³
3·0
1·9
1·7
1·5
1·8
1·8
2·5
2·4
3·5
crustal model
57°
58°
normal crust

FIGURE 45.

Model basement across a basement ridge on the Campbell Plateau with the calculated and observed anomalies.

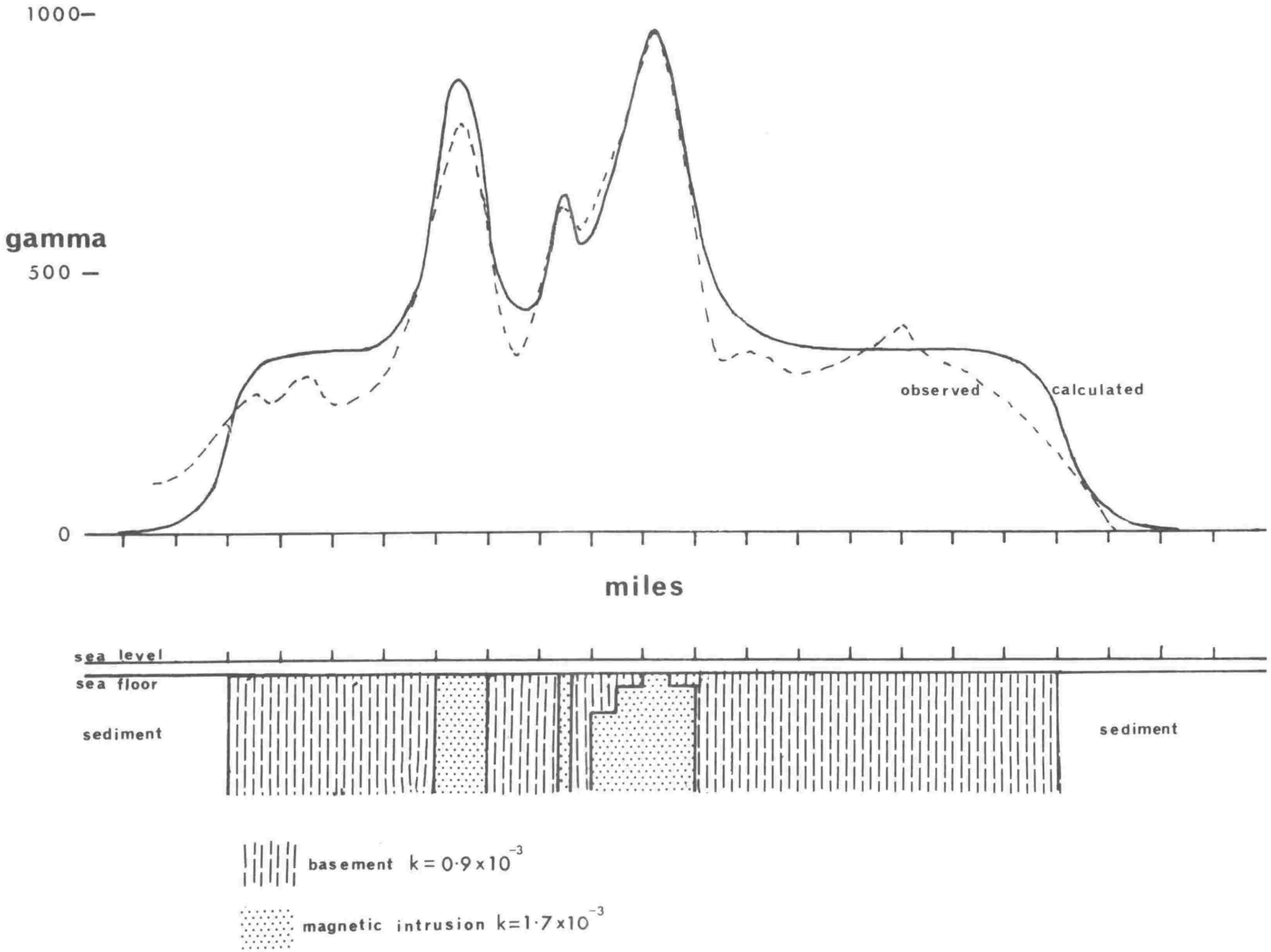
1000
gamma
500
0
observed
calculated
miles
sea level
sea floor
sediment
sediment
basement k = 0·9 x 10⁻³
magnetic intrusion k=1·7 x 10⁻³

FIGURE 46.

Basement model for the crest of the Pacific-Antarctic Ridge along track b with the calculated and observed anomalies.

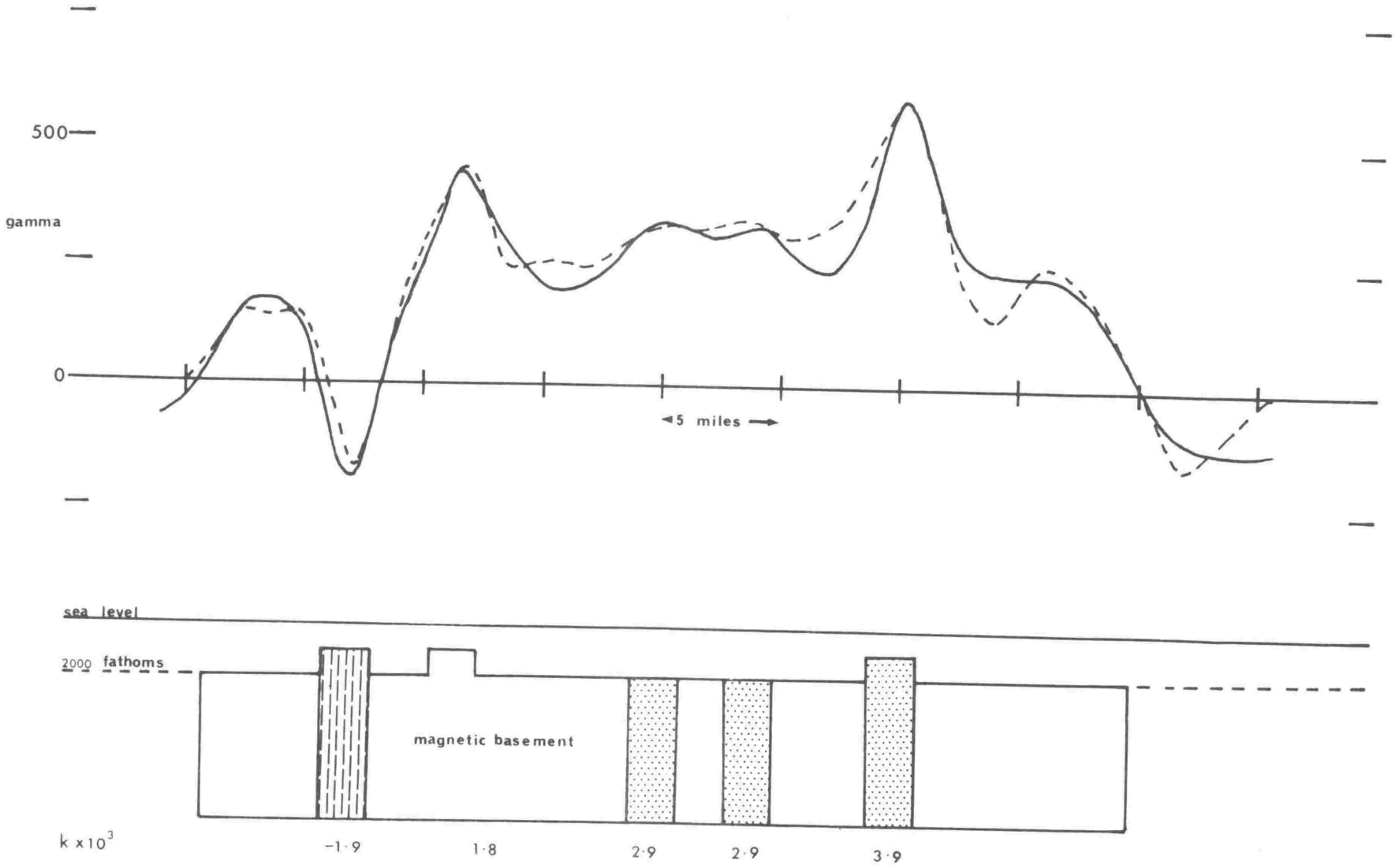
500
gamma
0
5 miles
sea level
2000 fathoms
magnetic basement
k x10^3
-1·9
1·8
2·9
2·9
3·9

FIGURE 47.

Basement model for the crest of the Pacific-Antarctic Ridge along track h with the calculated and observed anomalies.

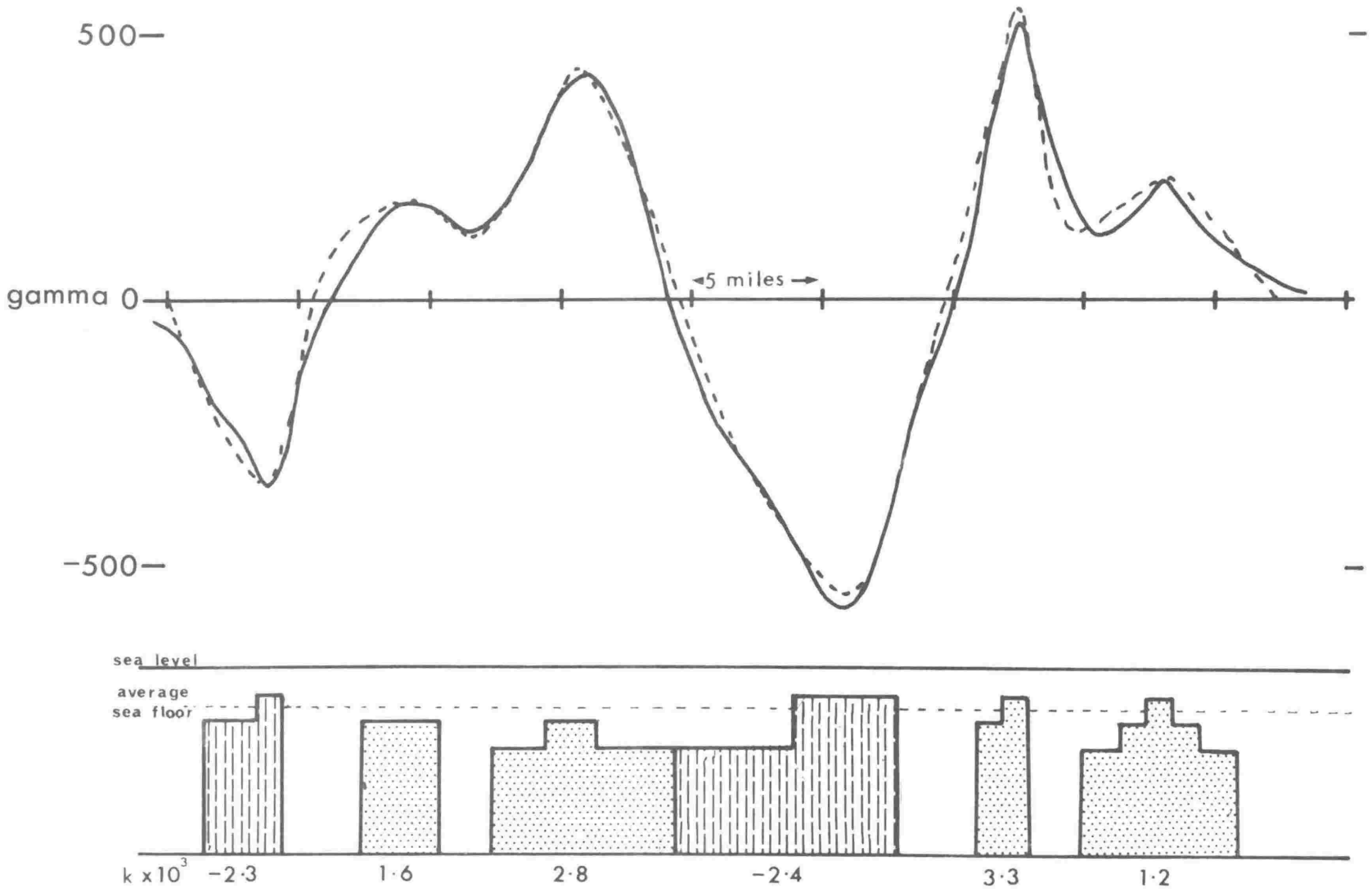
500—
gamma 0
5 miles
−500—
sea level
average
sea floor
k x10³
−2·3
1·6
2·8
−2·4
3·3
1·2

FIGURE 48.

Model of Balleny seamount 1 (67°08'S, 163°21'E) with the calculated and observed anomalies.

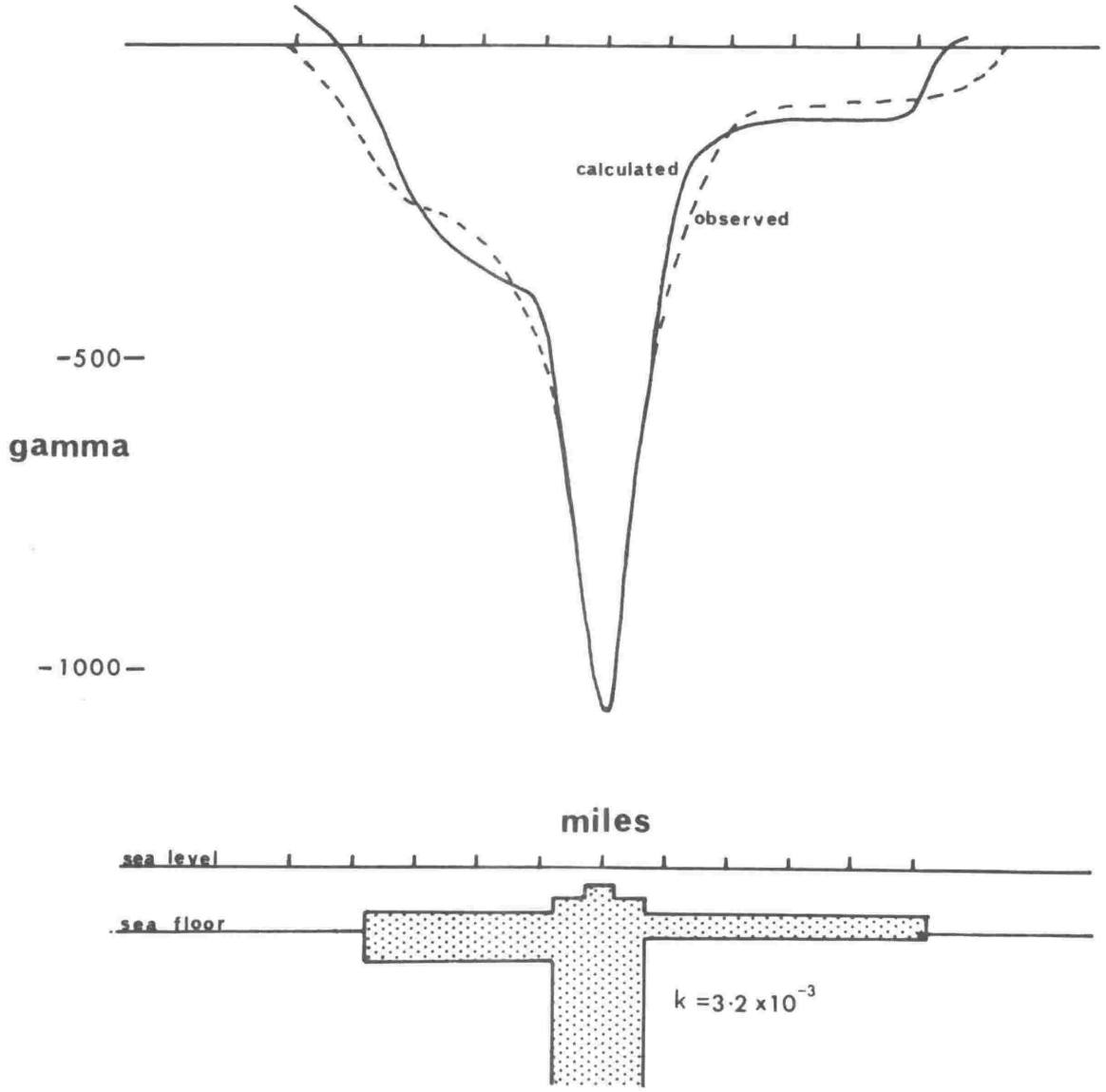
calculated
observed
-500-
gamma
-1000-
miles
sea level
sea floor
k =3·2 x10⁻³

FIGURE 49.

Model of Balleny seamount 2 (67°25'S, 167°47'E) with the calculated and observed anomalies.

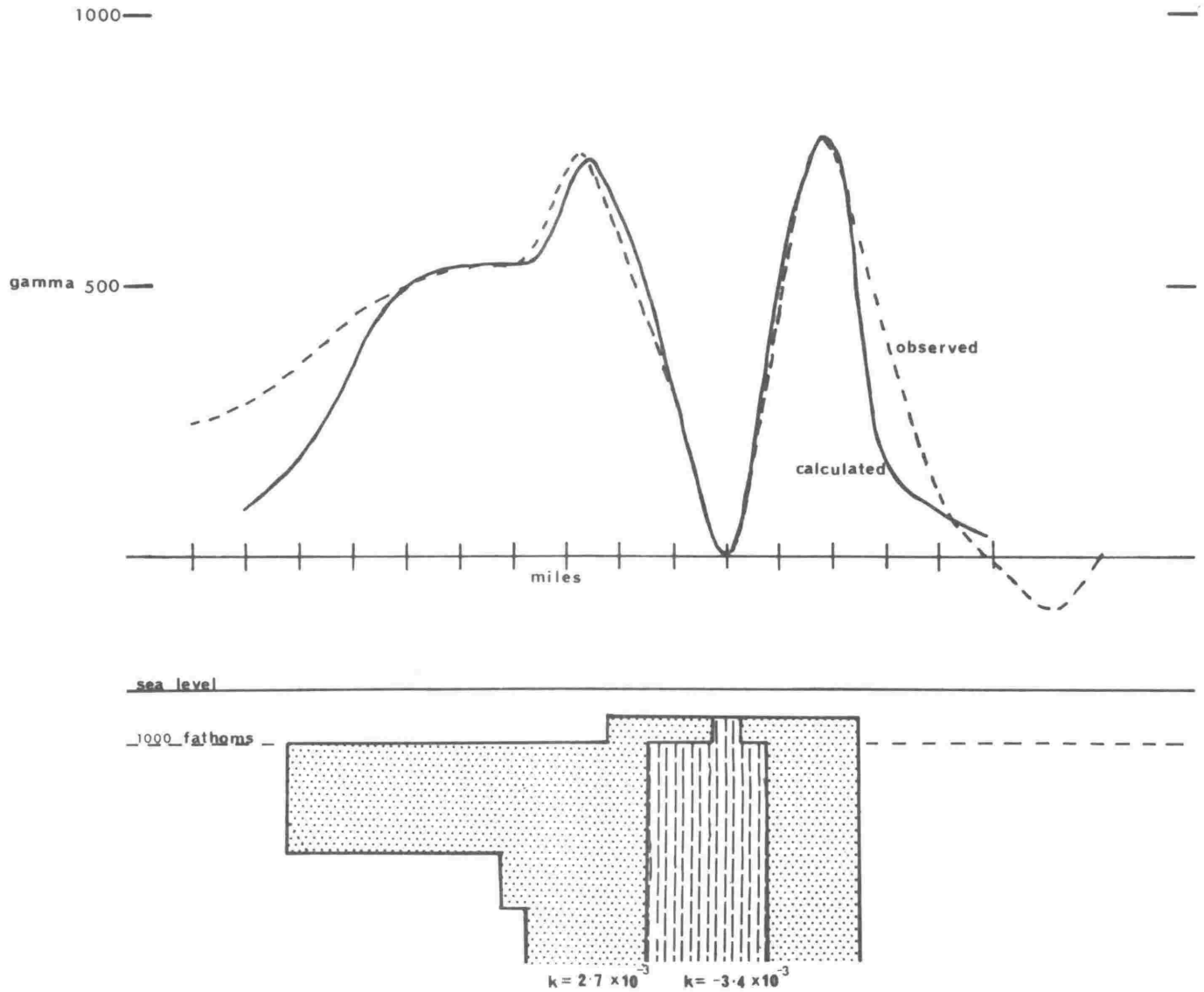
1000
gamma 500
observed
calculated
miles
sea level
1000 fathoms
k = 2·7 x10^-3
k = -3·4 x10^-3

FIGURE 50.

Magnetic anomaly profile across the Southwest Pacific Basin obtained in December 1965 (180° E) together with that obtained on track h (178° E) for comparison.

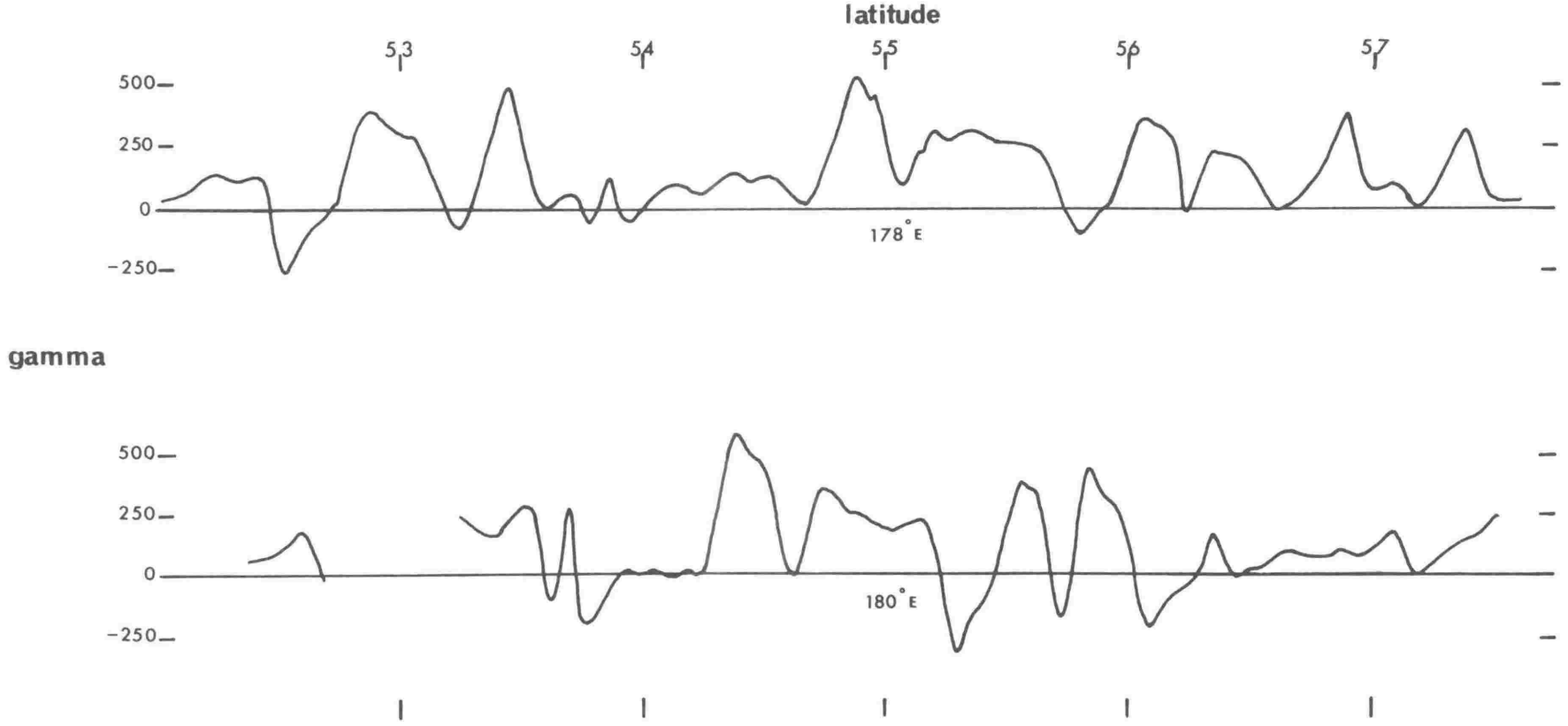
latitude
53
54
55
56
57
500
250
0
-250
178° E
gamma
500
250
0
-250
180° E

FIGURE 51.

Total field and bathymetry profiles across the Pacific-Antarctic Ridge obtained in December 1965 (180°E) together with those obtained on track h (178°E) for comparison.

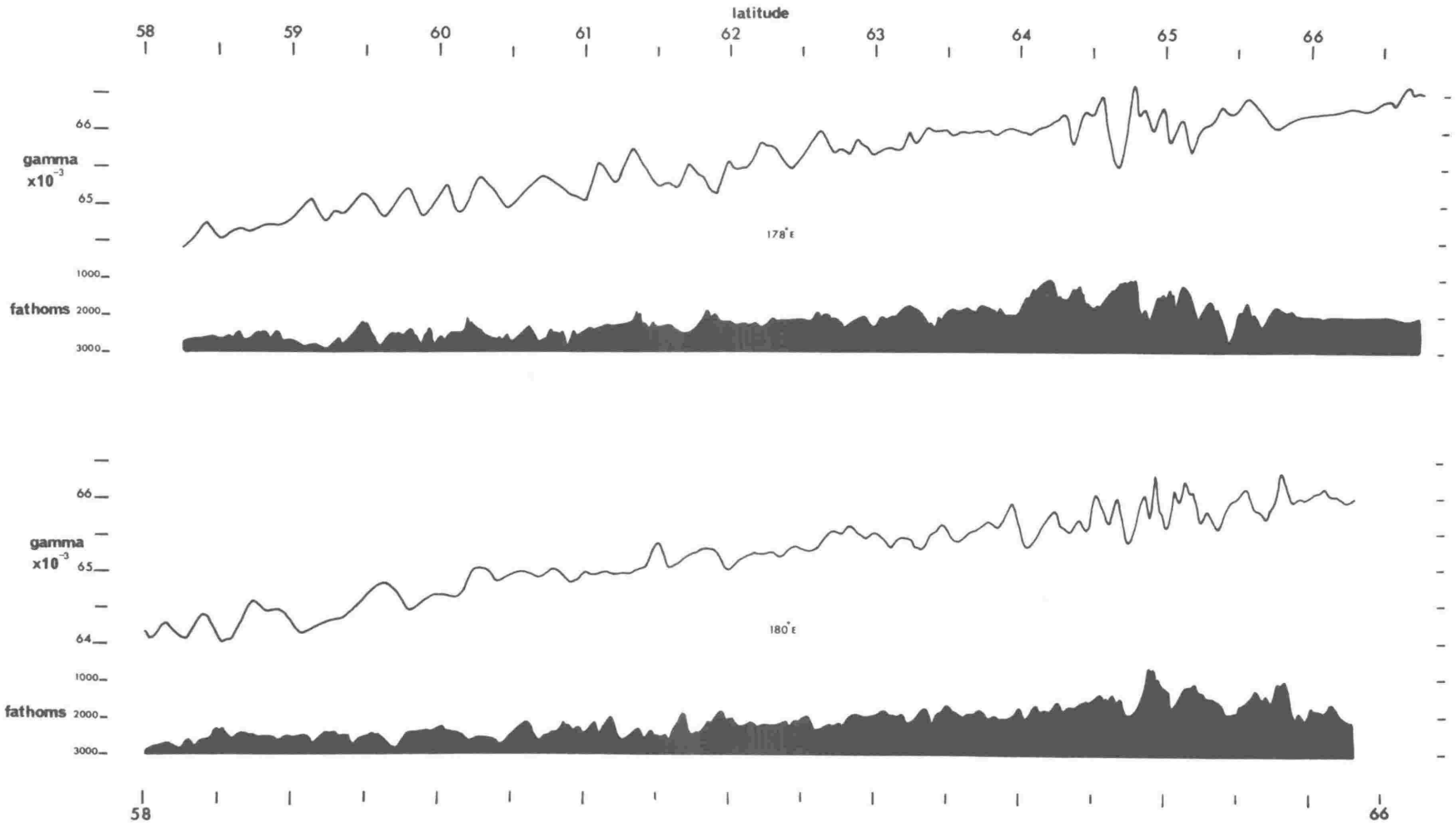
latitude
58
59
60
61
62
63
64
65
66
gamma
x10⁻³
66
65
178°E
1000
fathoms
2000
3000
gamma
x10⁻³
66
65
64
180°E
1000
fathoms
2000
3000
58
66